



University of Brasília – UnB
Faculty UnB Gama – FGA
Electronic Engineering

Electronic System for Data Acquisition and Control of a Automotive Brake Test Bench

Author: João Victor Avancini Guimarães
Advisor: Evandro Leonardo Silva Teixeira Ph.D.

Brasília, DF

2018



João Victor Avancini Guimarães

Electronic System for Data Acquisition and Control of a Automotive Brake Test Bench

Thesis submitted to the course of undergraduate in Electronic Engineering at the University of Brasília, as a partial requirement to obtain a Bachelor's degree in Electronic Engineering.

University of Brasília – UnB

Faculty UnB Gama – FGA

Advisor: Evandro Leonardo Silva Teixeira Ph.D.

Brasília, DF

2018

João Victor Avancini Guimarães

Electronic System for Data Acquisition and Control of a Automotive Brake
Test Bench/ João Victor Avancini Guimarães. – Brasília, DF, 2018-
125 p. : il. (some colors.) ; 30 cm.

Advisor: Evandro Leonardo Silva Teixeira Ph.D.

Graduation Thesis – University of Brasília – UnB
Faculty UnB Gama – FGA , 2018.

1. Electronic Instrumentation. 2. Braking Tests. I. Evandro Leonardo
Silva Teixeira Ph.D.. II. University of Brasilia. III. Faculty UnB Gama. IV. Elec-
tronic System for Data Acquisition and Control of a Automotive Brake Test Bench

CDU 02:141:005.6

João Victor Avancini Guimarães

Electronic System for Data Acquisition and Control of a Automotive Brake Test Bench

Thesis submitted to the course of undergraduate in Electronic Engineering at the University of Brasília, as a partial requirement to obtain a Bachelor's degree in Electronic Engineering.

Thesis approved. Brasília, DF, 30th of December of 2018:

Evandro Leonardo Silva Teixeira
Ph.D.
Advisor

Wellington Avelino do Amaral Ph.D.
Invited Lecturer

Edison Gustavo Cueva Ph.D.
Invited Lecturer

Eng. Ricardo Noronha
Internship Supervisor

Brasília, DF
2018

Acknowledgements

First of all I thank my parents Rita and Carlos and my siblings Pedro, Ana and Frederico for all their efforts, dedication and support over the years.

To my supervisor Prof. Dr. Evandro Leonardo Silva Teixeira for his patience, support and teachings given throughout my stay at the University of Brasilia.

To my friends Mairon, Wener and Joel for the comradeship along our stay at University of Brasília.

To Isiane for her companion, patience and support while I worked on this project.

To my work colleges during my internship at *Autotrac Comércio e Telecomunicações S/A* for sharing their experience and knowledge with me.

To the lecturers Julia Peterle, Aline Demuner, Graciela Ramos, Carmen Santos, Gerardo Pizo, Cristiano Miosso, Gilmar Beserra, Richard Pearl, Josh Reynolds, Eleanor Baldwin, Steve Hegarty, Wellington Amaral, Sébastien Rondineau and other teachers that I had the privilege of learning from over the years.

*“Science, my lad, is made up of mistakes, but they are mistakes which it is useful to
make, because they lead little by little to the truth.”*
(Jules Verne, A Journey to the Center of the Earth)

Abstract

This paper aims to design the automation of a testbench for brake tests. There are already consolidated standards rules for brake system testing, this research project is focused with respect to *SAE J2522* regulation that addresses on brakes tests on passenger vehicles. The major focus of the project is to ensure a resilient solution for the testbench in order to make possible the acquisition of all relevant physical information and to automate the tests.

Key-words: Electronic Instrumentation. Brake Test. Automotive Systems Simulation.

List of Figures

Figure 1 – Schematic for disk brake systems (NICE, 2017)	27
Figure 2 – Brake Tests Diagram of Execution	29
Figure 3 – <i>Crankshaft Position Sensor</i> (REMAN, 2016)	30
Figure 4 – Magnetic Sensor Signal (PETROLHEAD GARAGE, 2014)	31
Figure 5 – Thermocouple characteristic voltage output (BOJORGE, 2014)	32
Figure 6 – Thermocouple Measurement (ECIL, 2016)	33
Figure 7 – Distension (INSTRUMENTS, 2016a)	34
Figure 8 – Wheatstone bridge (INSTRUMENTS, 2016b)	34
Figure 9 – Piezo Accelerometer (UK, 2016)	35
Figure 10 – Instrumentation Amplifier (DESCONHECIDO, 2016)	36
Figure 11 – INA 118 (INSTRUMENTS, 2000a)	37
Figure 12 – ATmega16/32U4 Block Diagram (ATMEL, 2018)	39
Figure 13 – Duty Cycle Examples (RZTRONICS, 2016)	40
Figure 14 – ESD Test Waveform (LITTLELFUSE, 2015a)	42
Figure 15 – Campling action of a uni-directional TVS (RENESAS, 2016c)	43
Figure 16 – Campling action of a bi-directional TVS (RENESAS, 2016b)	43
Figure 17 – $V \times I$ characteristic of a uni-directional TVS (RENESAS, 2016e)	43
Figure 18 – $V \times I$ characteristic of a uni-directional TVS (RENESAS, 2016d)	43
Figure 19 – Project Problem Depuration	49
Figure 20 – Hardware Project Architecture	50
Figure 21 – Minimum Component Tachometer Diagram (TEXAS INSTRUMENTS, 2000)	52
Figure 22 – Tachometer with Adjustable Zero Speed Voltage Output, adapted from (TEXAS INSTRUMETS, 2018)	53
Figure 23 – Speed Acquisition Channel Circuit	55
Figure 24 – 1V2 voltage reference circuit	56
Figure 25 – Temperature Measurement Block Diagram	56
Figure 26 – AD8495 Functional Block Diagram (DEVICES, 2011)	57
Figure 27 – RFI	59
Figure 28 – Thermocouple Signal Conditioning Circuit	59
Figure 29 – Overvoltage Detection Circuit	60
Figure 30 – INA125 Schematic (INSTRUMENTS, 1997)	62
Figure 31 – Conditioning Circuit for the Load Cell	63
Figure 32 – 16-LFCSP (DEVICES, 2016)	64
Figure 33 – Adafruit ADXL335 - 5V ready (ADAFRUIT, 2018)	64

Figure 34 – Accelerometer Signal Conditioning Circuit	65
Figure 35 – Accelerometer Sensor Detection Circuit	66
Figure 36 – Weg CFW-08 Frequency Inverter (WEG, 2017)	67
Figure 37 – Sallen-Key Active Low Pass Filter (TEXAS INSTRUMENTS, 1999)	69
Figure 38 – PWM to Speed Reference Circuit	69
Figure 39 – PMOS low side driver (ELECTRONICS TUTORIALS, 2018)	70
Figure 40 – Digital Output Circuit	71
Figure 41 – Digital Input Circuit	72
Figure 42 – <i>ATmega32U4</i> pinout (PIGHIXX, 2018)	73
Figure 43 – MCU Core Circuit	74
Figure 44 – Crystal Oscillator Circuit	76
Figure 45 – USB Port Protection Circuit	76
Figure 46 – 5V Power Supply Circuit	77
Figure 47 – 4V1 voltage reference circuit	78
Figure 48 – PCB Top 2D View	79
Figure 49 – PCB Bottom 2D View	79
Figure 50 – PCB Top View	80
Figure 51 – Real PCB Assembled	80
 Figure 52 – Microcontroller Code Map	82
 Figure 53 – Materials Disposition	86
Figure 54 – Frequency Inverter WEG-CFW08	86
Figure 55 – Electric Motor WEG	87
Figure 56 – Brake Disc Machine	87
Figure 57 – Brake Disc Machine Pulley System	87
Figure 58 – Brake Disc Arrangment	88
Figure 59 – Load Cell Installation Scheme (CAIXETA, 2017)	88
Figure 60 – Load Cell Installed	88
Figure 61 – Thermocouples Installed	89
Figure 62 – CKP installed	89
Figure 63 – Test Application Main Screen	90
Figure 64 – Measurements of the first ten snubs of the test	92
Figure 65 – Temperature and Brake Force Measurements of The First Ten Snubs	92
Figure 66 – Temperature Variation During The Whole Test	93
Figure 67 – Deceleration During the Whole Test	93
Figure 68 – Analog Output in Respect with Duty Cycle	94
Figure 69 – Rotation in Respect with Duty Cycle	95

List of Tables

Table 1 – Thermocouples and their operation ranges	33
Table 2 – ASCII Commands Reference	83
Table 3 – Test Parameters Setup	91

List of abbreviations and acronyms

SAE	Society of Automotive Engineers.
GUI	Graphical User Interface.
ABS	Anti-lock Braking System.
CKP	Crankshaft Position Sensor.
GPIO	General-Purpose Input/Output.
SRAM	Static Random-Access Memory
EEPROM	Electrically Erasable Programmable Read-Only Memory.
DIP28	Dual In-line Package 28pins.
ISR	Interruption Service Routine.
IC	Integrated Circuit.
MCU	Microcontroller Unit.
I ² C	Inter-Integrated Circuit.
DAQ	Data Acquisition.
PWM	Pulse Width Modulation.
N-MOSFET	N channel Metal-Oxide-Semiconductor Field-Effect Transistor.
LPF	Low-Pass Filter.
TVS	Transient Voltage Supressor.
OPAMP	Operational Amplifier.
USB	Universal Serial Bus.
UART	Universal Asynchronous Receiver-Transmitter.
USART	Universal Synchronous-Asynchronous Receiver-Transmitter.
ESD	Electrostatic Discharge.
EMI	Electromagnetic Interference.

PCB	Printed Circuit Board.
RFI	Radio Frequency Interference.
DAC	Digital-to-Analog Converter.
ADC	Analog-to-Digital Converter.
SNR	Signal-to-Noise-Ratio.
RTD	Resistance Temperature Detector.

List of symbols

Pa	Pascal: Unit used to measure pressure.
kPa	10^3 Pascal.
MPa	10^6 Pascal.
°C	Celsius Degree: Unit used to measure temperature.
kph	Kilometer per hour: Unit used to measure speed.
m	Meters: SI unit used to measure distance.
cm	10^{-2} Meters.
s	Seconds: SI unit for measuring time.
ms	10^{-3} Seconds.
hp	Horsepower: Unit used to measure power.
kB	KiloBytes: Used to measure memory size.
V	Volts: SI unit for measuring electrical potential.
mv	10^{-3} Volts.
Ω	Omega: SI unit for measuring electrical resistance.
A	Ampere: SI unit for measuring electrical current.
mA	10^{-3} Ampere.
g	Earth gravity acceleration ($9.8m/s^2$).

Summary

1	INTRODUCTION	23
1.1	Purpose of the project	24
1.2	Text Structure	25
2	LITERATURE REVIEW	27
2.1	Working principles of disk brake systems	27
2.2	The <i>SAE J2522</i> regulation	28
2.2.1	Monitored Parameters	28
2.2.2	Brake Tests	29
2.3	Review of basic Electronic Sensors, Devices and Concepts Relevant to this thesys	30
2.3.1	Speed Measurement	30
2.3.2	Temperature Measurement	31
2.3.3	Brake Force Measurement	33
2.3.4	Vibration Measurement	34
2.3.5	Instrumentation Amplifier	36
2.3.5.1	Important features to consider in a amplifier	37
2.3.6	System Controlling	38
2.3.6.1	Microcontroller basic characteristics	38
2.3.6.2	Microcontroller Architecture and Most Important Parts	39
2.3.6.3	Pulse Width Modulation	40
2.3.7	Circuit Protection	41
2.3.7.1	Low Pass Filters	41
2.3.7.2	Transient Voltage Supression Diodes (TVS)	42
2.3.7.2.1	TVS diodes principle of operation	42
2.3.7.2.2	Selecting TVS Diodes	42
3	METHODOLOGY	45
3.1	Lieterature Review	45
3.2	Problem Description	45
3.3	Project Conception	45
3.4	Case Study	45
4	ACQUISITION AND CONTROL SYSTEM	47
4.1	Monitored Parameters	47
4.2	Functional Requirements of the Testbench	47

4.3	Problem Analysis	48
4.3.1	Brake System Simulator	48
4.3.2	Higher Layer Hardware	49
4.3.3	Lower Layer Hardware	49
4.3.3.1	Lower Level Hardware Interfaces	50
4.4	Speed Acquisition Channel	51
4.4.1	CKP Signal Conditioning	51
4.4.1.1	LM2907 Basic Tachometer Circuit	52
4.4.1.2	LM2907 Designed Circuit	54
4.4.2	1V2 Reference	55
4.5	Temperature Acquisition Channel	56
4.5.1	Thermocouple Signal Conditioning	56
4.5.2	Input Protection and Filtering	57
4.5.3	Thermocouple Sensor Detection	60
4.6	Brake Pressure Acquisition Channel	61
4.6.1	Load Cell Signal	61
4.6.2	Load Cell Signal Conditioning	61
4.6.3	Load Cell Sensor Detection	63
4.7	Vibration Acquisition Channel	63
4.7.1	Accelerometer	63
4.7.2	Signal Conditioning Circuit	65
4.7.3	Sensor Detection Circuit	65
4.8	Speed Reference Output Channel	65
4.8.1	Speed Control	65
4.8.2	Filter characteristics definition	66
4.8.3	Sallen-Key Low Pass Active Filter	68
4.8.4	Complete Circuit	69
4.9	Digital Interfaces	70
4.9.1	Digital Outputs	70
4.9.1.1	Low-side Driver	70
4.9.1.2	Digital Output Circuit	70
4.9.2	Digital Inputs	71
4.10	MCU	72
4.10.1	MCU circuit	73
4.10.1.1	Core Circuit	73
4.10.1.2	Crystal Oscillator Circuit	75
4.10.1.3	USB Port Protection Circuit	75
4.11	Voltage Supplies	76
4.11.1	Power Supplies	76

4.11.1.1	5V Supply	77
4.11.2	Voltage References	77
4.11.2.1	4V1 Reference	77
4.12	Circuit Fabrication and Assembly	78
4.12.1	PCB Design	78
5	FIRMWARE PROJECT	81
5.1	Microcontroller programming basics	81
5.2	Code Map	81
6	EXPERIMENTAL TESTS	85
6.1	Materials	85
6.2	Test Application	89
6.3	Brake Test	91
6.3.1	Full Stop Test	91
6.3.2	Results and Discussion	91
6.4	Analog Output Tests	94
6.4.1	Analog Output Duty Cycle Tests	94
6.4.2	Results and Discussion	94
7	CONCLUSIONS AND FUTURE ENDAVOURS	97
7.1	Conclusions	97
7.2	Future Endavours	98
REFERENCES		99
APPENDIX		105
APPENDIX A – SCHEMATIC PRINTS		107
APPENDIX B – FIRMWARE CODE		117

1 Introduction

With the advancement of technology, cars are leaving the factory each time with more power for more affordable prices. In 1995 the best-selling car in Brazil ([HERNANDES, 2017](#)), (*Volkswagen Gol Plus 1.0*), had 49.8hp of maximum power and brand-new would accelerate from nought to 100kph in 22.4 seconds ([CNW, 2017b](#)). On the other hand, the sales champion of 2015 , *Volkswagen Gol 1.0*, had 76hp of maximum power and could do the same task in 13.3 seconds ([CNW, 2017a](#)), almost half the time from the previous. Interisting fact is that even though the latter is 20 years younger, both cars have similar brake systems: disk brakes in the front wheels and drum ones in the back. This enhancement on vehicle accelerations naturally imply on higher top speeds, which should lead to a bigger concern in brake systems effectiveness.

During the development of any solution or enhancement on any technology or product, testing is fundamental. In the matter of brake systems, the fact stated on the previous sentence can also be considered true. On the process of developing more effective brake systems, it is important to perform brake tests.

Although brake tests are so importatant ([ABENDROTH, 1985](#)), performing this tests with full scale vehicles are obviously expensive and this somehow makes extensive testing unfeasible. Also the time required for each test might be a constrain. The automotive industry has being using testbenchs and controlled environments in order to provide relevant and reliant information about quality and performance of automotive systems with lower costs and reduced testing time. Small scale tests do not have the purpose of fully replacing full scale ones, but the savings in costs and time that they could provide can be used for mass testing, and this can already somehow show their utility and relevance ([GARDINALLI, 2005](#)).

Evaluating the brake efficiency of a vehicle as a whole, involves a lot of factors, a small scale test plataform will not provide results that could be used to fully address the quality of a car break system, instead, it is possible to focus the results on the performance of individual componentes of the system such as pads, disks and calipers ([HALDERMAN; MITCHELL, 2016](#)), and evaluating the performance of this components is a good start for evaluating the braking capacity of a brake system.

Governament and legal authorities have been creating strict regulations for manufacturers to follow in order to ensure that cars have a higher standard of safety. Braking tests have been regulated for some time. A international standard for brake testing is the regulation *SAE J2522* ([SAE, 2016](#)), which gives a the description of how break tests should be conducted for systems used in low weight passengers cars. The brake system

is a critical part of an automobile, thanks to this system it is possible to use the latter under safe conditions both in urban and rural areas. There are some ideal requirements that a brake system should be able to attend ([KAWAGUCHI, 2005](#)):

- Reduce the speed of a moving vehicle, increasing the deceleration of the same.
- Stop the vehicle completely.
- Maintain the vehicle speed, preventing unwanted acceleration in downhill paths.
- Keep the vehicle motionless while it is parked.

Another point of view should also be considered during this analysis, the manufacturers point of view. More effective brake systems means more research and probably more expensive materials, generating more cost to manufacturers and consequently more cost to customers. Theoretically this would meant that manufactures need to choose a trade-off between quality and cost. However, the point in which this trade-off is setted is determined by governament regulations. Moreover if there was no general regulations each car manufacturer would have a standard that they judge is sufficient. In Brazil, according to Resolution N.519 ([CONTRAN, 2015](#)) from the National Traffic Council (*CONTRAN - Conselho Nacional de Trânsito*), the minimal requirements of perfomance of brake systems from any vehicle with 750kg or less should meet the following regulations from Brazilian Association of Technical Standards (*ABNT - Associação Brasileira de Normas Técnicas*): *NBR 10966-1, NBR 10966-2, NBR 10966-3, NBR 10966-4, NBR 10966-5, NBR 10966-6, NBR 10966-7* and *NBR 16068*. Most of these regulations are based in the european regulation ECE-13/05.

Considering the importance of regulatory standards, the need for brake tests becomes even more evident as it is mandatory to ensure that brake-systems will attend to regulations requiremementes. Only with extensive testing it is possible to ensure that a particular system will attend to all standards regarding it's category of operation.

Making all these considerations, a *Break-Testbench* can be a useful device for the automotive industry and research. Considering that this device would be able to simulate a replica of real evironments and situations that a brake system is submitted, this testbench could allow manufactures and suppliers to avoid expenses in full scale tests as they would be able to test different parts of the system in a assisted and controlled evironments.

1.1 Purpose of the project

The purpose of this project is to develop, implement and test an electronic instrument system for monitoring and controlling a small scale brake-testbench based on

the information from the international regulation *SAE J2522* ([SAE, 2016](#)). The system should be able to perform brake tests by controlling the mechanical parts while acquiring relevant data with the aid of sensors and transducers.

1.2 Text Structure

The rest of this thesis was divided on chapters briefly explained below.

Chapter 2, Literature Review: This chapter will explore some concepts and aspects of engineering and of brake tests that are considered fundamental to following parts of this paper.

Chapter 3, Methodology: This is where the strategy for developing this paper and the engineering solutions it proposes are discussed.

Chapter 4, Acquisition and Control System: On this chapter the problem this project tries to solve will be defined in a specific way and the project requirements, both from hardware and software will be enumerated. Also, based on these requirements the parameters and the proposed solutions will be discussed.

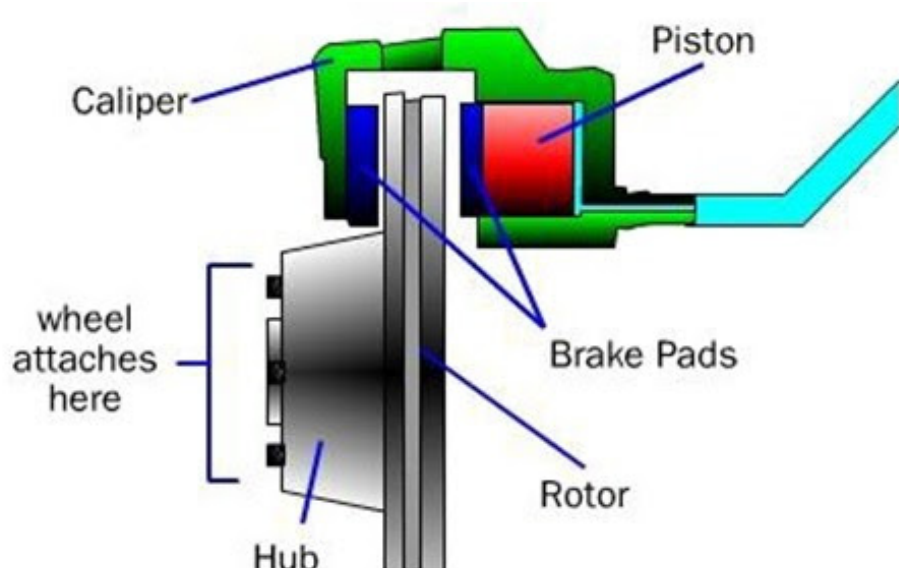
Chapter 5, Experimental Tests: As the title already states, this chapter will deal with the experimental tests needed to validate the developed solution.

Chapter 6, Conclusions and Future Endeavours: This chapter is about among the possible conclusions that can be made after the development of this project and will also deal with the possible improvements and uses for the development solution.

2 Literature Review

2.1 Working principles of disk brake systems

In general terms, a disc break can be summarized as a type of brake that uses calipers to squeeze pairs of pads against a disc coupled to a shaft in order to create friction. This generated friction ought to retard the rotation of this shaft coupled to the disk. A moving car, or being more specific, a rotating shaft has a certain amount of kinetic energy, the brakes of a car are designed to convert this kinetic energy to heat (through friction) in order to decelerate the car ([LIMPERT, 1999](#)). Figure 1 shows a schematic for a typical disk break.



WORKING OF DISK BRAKES

Figure 1 – Schematic for disk brake systems ([NICE, 2017](#))

As Figure 1 shows, some of the main components of a typical disk brake system and their respective functions are ([CARPARTS, 2018](#)):

- *Caliper*: Fits over the rotor like a clamp, houses the pads and pistons. This part does not tend to wear out quickly, usually, damages on this part are caused by using outworn pads or disks ([GOODYEAR, 2018](#)).
- *Pads*: There are two brake pads on each caliper, this is the part that is effectively in contact with the disk. Pads are used in order to prevent disk wear and caliper wear,

this parts are made with specific materials that provide better performance, hence more friction with less dissipated heat. Pads tend to wear out quickly in a vehicle and should be checked and replaced quite often.

- *Piston*: Most of brake discs are activated through a hydraulic mechanism, when the break pedal is pressed the brake fluid goes to the piston and the piston squeezes the pads against the disk.
- *Rotor*: The disk rotor is the main component of the system, it is directly connected to the wheel's shaft. The rotor wears with time, if break pads are replaced accordingly the rotor tends to last more than the pads. Usually a vehicle will undergo more than one brake pads replacement before having its disks replaced.

2.2 The SAE J2522 regulation

More related to this project is the *SAE J2522*, entitled *Dynamometer Global Brake Effectiveness*, at the beginning it already states the its utility with the following:

“The SAE Brake Dynamometer Test Code Standards Committee considers this standard useful in supporting the technological efforts intended to improve motor vehicle braking systems overall performance and safety”

This regulation ([SAE, 2003](#)) was developed to be used in conjunction with other test standards in order to address the friction of a certain material to check its adequacy for a certain application. It is important to state that this paper is based on the *SAE J2522*, it is not a faithful application of the standard though. This paper is more concerned about the settings of the tests mentioned on the regulation rather than the formulas and criteria for a materials engineering analysis.

All the tests mentioned on the regulation can generalised on repetitive cycles of accelerating the rotor to a specified speed and applying brake force (may vary along the test) until the rotor reaches a lower limit of speed. On the regulation, sometimes the deceleration ratio is also defined but not always. Initial temperature is also defined, some tests can only be performed if the brake parts are under a certain temperature.

2.2.1 Monitored Parameters

According to Regulation *SAE J2522* ([SAE, 2003](#)), in order to perform the brake tests specified it is mandatory to evaluate the following parameters:

- *Temperature of the brake pads*: It is important during the entire test to be fully aware of the temperature of the brake system, firstly by the safety factor (there is a maximum operating temperature for the system), also by the wear of the system

that is tied to the temperature therein. Last but not least is the fact that knowing the temperature it is possible to carry out tests based on it, being possible to conduct tests in known temperature ranges.

- *Braking pressure*: The pressure to be measured is the pressure that the brake caliper is applying to the rotor over time, knowing the magnitude of this force means having control over how much the temperature increases according to braking and how much the rotor speed decreases as a function of braking.
- *Rotation Speed*: Without knowledge of rotor speed it would be impossible to determine whether the brake is being effective or how effective it is. Speed monitoring is the most critical parameter for system operation, without it there is no utility to the rest of the equipment.

Another interesting parameter to monitor that is not specified on Regulation *SAE J2522* is the vibration on the caliper, usually when the magnitude of this vibration is considerably high it usually indicates that this part is already worn out ([GOODYEAR, 2018](#)) and it may damage the rotor by bending it over time. Is is also relevant to mention that vibration is measured in terms of g ($9.8 \text{ m} \cdot \text{s}^2$).

2.2.2 Brake Tests

All tests specified on the regulation follow a certain pattern of execution order which is synthesized in Figure 2.

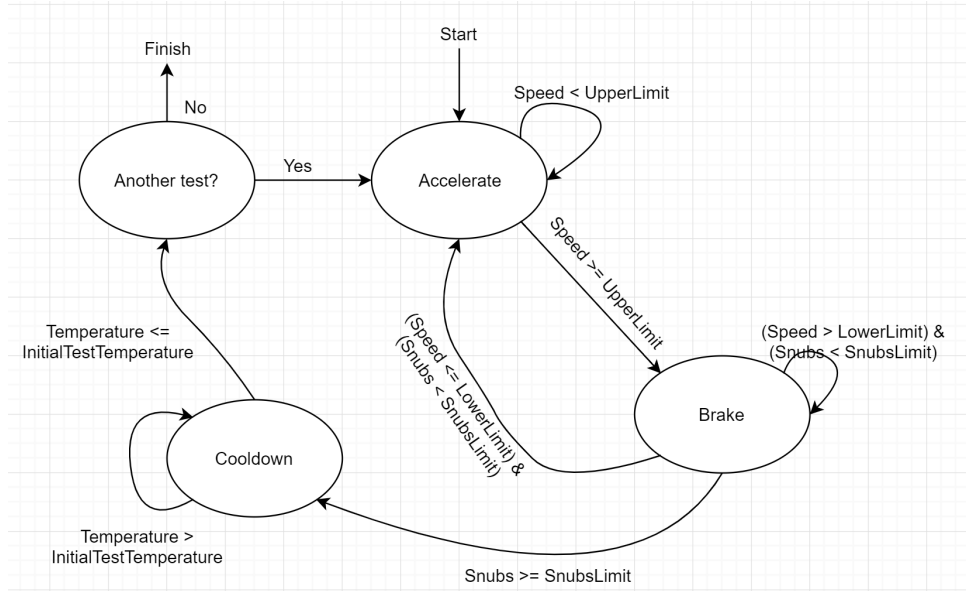


Figure 2 – Brake Tests Diagram of Execution

The system is accelerated to a top speed (**Upper Speed Limit**), than the brake actuates with a known pressure (**Brake Pressure**) until the system reaches a cer-

tain speed (**Lower Speed Limit**), this process is repeated for certain number of times (**Snubs**) and after each test the system must rest (**Coldown**) until the brakes are cooled enough regarding a defined temperature (**Initial Test Temperature**), only after the brakes reach this temperature another test can be performed.

2.3 Review of basic Electronic Sensors, Devices and Concepts Relevant to this thesys

2.3.1 Speed Measurement

As it was specified in Item 2.2.1 from Section 2.2.1, monitoring the rotor speed is mandatory in order to perform brake tests. There are many different ways to measure speed in rotors and shafts. On the automotive environment this measurements are done using magnetic sensors.

The name used for the sensor in the automotive environment is Crankshaft Position Sensor (CKP), it has this name because most of the time this sensor is mounted aligned with the crankshaft and is used to monitor both the speed and the position of the crankshaft. A typical CKP sensor is shown in Figure 3.



Figure 3 – Crankshaft Position Sensor (REMAN, 2016)

This sensor is widely used in the automotive industry to determine the angular position of the vehicle's crankshaft and its rotation speed. There are several types of CKP sensors, the most common are the variable reluctance type because they have low cost and good accuracy (SCHROEDER, 2002).

As the gear in question rotates each tooth of the gear aligns with the variable reluctance sensor, a magnetic flux in the sensor coil changes as the air gap between the sensor and the gear changes. This change in the magnetic field generates induces a voltage pulse at the sensor output. This type of sensors have an analog voltage output where amplitude and frequency vary proportionally to the speed of rotation of a gear, as Figure

4. With this type of sensor it is possible to extract data of linear velocity, angular velocity and angular position. However, only the angular velocity data (frequency) is important to be measured for brake tests specified by the regulation ([SAE, 2003](#)).

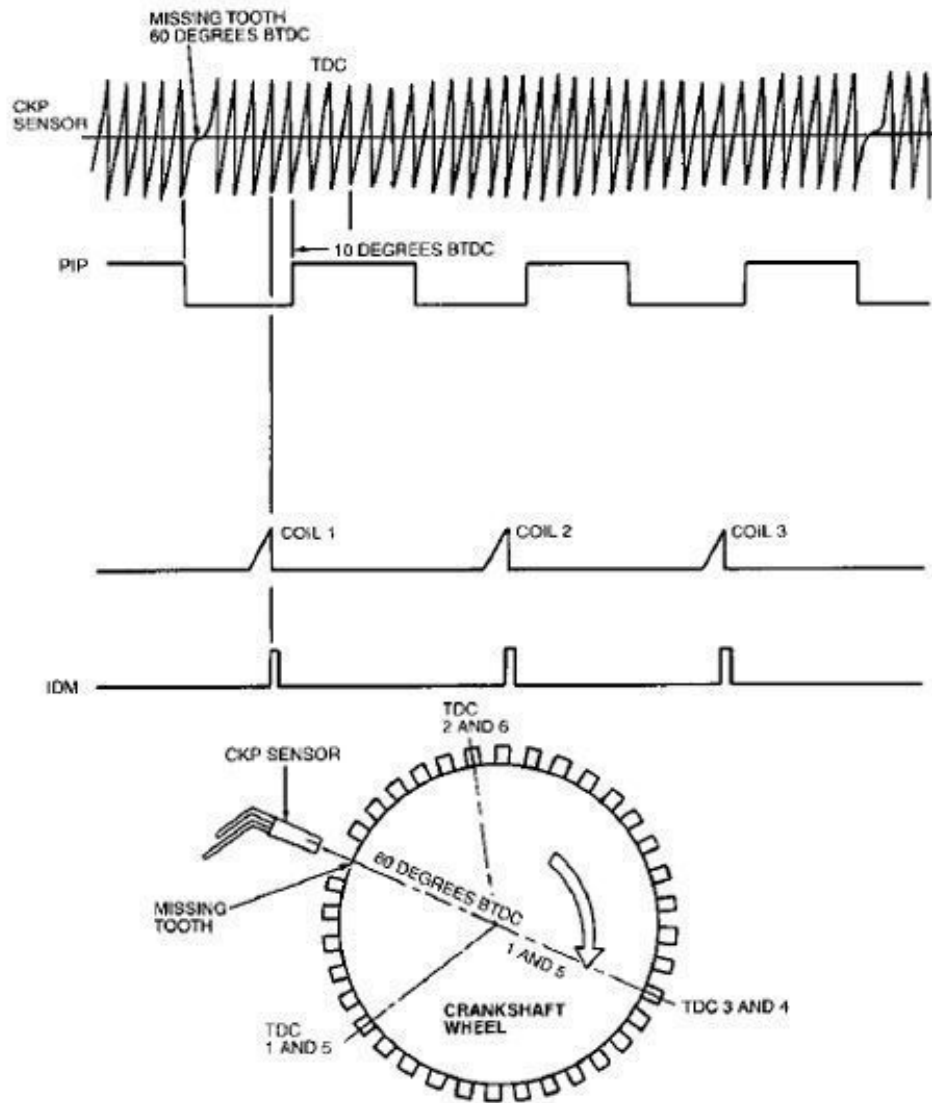


Figure 4 – Magnetic Sensor Signal ([PETROLHEAD GARAGE, 2014](#))

2.3.2 Temperature Measurement

As it was explained in Section 2.1, from a physics point of view a brake can be seen as a device to convert kinetic energy into thermal energy (heat). Whereas, considering this fact it is possible to address that the performance of a break system is therefore directly related to the variation of temperature during braking. Moreover, as it was explained in Item 2.2.1 from Section 2.2.1, SAE J2522 ([SAE, 2003](#)) specifies that it is mandatory to measure temperature in order to perform brake tests.

According to (GUMS, 2018), the four main types of temperature transducers are: Thermocouples, RTDs (Resistance Temperature Detectors), Thermistors and Semiconductor based ICs. It is stated by (NEWTON, 2016) that brake pads from production passenger cars operate at the temperature range from 100°C to 650°C. Among the most common type of temperature transducers, thermocouples operate across the widest temperature range, from -200 °C to 1750 °C (AMETHERM, 2018). Moreover, regulation *SAE J2522* (SAE, 2003) states that temperature measurements for performing specified brake tests should be done with a Thermocouple. Taking the sum of all this facts, thermocouples are the reasonable choice for this kind of application.

A thermocouple is a device that has this junction of two different metals and has a known voltage generated output proportional to the heat transfer on the junction. In theory any combination of two different metals could be used, but there are standardized combinations that produces more stable and predictable voltage outputs (POLLOCK, 1991). This relation between heat transfer and voltage is known not to be linear as Figure 5 shows (E,J,K,T,R,S and B are designators for normalized thermocouples junction types).

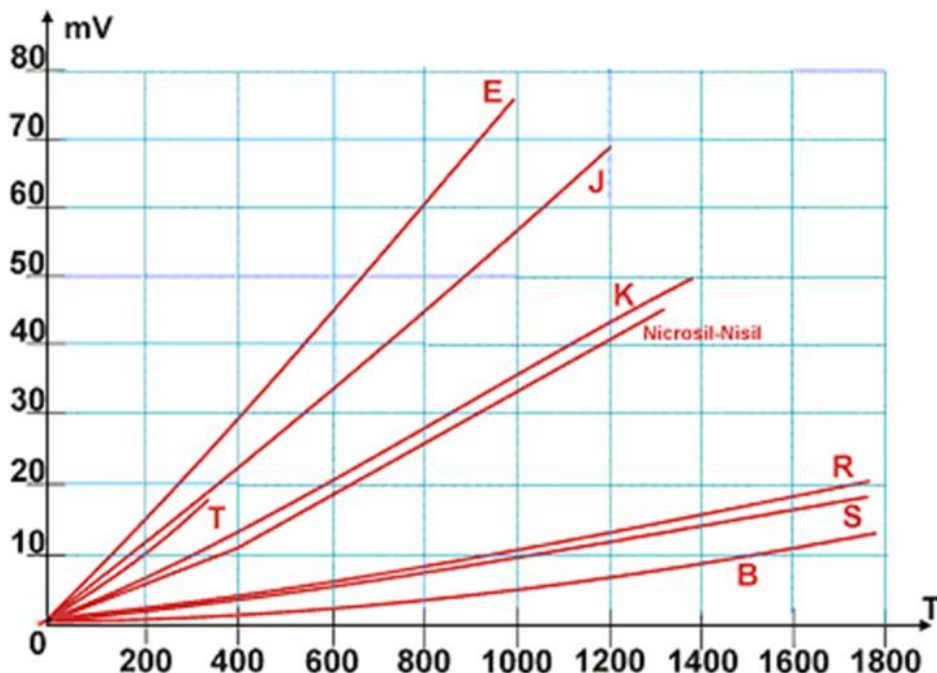


Figure 5 – Thermocouple characteristic voltage output (BOJORGE, 2014)

Thermocouple actually have two junctions, a hot junction (the one that is submitted to heat transfers) and a cold junction (also called reference junction). What the thermocouple really measures is the difference between the temperature of this two junctions, this means that in a hypothetical situation which the hot junction is submitted to a 100°C and the cold junction is submitted to a environmental temperature of 25°C, after thermal equilibrium is reached the thermocouple voltage will be proportional to a

temperature of 75°C. Hence the thermocouple will only produce a "real" output voltage when the cold junction is submitted to a 0°C (in some calibrations procedures the cold junction is actually submitted to 0°C) (KINZIE; RUBIN, 1973).

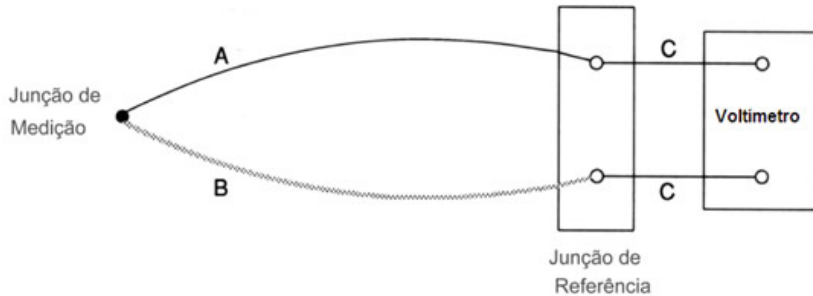


Figure 6 – Thermocouple Measurement (ECIL, 2016)

There is a big variety of thermocouples available, table 1 shows the most common thermocouples and their temperature range.

Table 1 – Thermocouples and their operation ranges

Thermocouple Type	Range of Operation (°C)
J	0 a 750
K	-200 a 1250
E	-200 a 900
T	-250 a 350

2.3.3 Brake Force Measurement

Brake pressure can be interpreted as the force that the brake system applies to the disc in a distributed way along the area of the pads. Considering this, in order to find out the break pressure the force applied to the calipers must be measured.

Force transducers can be defined as devices that converts a signal from one physical form to a corresponding signal having a different physical form (PALLĂ; WEBSTER et al., 2012) and they are used with instrumentation of varying complexity. One of the many force transducers is the load cell, they are devices formed by strain gauges which their electrical resistance varies proportionally to their distension. Distension is a quantification of the deformation of a body, it can also be defined as a fractional change of the body of a body. Distension may be negative (compression) or positive (traction).

Generally, the length variation in a strain gauge is very small and this makes them very susceptible to measurement errors. As a result, the use of a Wheatstone bridge is very common, it is formed by four resistive arms and an excitation voltage applied to the bridge (WINDOW; HOLISTER et al., 1982).

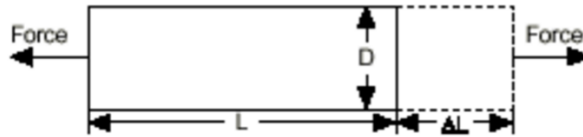


Figure 7 – Distension (INSTRUMENTS, 2016a)

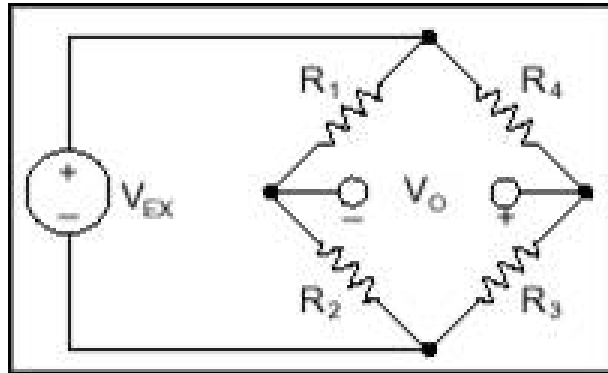


Figure 8 – Wheatstone bridge (INSTRUMENTS, 2016b)

The voltage output V_O can be obtained from the Equation 2.1, V_O the load cell signal output is a differential pair signal.

$$V_O = \frac{R_3}{R_3 + R_4} - \frac{R_2}{R_1 + R_2} \quad (2.1)$$

According to (DILLON; GRIFFEN; WEIHS, 1989) the main advantages and disadvantages of Load Cells are:

- *Accuracy*: usually less than 0.1%.
- *Rigid in Construction*: it is extremely resistant to impact and to any mechanical stress.
- *Calibration*: load cells are usually already calibrated by manufacturers and vendors.
- *Size and Weight*: load cells are bigger and heavier than most force transducers, for applications where size and weight is a important requirement they may not be suitable.

Taking all this characteristics into concern the load cell is the most suitable transducer for a automotive test environment.

2.3.4 Vibration Measurement

Even though measuring vibration is not mandatory in order to perform break tests, it can provide useful data in order to address the wear of the caliper of a disc break, and

as excessive vibration can stress the rotor enough to cause it to bend (as explained in Section 2.2.1).

A body is said to vibrate when it describes an oscillatory movement around a reference point (FERNANDES, 2000). For the measurement of vibration in machines it is more common the measurement of the acceleration as a function of g ($9.8m/s^2$). The same is measured as a function of g as a function of Einstein's Principle of Equivalence, where the acceleration of a reference data is not distinguishable from the gravitational action on it (JR, 1968).

Accelerometers are sensors that measure acceleration itself, that is, the acceleration that the sensor itself is subjected to. Accelerometers are widely used in the automotive industry, initially only in the Air Bag system and currently even for vehicle stability control.

Currently the most common accelerometers are those based on the piezoelectric effect, this effect discrives the variation of electrostatic force or electric voltage in a material when subjected to a force.

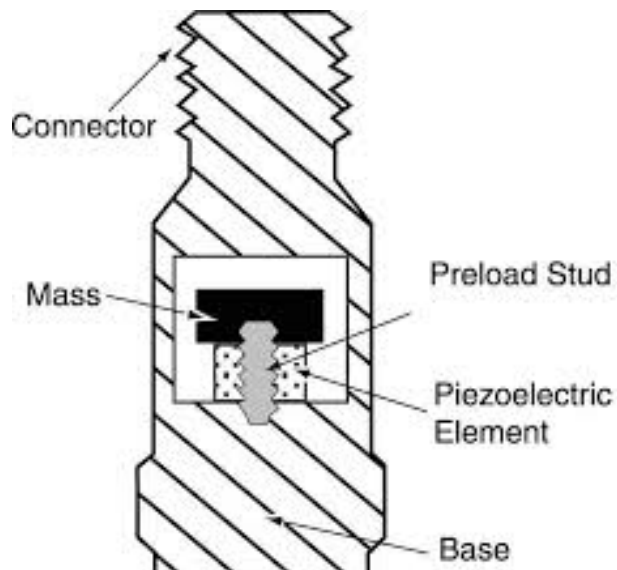


Figure 9 – Piezo Accelerometer (UK, 2016)

By measuring this variation of electrostatic force or electrical voltage it is possible to determine the acceleration that the sensor has undergone. In Figure 9 we can observe that there is a mass in the piezoelectric material, so when the sensor is submitted to some movement, based on the principle of inertia the mass will exert a force of traction or compression which will generate a voltage variation at the sensor output (PATRICK, 2007).

2.3.5 Instrumentation Amplifier

In general, sensors and transducers have very low voltage output levels (specially passive transducers), and therefore an amplification is fundamental. The most commonly used amplifier circuit in instrumentation engineering is the common joint differential amplifier more commonly referred as *Instrumentation Amplifier* (Figure 10), which is very stable and significantly reduces the output signal noise (WAIT; HUELSMAN; KORN, 1975).

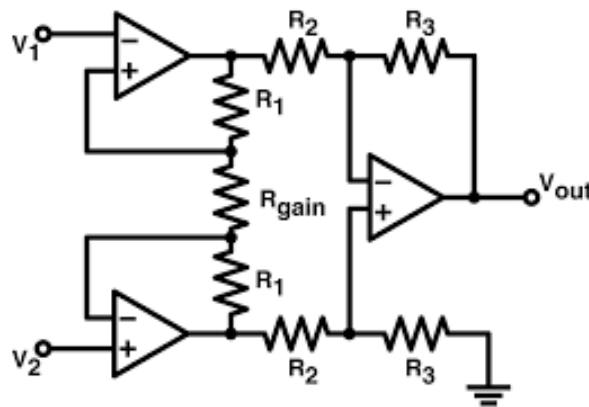


Figure 10 – Instrumentation Amplifier (DESCONHECIDO, 2016)

The instrumentation amplifier has two stages, the first stage consists in amplifying both inputs of a sensor, with the gain of this amplification stage controlled by R_{gain} in Figure 10. The second stage consists in taking the difference of the two input signals. If the differentiation happens before the amplification, noise may be so big in the input signals that some signal information might be lost. In the instrumentation amplifier noise and signal is amplified on the first stage, considering that the noise is similar in both inputs the differential stage will take out the noise and only output the difference between both inputs. One advantage of this amplifier is that it has high input impedances, that means it will not drain significant current from the signal, i.e., it will not interfere with the measure (THOMSEN et al., 2003). Another advantage is that the gain of this amplifier can be adjusted with just one resistor (METTINGVANRIJN; PEPER; GRIMBERGEN, 1994).

The gain of the instrumentation amplifier is given by the following 2.3.5 (COUNTS; KITCHEN, 2006).

$$V_{out} = (V_2 - V_1) \cdot \left(1 + \frac{2 \cdot R}{R_{gain}} \right) \quad (2.2)$$

Something interesting to notice is that if we take out the R_{gain} (open load), the gain of the amplifier is equal to one. Besides this advantageous behavior of the instrumen-

tation amplifier, it is quite hard to make it work with seven resistors and three operation amplifiers because of components imprecision. Hence, it is more practical to work with ICs that ensure the symmetry of between those components. As an example, there is the Texas Instruments INA118 ([INSTRUMENTS, 2000b](#)), which is one of many encapsulated solutions for the instrumentation amplifier, the schematic of this component is shown in Figure 11.

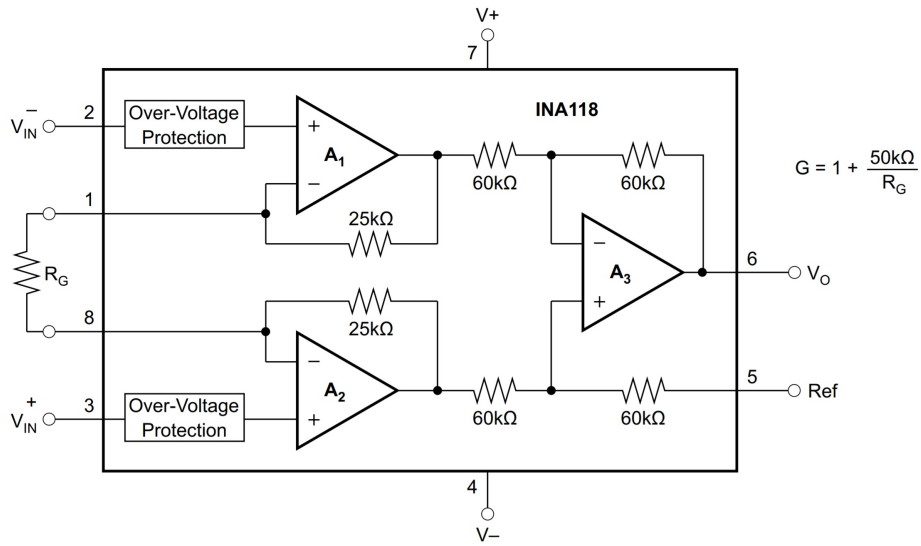


Figure 11 – INA 118 ([INSTRUMENTS, 2000a](#))

2.3.5.1 Important features to consider in a amplifier

There are some important factors when choosing a OPAMP in a certain application, according to ([INC.\(NORWOOD, 2011\)](#)), some of the important features to know in a amplifier are:

- *Common-Mode Voltage Range (CMVR)*: Allowable input voltage range at both inputs before clipping or excessive nonlinearity.
- *Common-Mode Rejection Ratio (CMRR)*: The ratio of common-mode voltage range (CMVR) to the change in the input offset voltage over this range, expressed in dB.
- *Gain Bandwidth Product (GBW)*: The product of open-loop and bandwidth at a specific frequency.
- *Input Bias Current (I_B)*: The current at the input terminals.
- *Operating Supply Voltage Range*: The supply voltage range that can be applied to an amplifier for which it operates within specifications. Many applications implement op amp circuits with balanced dual supplies, while other applications for energy conservation or other reasons, use single-supply.

- *Supply Current:* The current required from the supply voltage to operate the amplifier with no load.

2.3.6 System Controlling

In order to automate break tests a system block that should be able to interface both sensor signals and user commands to the system is needed. Summarizing, this block should be responsible to handle the interface between the electric signals and higher level user instructions.

At the design of this block of the solution a important thing should be considered, data acquisition. According to ([NATIONAL INSTRUMENTS, 2018](#)) DAQ (Data Acquisition) can be defined as the process of measuring an electric or physical phenomenon, such as voltage, current, temperature, pressure or sound.

As mentioned in Section 1.1: "*The system should be able to perform brake tests by controlling the mechanical parts while acquiring relevant data with the aid of sensors and transducers*". There is a type of device that is able to perform data acquisition and system control, the microcontroller.

2.3.6.1 Microcontroller basic characteristics

A microcontroller is a compact computer on a single integrated circuit chip, in most cases a microcontroller (also referred by the acronym MCU) includes a processor, volatile and non-volatile memory, input/output ports and other peripherals. The great thing about the microcontrollers is their low cost, many small appliances that do not require a powerful hardware are only economically viable because of those devices. The components a microcontroller has may vary, it is a responsibility of the project designer to decide the microcontroller that has the best fit (technically and economically) for the project.

Microcontrollers differ from microprocessors only in one thing, MCUs can be used standalone while microprocessors need other peripherals to be used. By reducing the size and cost compared to a design that uses a separate microprocessor, memory, and input/output devices, microcontrollers make it economical to digitally control even more devices and processes. "A microprocessor can be considered the heart of a computer system, whereas a microcontroller can be considered the heart of an embedded system"([ROUSE, 2012](#)).

A great thing about microcontrollers is that they can provide real-time response to events, so for instrumentation they are crucial. With them it is possible to acquire signals with good sampling rates without loss of relevant information ([BARTZ; ZHAKSILIKOV; OGAMI, 2004](#)).

2.3.6.2 Microcontroller Architecture and Most Important Parts

In order to understand how a typical MCU parts are, Figure 12 show the block diagram of the ATmega32U4, a MCU manufactured by Microchip.

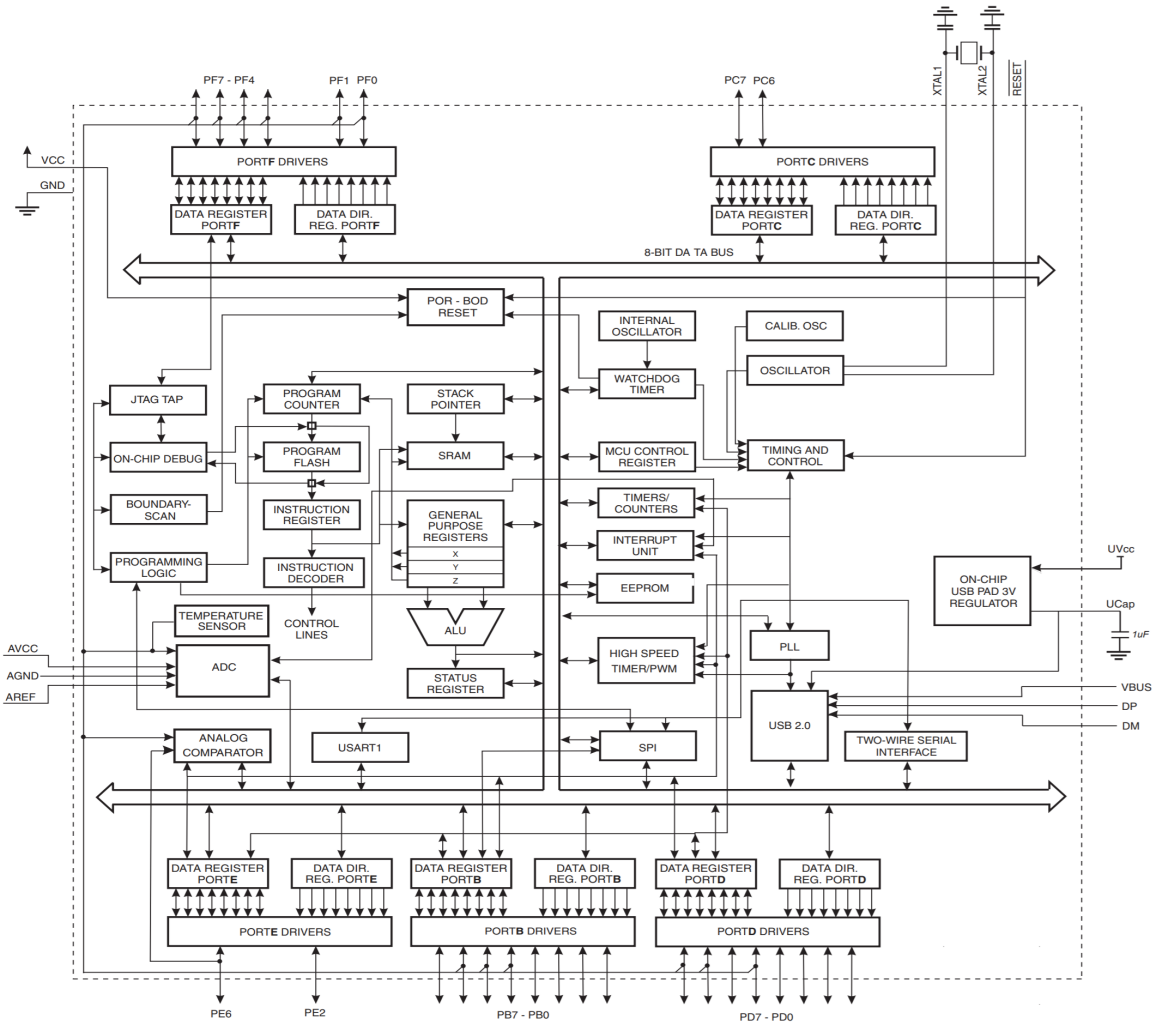


Figure 12 – ATmega16/32U4 Block Diagram ([ATMEL, 2018](#))

The most important blocks of this device are:

- *Timing and Control:* This circuit block represents the part of MCU responsible for maintaining the clock signals and handle time events.
- *Program Flash:* This is a non-volatile memory used to store the code, MCUs can execute code directly from the flash memory.
- *Port Drivers:* These are the device *I/Os (inputs/outputs)*, they can be digital or analog ports (except for outputs which can only be digital).

- *ADC (Analogic to Digital Converter)*: MCUs are by nature digital devices, when acquiring a analog signal, they first make a conversion to a digital value and then copy this data to a register.
- *USB 2.0*: Although not being a common feature, some MCUs include a USB (Universal Serial Bus) port. When interfacing with other USB devices, already having this feature inside the MCU saves space and costs when integrating the MCU in a circuit board.
- *High Speed Timer/PWM*: As mentioned in Item 2.3.6.2, MCUs do not have analog outputs, the high speed is used to generate a special digital output signal which will be explained on Section 2.3.6.3.

2.3.6.3 Pulse Width Modulation

Pulse Width Modulation (PWM), is a way of modulation for encoding information on a digital pulse train signal. There are many ways of encoding and extracting this message in and out of the PWM signal and this type of modulation can be used for a wide variety of applications such as controlling the charge delivered to a load and transmitting information (STANDARD, 1996). PWM signals have a fixed high and a fixed low voltage level, there are two parameters that can be varied on a PWM signal: oscillation frequency and duty cycle. Figure 13 shows how the duty cycle affects a PWM signal.

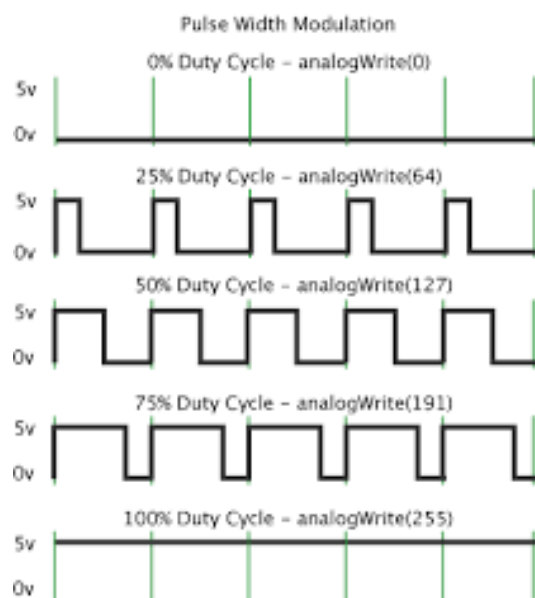


Figure 13 – Duty Cycle Examples (RZTRONICS, 2016)

Duty cycle can be defined mathematically by the Equation 2.3 (JAMES, 2001), where $D\%$ is the duty cycle in percentage, PW is the pulse width (pulse active time) and

T is the wave period.

$$D(\%) = \frac{PW}{T} \quad (2.3)$$

One useful way of using a PWM duty cycle variation is by encoding a analog voltage level proportional into it's percentage (HOLMES; LIPO, 2003), meaning that 100% duty cycle would represent maximum voltage amplitude and 0% the minimum voltage. This means it is possible to extract a analog voltage level by taking a PWM average level (ALTER, 2008), this is a practical way for designing digital to analog converters.

2.3.7 Circuit Protection

A important feature of any electronic product/appliance is the immunity against undesired inputs. In DAQ systems this is a relevant issue, the inputs of this systems must be protected from possible damage that may be caused by unintentional/accidental high voltage inputs, surges, etc (MATHIVANAN, 2007).

According to (LITTLELFUSE, 2015b), Voltage Transients are defined as short duration surges of electrical energy and are the result of the sudden release of energy previously stored or induced by other means. There are many things that can cause voltage transients (commonly referred just by transients) and those can be divided in two groups:

- Repeatable Transients: Usually caused by the operation of inductive loads such as motors, generators and switching circuits.
- Random Transients: Uncorrelated transients generated by exclusive events such as lightning, ESD and unpredictable events.

In order to enhance energy efficiency, devices are now operating at lower voltages (SOUZA et al., 2017). With the miniaturization of electronic components, those have become even more sensitive to electrical stress (LITTLELFUSE, 2015b).

In automotive environment, many of the supporting electrical components of the vehicle can generate transients, specially from inductive load switching. When the inductive load is switched off, the collapsing magnetic field is converted into electrical energy that turns into a transient (LITTLELFUSE, 2015b).

2.3.7.1 Low Pass Filters

According to (LITTLELFUSE, 2015b), a ESD pulse (fastest common transient pulse) has a overall duration period of less than 100ns (50% of the peak value) and a rising time that lasts less than 1.2μs. Figure 14 shows an example of a ESD Test Waveform.

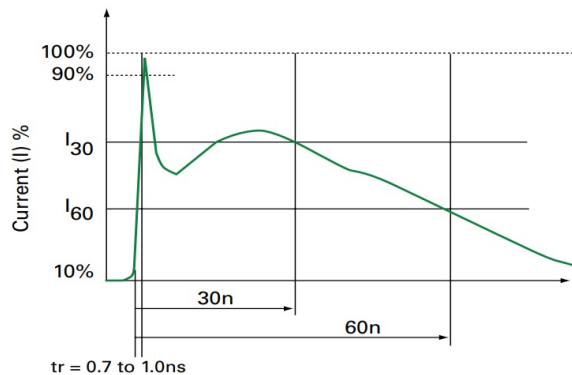


Figure 14 – ESD Test Waveform ([LITTLELFUSE, 2015a](#))

Considering that a signal has a frequency that is lower than the frequency of the transient it is vulnerable to, using a low pass filter to provide suitable attenuation for that transient and still letting the signal frequency on the passband, it is possible to protect that part of the circuit against this particular transient ([STANDLER, 1988](#)).

2.3.7.2 Transient Voltage Supression Diodes (TVS)

2.3.7.2.1 TVS diodes principle of operation

Transient Voltage Supression Diodes or TVS Diodes are nowadays the most popular choice for protection components in circuit due to their fast response, low clamping voltage and longevity. Under normal operation TVS diodes are high-impedance devices, interacting as a open circuit to the protected component, during a transient event the TVS diode junction provides a low-impedance path for the transient current ([RENESAS, 2016a](#)).

There are both uni-directional and bi-directional, the first has a operation curve similar as the one from a Zener diode, during positive transients the device limits the input voltage to it's clamping voltage and during negative transients the spike is clamped to the diode drop. On the other hand, bi-directional TVS diodes are always reverse biased during both negative and positive transients. Figures [15](#) and [16](#) show respectively the action of a uni-directional TVS and a bi-directional TVS during transient events.

The *Voltage X Current* curve of both uni-directional and bi-directional TVS diodes can be seen repectively on Figures [17](#) and [18](#).

2.3.7.2.2 Selecting TVS Diodes

According to ([WALTERS, 2016](#)), the following parameters of TVS devices are important to consider in order to choose one for protecting a particular circuit net:

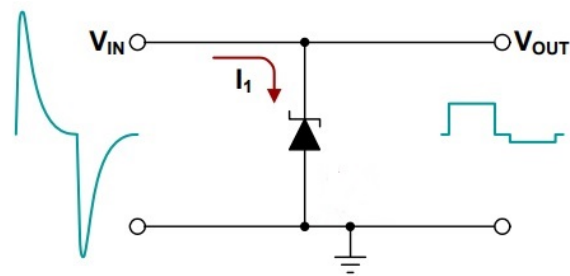


Figure 15 – Campling action of a uni-directional TVS (RENESAS, 2016c)

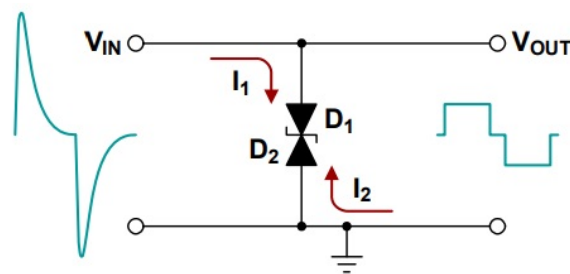
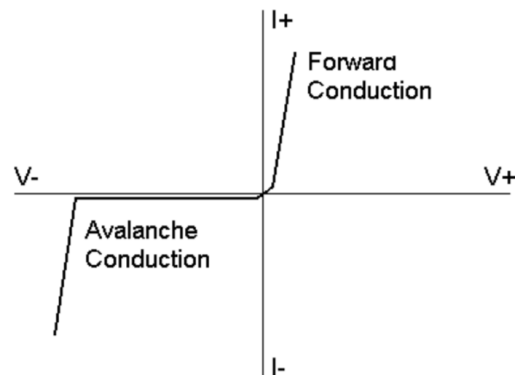
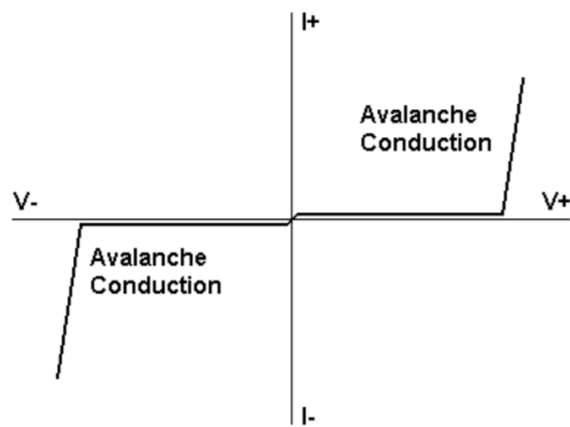


Figure 16 – Campling action of a bi-directional TVS (RENESAS, 2016b)

Figure 17 – $V \times I$ characteristic of a uni-directional TVS (RENESAS, 2016e)Figure 18 – $V \times I$ characteristic of a uni-directional TVS (RENESAS, 2016d)

- V_C (Clamping Voltage): the voltage limit that the TVS will allow on the point of intended protection. This voltage should be slightly lower than the point of intended protection absolute maximum voltage rating.
- V_{WM} (Rated Standoff Voltage): this is the maximum voltage in which the TVS still works as a high-impedance device. Therefore, the first step when selecting a TVS device is to know the peak voltage at the point of intended protection during normal operation and then select a TVS device with an appropriate V_{WM} .
- P_{PP} (Peak Pulse Power): in order to ensure the durability of the TVS device, the maximum power it needs to dissipate should be known. This P_{PP} is calculated by multiplying the TVS device V_C (Clamping Voltage) and the I_{PP} (Peak Impulse Current, peak current for the transient event).

3 Methodology

In order to achieve the goals of this project the endeavours were divided into three

3.1 Literature Review

This stage can be considered the most important of the whole project because it layers the foundations for development of all that follows. This stage comprehended the knowledge needed in all further stages and steps of the project, even on the further stages of development it was necessary to review some of the information acquired on this part in order to achieve best results. On the Literature Review stage, concepts, components and other necessary information to make the foundations for the project were addressed. For instance it will be on this stage that the brake tests parameters and requirements will be analysed in order to choose the proper solutions for this project.

3.2 Problem Description

This particular stage consisted on the depuration of the problem in question, leading to a study of the requirements that were necessary to ensure in order to develop and execute the project.

3.3 Project Conception

After a deep problem analysis it was possible to address a more detailed solution description, in this stage the general solution was splitted in many smaller ones that were defined according to the requirements of the previous stage. All this solutions were focused in functionality, this is a project of electronic instrumentation, so the goal was not to develop electrical/electronic solutions from the beginning, it was evaluating the requirements and finding a group of components/solutions that combined in a particular and unique way could lead to this project achieving its goals.

3.4 Case Study

After the particular and smaller solutions are developed, tested and considered functional, the general solution of this project will be tested as a whole thing. This being doing a brake test that is capable of proving the functionality and usability of the developed technology.

4 Acquisition and Control System

4.1 Monitored Parameters

As mentioned before this paper will be based in the *SAE J2522* regulations, this regulation says that to evaluate the efficiency of a brake system it is mandatory to monitor temperature on the brake pads, the pressure applied on the disk and the speed of the rotor throughout all the process. Monitoring the vibration is not mandatory but has some advantages.

- *Temperature of brake pads:* During all test it is mandatory to have full knowledge of the temperature of the break pads, firstly because of security reasons (there is upper limit for temperature in any system) and also because of the wear of parts that is related to temperature.
- *Pressure applied on the disks:* Knowing the magnitude of this force means being able to relate the pressure applied and the deceleration, knowing how the pressure applied increases the temperature of the pads and evaluate how this promotes wear of the parts.
- *Rotation speed:* Without knowing how the speed of the rotor varies over time it would be impossible to determine the acceleration and deceleration rates among many other issues.
- *Vibration:* As mentioned before this is not mandatory but rather interesting, measuring vibration makes it possible to determine how the extensive use can wear out the parts and reduce stiffness among other properties. Also it is natural that the system will vibrate during braking, minimal vibration or too much vibration can indicate a fault that in the future could damage the system.

4.2 Functional Requirements of the Testbench

According to the specification of the *SAE J2522* and according to parameters considered to be important, some requirements for the testbench were defined.

1. Measure a braking pressure up to 250kgf.
2. Measure temperatures up to 600 °C
3. Measure temperatures with a minimal resolution of 7.5 °C.

4. Accelerate the rotor to a speed up to 600 RPMs.
5. System must have a sampling period of 50ms.
6. The system hardware must be able to operate under temperatures up to 40°C.
7. System must have two acquisition channels for temperature.
8. System must have a channel for braking force acquisition.
9. System must have two digital outputs to control relays.
10. System must have a channel for acquiring frequency.
11. The system must work with real time acquisition.

Also some other optional requirements were created for making the system more versatile for future tests, those being:

- Having a additional braking force acquisition channel.
- Having a additional input digital channel.
- Having three digital input channels.
- Having two analog outputs.
- Having a vibration acquisition channel
- Having a built-in USB to UART transceiver to make the system more practical to use.
- System being easily reprogrammable.

4.3 Problem Analysis

The project solution can be divided in the structure showed in Figure 19.

4.3.1 Brake System Simulator

The *Brake System Simulator* block as the name says comprehends the hardware responsible for simulating the environment of a brake system, the two basic components are the **Brake** component itself (in this case being a disc brake system and peripherals) and a **Electric Motor** to accelerate the rotor in order to simulate the speed a vehicle wheel might be submitted. A **Transducers/Sensors** block was also added, without acquiring a physical/mechanical quantities such as temperature and pressure, a brake test

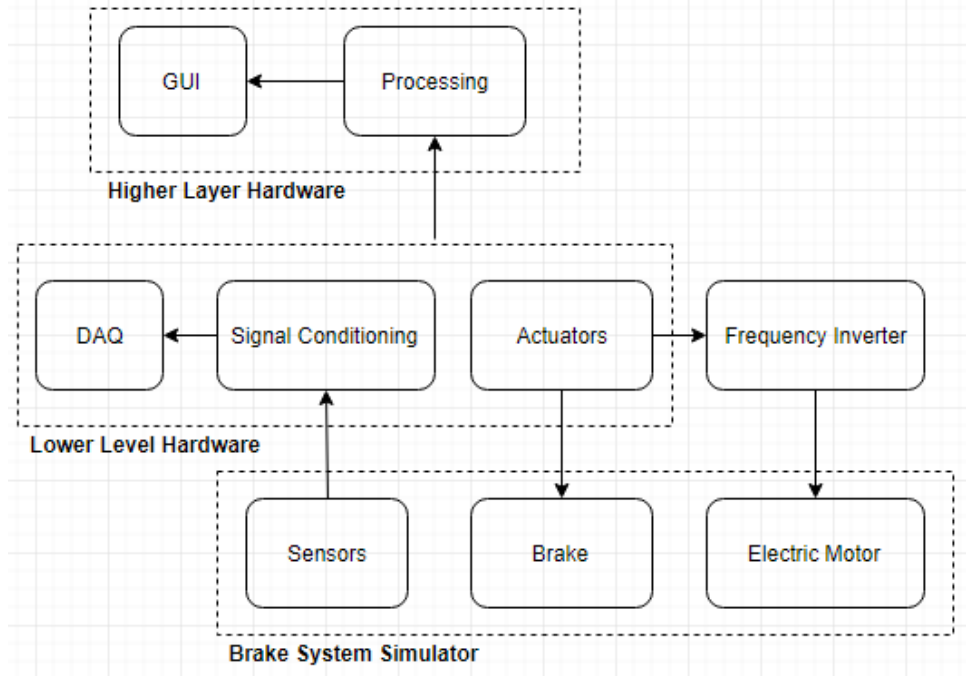


Figure 19 – Project Problem Depuration

would be useless because no possible technical analysis could be done afterwards. The **Transducers/Sensors** block was placed inside the *Brake System Simulator* block because the sensors and transducers will be placed arround the components of this major block.

4.3.2 Higher Layer Hardware

This layer needs to do all the heavy data processing, *i.e.*, converting and dealing with the information that flows through all the structure. The *GUI* block is the one responsible for acquiring and displaying computer information in a human-friendly format. Although developing this part of the solution is not part of this thesys it is important to understand its importance.

4.3.3 Lower Layer Hardware

This layer of hardware will make the translation from physical/mechanical quantities to computer data and *vice versa*, *i.e.*, converting physical/mechanical quantities to voltage and than to bytes of information and also on the opposite way (bytes to voltage and voltage to physical/mechanical quantities). Tranducers signals are not always ready to read, as mentioned in Section 2.3.5, Instrumentation Engineering also involves doing Signal Conditioning to amplify and filter this signals. Controlling the system also involves designing circuits to generate the desired digital and analog output channels.

Based on the matters analysed on the previous sections of this paper a hardware architecture was defined and it displayed on the following Figure 20.

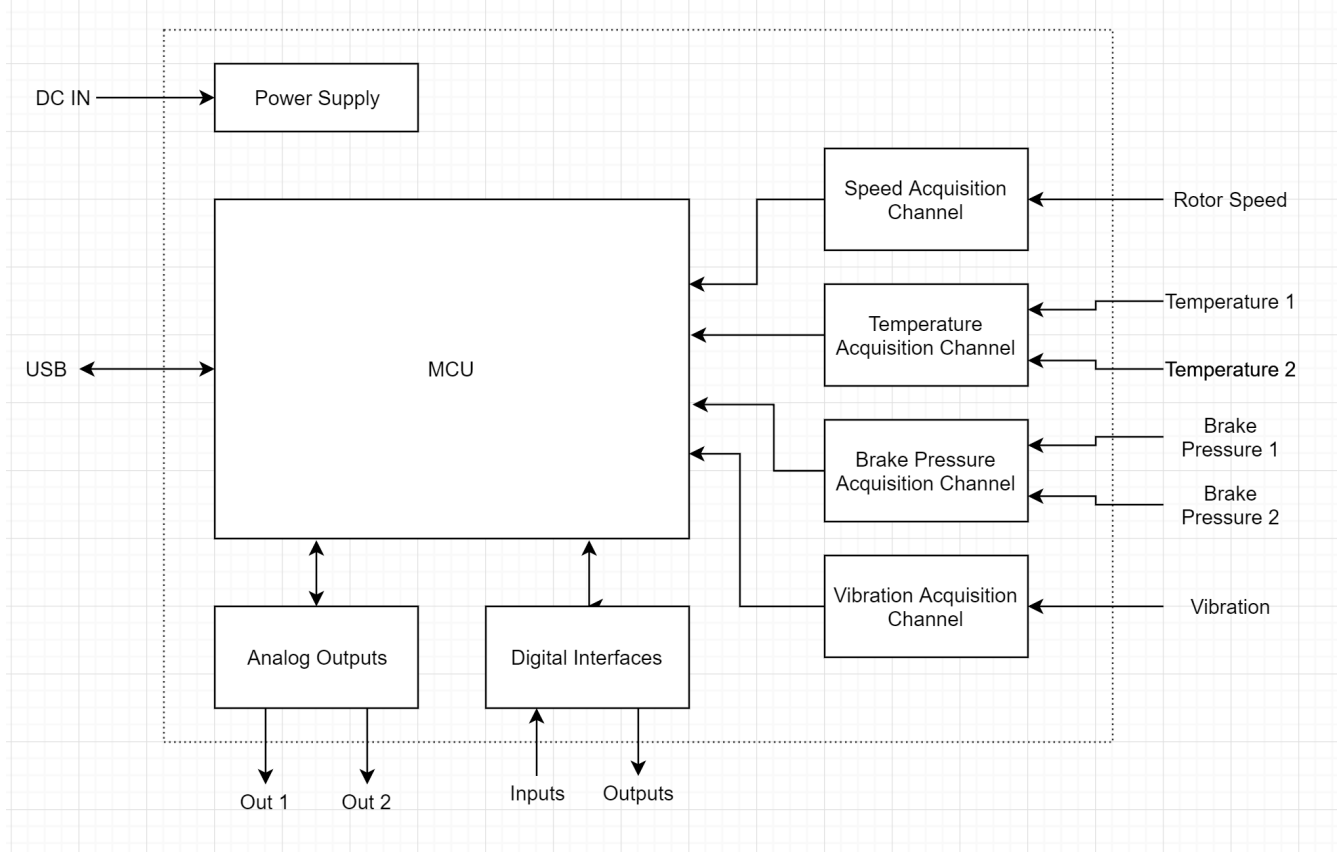


Figure 20 – Hardware Project Architecture

It is possible to see that each type of transducer will have a specific circuit in order to perform signal conditioning as better as possible according to the type of transducer parameters. Also it is possible to observe that there will be special circuits to interface the MCU with digital outputs and inputs alongside with analog outputs. Regarding the analog outputs, it is also interesting to have a feedback path to the MCU so adjustments can be made in order to guarantee that the analog outputs voltages are correct according to the desired quantities. Moreover, a power supply block should be designed to generate a stabilized voltage to power up all the circuit modules. Last but not least, a communication port (USB) was placed, through this port the communication with the upper layer of hardware will be done.

4.3.3.1 Lower Level Hardware Interfaces

Based on the previous considerations and considering possible future usages for the designed product, this are the following hardware interfaces.

- *Sensor Inputs:*

- Speed Sensor.
- Temperature Sensor 1.
- Temperature Sensor 2.
- Brake Force Sensor 1.
- Brake Force Sensor 2.
- Vibration Sensor 1.

- *Digital Interfaces:*

- Output 1.
- Output 2.
- Output 3.
- Input 1.
- Input 2.
- Input 3.

- *Analog Outputs:*

- Output 1.
- Output 2.

- *Communication Ports:*

- USB Port 1.

The schematic will all the circuits implemented on this project is located at Appendix [A](#).

4.4 Speed Acquisition Channel

4.4.1 CKP Signal Conditioning

As mentioned in Section [2.3.1](#), a CKP sensor has a analog signal with variable amplitude. For this project the only important parameter to extract from the sensor output signal in order to obtain the wheel speed is its frequency (angular velocity). The most practical way to obtain this data is to use a tachometer interface circuit, for this project the LM2907 from *Texas Instruments* ([TEXAS INSTRUMENTS, 2000](#)) will be used. LM2907 is a *frequency-to-voltage* converter with a ground-referenced tachometer input with $\pm 28V$ maximum voltage, making it versatile for many different sensor models.

4.4.1.1 LM2907 Basic Tachometer Circuit

The conditioning circuit for this project was based on the *Minimum Component Tachometer Diagram* from Figure 21 and *Tachometer with Adjustable Zero Speed Voltage Output* from Figure 22 suggested by LM2907 datasheet ([TEXAS INSTRUMENTS](#), 2000).

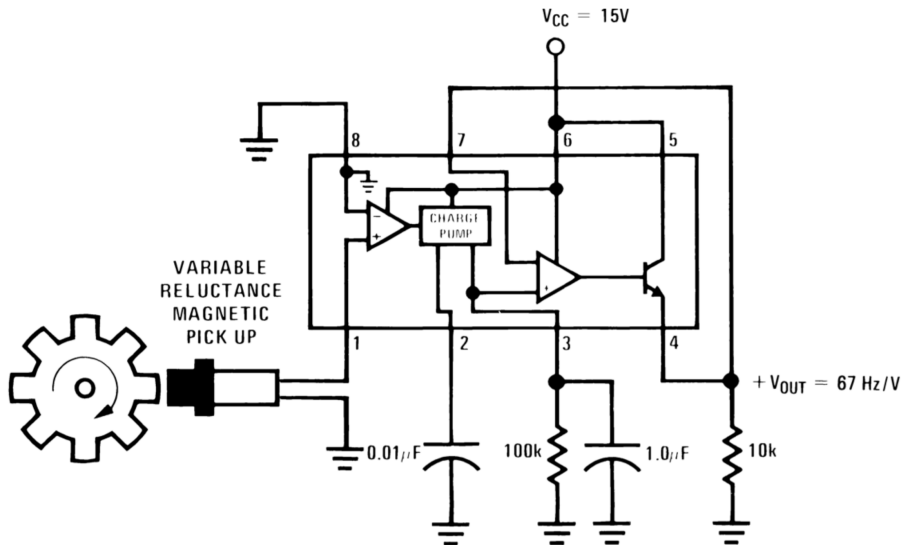


Figure 21 – Minimum Component Tachometer Diagram ([TEXAS INSTRUMENTS](#), 2000)

According to the datasheet ([\(TEXAS INSTRUMENTS, 2000\)](#)), in order to configure the gain of the frequency-to-voltage converter, C1, R1 and C2 must be configured in respect to the following design requirements.

- **C1:** This capacitor is charged and discharged every cycle by a $180\mu\text{A}$ typical current source. C1 must not be sized lower than 500-pF due to its role in internal compensation.
- **R1:** Higher of R1 values increase the output voltage for a given frequency, but too large will degrade the output's linearity. Because the current pulses are a fixed magnitude of $180 \mu\text{A}$ typical, R1 must be big enough to produce the maximum desired output voltage at maximum input frequency. At maximum input frequency the pulse train duty cycle is 100%, therefore the average current is $180 \mu\text{A}$ and $R_1 = V_o(\text{max}) / 180 \mu\text{A}$.
- **C2:** This capacitor filters the ripple produced by the current pulses sourced by the charge pump. Large values reduce the output voltage ripple but increase the output's response time to changes in input frequency.

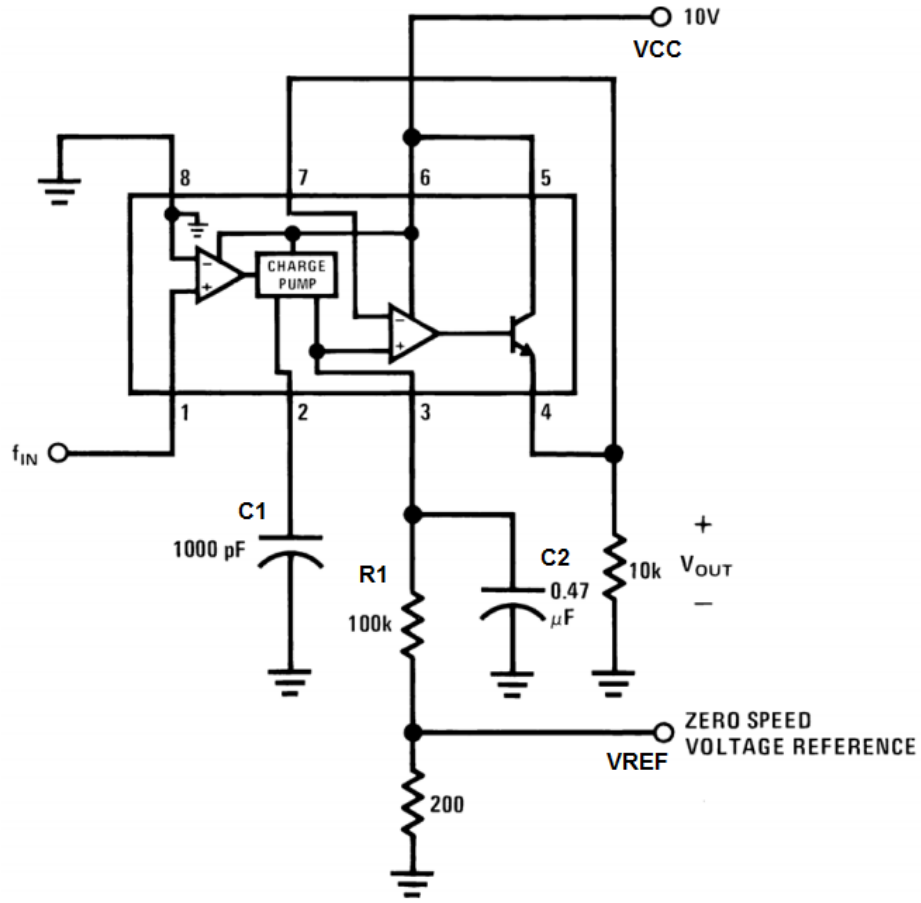


Figure 22 – Tachometer with Adjustable Zero Speed Voltage Output, adapted from ([TE-XAS INSTRUMETS, 2018](#))

The output voltage (V_O) can be calculated using Equation 4.1, V_{CC} is the supply voltage and f_{IN} the input frequency.

$$V_O = V_{REF} + (V_{CC} \cdot f_{IN} \cdot C1 \cdot R1) \quad (4.1)$$

As said in Item 4.4.1.1, C2 controls the voltage ripple on the output(V_{RIPPLE}), this ripple is given by Equation 4.2. According to the datasheet, I_2 has a typical value of 180uA.

$$V_{RIPPLE} = \frac{V_{CC}}{2} \cdot \frac{C1}{C2} \cdot \left(1 - \frac{V_{CC} \cdot f_{IN} \cdot C1}{I_2} \right) \quad (4.2)$$

Finally, the last thing to consider is the maximum attainable input frequency, determined by V_{CC} , C1 and I_2 (180uA) in Equation 4.3.

$$f_{MAX} = \frac{I_2}{C1 \cdot V_{CC}} \quad (4.3)$$

4.4.1.2 LM2907 Designed Circuit

The first parameter to be calculated is the maximum frequency, functional requirement from Item 4 in Section 4.2 says the the system should be able to reach 200kph. Hence, to know the relation between frequency and speed on a wheel it's important to know the wheel's diameter.

According to (TODAS..., 2018), the smallest commercial tyre size in terms of diameter in Brazil is the standard 165/70R13 which has a diameter (D) of 561.2mm and the one with the biggest diameter (D) is the standard 265/50R20 having 773mm. Using Equation 4.4 to calculate the overall length of the wheel gives a approximately length of 1.762m for the smaller tyre and a approximately length of 2.428m for the bigger one.

$$C = \pi \cdot D \quad (4.4)$$

Considering this upper limit speed of 180kph, calculated values of tyre circumference length, we have maximum frequencies of approximately 28.36Hz (for the smaller tyre standard) and 20.59Hz (for the bigger tyre standard).

According to (TEXAS INSTRUMENTS, 2000) the input common mode voltage is equal to $V_{CC} - 1.5V$, and as V_{CC} is equal to 5V (check Section 4.11.1.1) the maximum output voltage V_O is equal to 3.5V. Considering a safer upper frequency limit of 150Hz (approximately six times the maximum calculated frequency of 31.52Hz, this multiplication factor will be explained better in Section 6.1) applied to Equation 4.1 with the $V_{CC} = 5V$, the desired offset voltage V_{REF} (1.225V, check Section 4.4.2) and the maximum output voltage $V_O = 3.5$ gives a time constant ($R1*C1$) of 0.003. Using the recommended capacitor values from 21 and commercial resistor values it is possible to achieve this time constant using $R1=300k\Omega$, with this values V_O can be described by Equation 4.5.

$$V_O = 1.225V + 0.015 \cdot f_{IN} V Hz \quad (4.5)$$

For instance applying the upper frequency value of 28.36Hz calculated previously will give a $V_O = 1.6504V$.

Figure 23 shows the designed circuit for the speed acquisition channel.

In addition to the components from the circuit *Tachometer with Adjustable Zero Speed Voltage Output* on Figure 22, the following features have been added:

- **TVS Diode:** In order to protect the the IC's input the SMBJ15CA TVS diode from Littelfuse was added. This diode has a maximum clamping voltage of 26V, the maximum input voltage is $\pm 28V$, thus the TVS will help protecting the input from overvoltages.

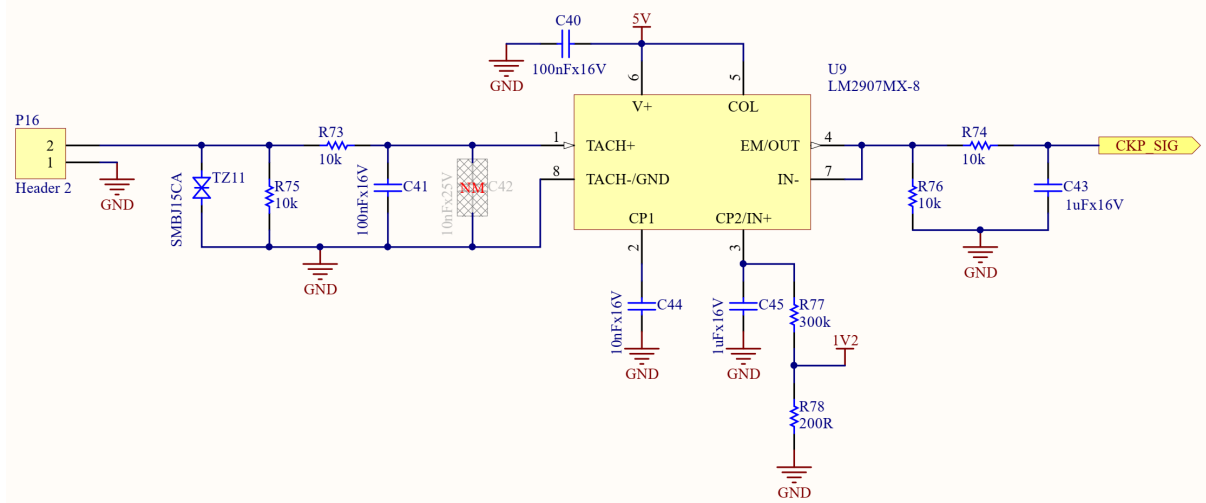


Figure 23 – Speed Acquisition Channel Circuit

- **LPF at the input:** As the maximum frequency was determined to be 31.52Hz, it is possible to filter all the upper frequencies in order to avoid any noise to enter the circuit. R73, C41 and C42 form a LPF with a cutoff frequency of approximately 160Hz.
- **LPF at the output:** R74 and C43 form a LPF to that is used to filter any external post-conversion noise, it has a approximate frequency of 16Hz.
- **R78:** This resistor is recommended by ([TEXAS INSTRUMENTS, 2000](#)) in order to use the voltage reference functionality.

4.4.2 1V2 Reference

The 1V2 reference from the circuit of Section 4.4.1 is achieved using the LM4040CYM3-1.2 from *Microchip* ([MICROCHIP, 2017b](#)). This is a 1.225V precision voltage reference with a tolerance of $\pm 1.15\%$ and maximum operating output current of 10mA. The only external component needed is a bias resistor which can be calculated using 4.6 ([MICROCHIP, 2017b](#)).

$$R_{BIAS} = \frac{V_S - V_{OUT}}{I_L - I_Q} \quad (4.6)$$

The used V_S *Voltage Supply* will be the 5V obtained in the circuit from Figure 46 in Section 4.11.1.1. According to the datasheet, the minimul operating voltage (I_Q in this case) is 100uA. Moreover, V_{OUT} is naturally 1.225V. The minimum bias current (load current I_L) is of 500nA (according to the ([TEXAS INSTRUMENTS, 2000](#))). Hence, any value of resistance that guarantee that the current that flows through the regulator is less than 10mA is acceptable.

Using a $1\text{k}\Omega$ resistor a current of 4mA can be achieved. Figure 24 shows the circuit for the $1\text{V}2$ reference, the capacitors are just a bypass capacitors recommended by the datasheet.

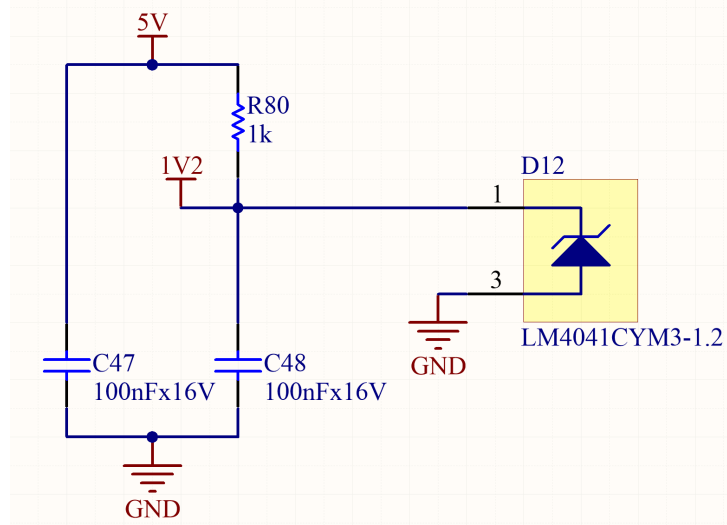


Figure 24 – $1\text{V}2$ voltage reference circuit

4.5 Temperature Acquisition Channel

Figure 25 shows the solution overview for the thermocouple circuit.

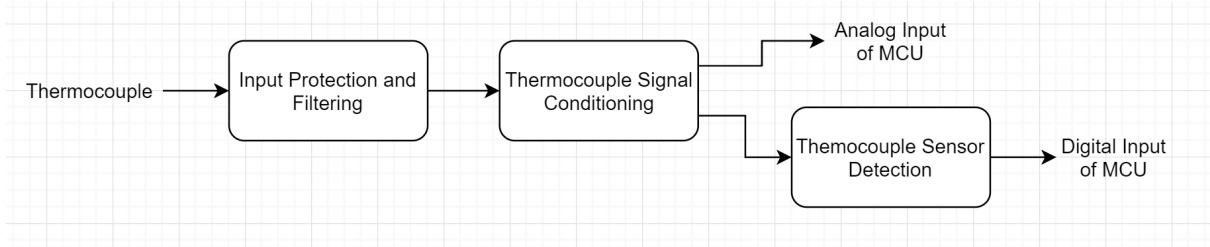


Figure 25 – Temperature Measurement Block Diagram

The function of each block will be explained in the following sections.

4.5.1 Thermocouple Signal Conditioning

For this project it was defined that thermocouples of type K (formed by the junction of two metal leagues: Alumel and Cromel) would be used in this project. This is because this specific type of thermocouple has a wide range of operation ($-200^\circ\text{C} - 1200^\circ\text{C}$), so according to the requirements they are never too close from the boundary values, a thermocouple of type T or even a type J would not be suitable. Other appealing factor is that this type of thermocouple is quite common so getting eventual replacements would be easier, in comparison with type E thermocouples.

As mentioned in sub-section 2.3.2, besides amplification and linearization, the thermocouple signal also needs cold junction temperature difference compensation. There is an integrated solution from *Analog Device* called AD8495, this IC functional diagram is displayed on Figure 26.

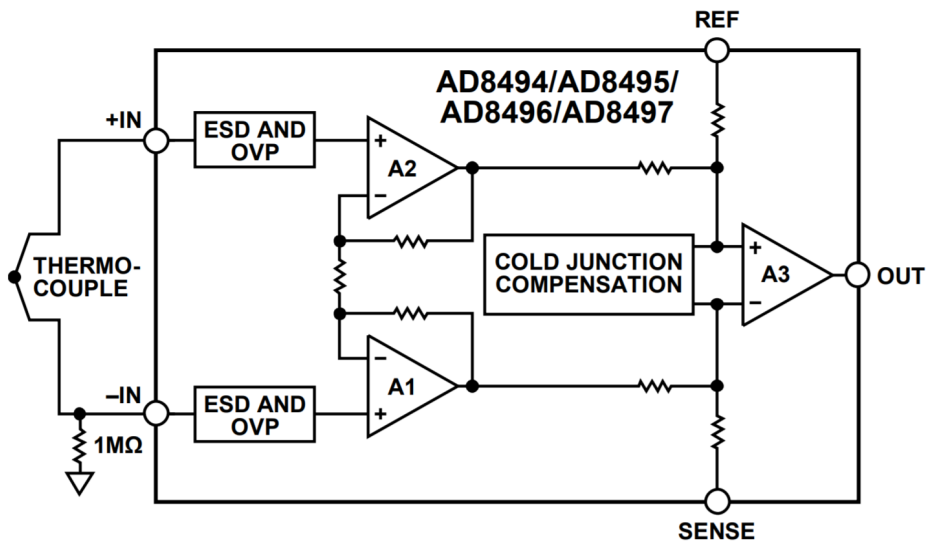


Figure 26 – AD8495 Functional Block Diagram ([DEVICES, 2011](#))

This IC produces a linearized output with a fixed gain of $5\text{mV}/^\circ\text{C}$, it is a quite practical solution as it can be powered with single-supply voltage source and it's output saturates to the power supply voltage if the thermocouple is disconnected ([ANALOG DEVICES, 2010](#)).

4.5.2 Input Protection and Filtering

Although this IC already has overvoltage and ESD protection, thermocouples tips can pick a load of unwanted noise and transients. Hence, additional protection and external filtering is also recommended by ([DUFF; TOWEY, 2010](#)). First thing to do is to add current-limitt series resistors, the drawback is doing that is that resistors in the circuit net increases the overall noise. This type of noise is called Johnson-Nyquist Thermal Noise or more commonly just by Johnson Noise, thermal agitation of electrons in a resistor gives rise to random fluctuations in the voltage across its terminals ([ROMERO, 1998](#)). Moreover, it can be calculated using the following Equation 4.7 where K is the Boltzamann's constant $1.38 \cdot 10^{-23}$, R is the resistance in ohms (Ω) and T the temperature in kelvin (300K at room temperature) ([BRYANT et al., 2000](#)).

$$\text{Noise}(nV\sqrt{\text{Hz}}) = \sqrt{4 \cdot K \cdot R \cdot T \cdot 10^9} \quad (4.7)$$

Because the protection circuit includes two equal resistors, whose noise is uncorrelated, that is, the two noise sources are independent of each other—the above result must be multiplied by the square root of 2 (the root sum square of the two noise voltages) and it is considered as a general rule design to tolerate additional Johnson Noise from 10 to 30% to the amplifier IC (BRYANT et al., 2000). (DUFF; TOWEY, 2010) suggests using current-limiting resistors of 100Ω , according to the AD8495 datasheet (ANALOG DEVICES, 2010), the chosen amplifier (AD8495) has a voltage noise density of $32\text{nV}\sqrt{\text{Hz}}$. Combining this resistors noise with the amplifier noise will produce a overall noise of $32.485\text{nV}\sqrt{\text{Hz}}$, which is just 1.5% above the amplifier's own noise. Additional protection can be achieved using TVS to protect the inputs from differential input overvoltage, considering a bidirectional TVS with a 10V breakdown voltage, the device will theoretically limit the differential voltage between 10V and -10V, the AD8495 has overvoltage protection from -25V to 20V when powered with 5V, so this will help protecting the amplifier inputs.

With the overloads protection done, another important feature to do is to filter unwanted signals in the inputs to avoid them to be amplified later, this is done by filtering Radio Frequency Interference (RFI), signal lines (specially for low level signals) are quite susceptible to RF interference (COUNTS; KITCHEN, 2006). Interference that occurs on both lines are usually reduced by the amplifiers own CMRR (check Section 2.3.5.1), but only on a limited bandwidth, also the in-amp rectifier cannot filter differential RF interference. The chosen amplifier (AD8495) has a -3dB bandwidth at 25kHz, (DUFF; TOWEY, 2010) suggests setting a common-mode cutoff filter frequency at 160kHz (in order to guarantee the filter will not attenuate signals inside the 25kHz bandwidth). The standard circuit for the RFI filter is displayed on Figure 27, resistors R and capacitors C_C are used to filter common-mode interference. Capacitor C_D is connected across the bridge output to reduce any common-mode rejection errors due to the components mismatch, that way filtering any differential interference. C_D is usually chosen to be ten times larger than C_C (ANALOG DEVICES, 2010).

The -3dB common-mode bandwidth of this filter from Figure 27 is given by Equation 4.8 (COUNTS; KITCHEN, 2006).

$$BW_{CM} = \frac{1}{2 \cdot \pi \cdot R \cdot C_C} \quad (4.8)$$

The -3dB differential bandwidth of this filter from Figure 27 is given by Equation 4.9 (COUNTS; KITCHEN, 2006).

$$BW_{DIFF} = \frac{1}{2 \cdot \pi \cdot R \cdot (2 \cdot C_C + C_d)} \quad (4.9)$$

Using the values for the current limiting resistors (100Ω), Equation 4.8 and the

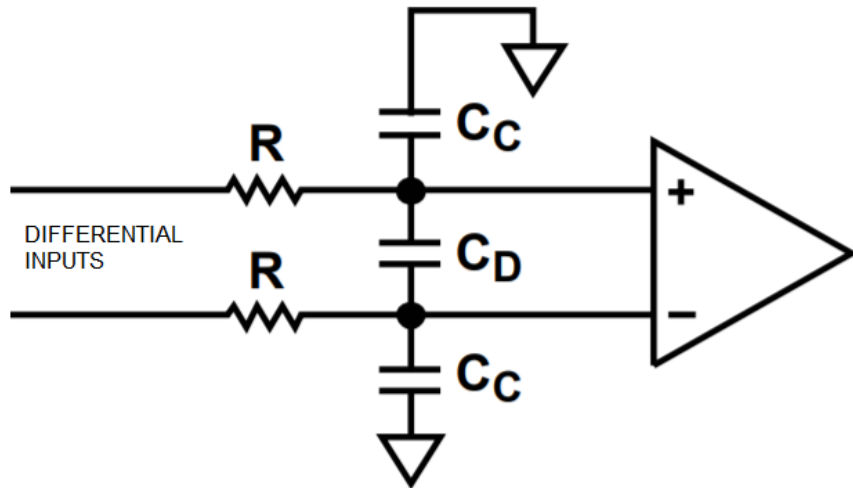


Figure 27 – RFI

suggested cutoff frequency of 160kHz (DUFF; TOWEY, 2010), it is possible to calculate a value of 10nF for C_C . Choosing a C_D value ten times larger than C_c implies on using a C_D value of 100nF, that used on Equation 4.9 will produce a differential interference filter cutoff frequency of 13kHz.

With all this considerations, the Thermocouple Signal Conditioning Circuit can be seen in Figure 28.

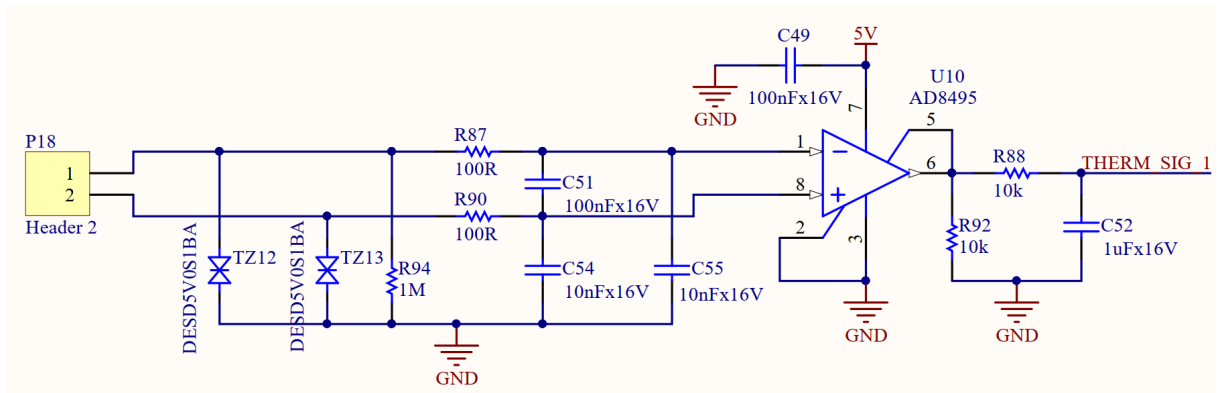


Figure 28 – Thermocouple Signal Conditioning Circuit

Besides the RFI filter and the amplifier, only a few components were added. First a TVS diode with a standoff voltage of 5V was placed on each of the thermocouple signal tracks. According to (ANALOG DEVICES, 2010), in order to implement sensor disconnection detection a 1M resistor should be added to the the thermocouple negative track. More over a post amplification LPF with a cutoff frequency of approximately 16Hz was placed in order to filter any remain of noise uncorrelated to the thermocouple signal.

4.5.3 Thermocouple Sensor Detection

A important feature of any acquisition system is to detect when a sensor is disconnected from the the acquisition system input ([O'MAHONY; GELFAND; MERRICK, 2011](#)), because a signal acquisition circuit without the signal source will generate outputs that are uncorrelated to what the system was designed to measure/sense on the outside world. The AD8495 has a quite useful feature ([ANALOG DEVICES, 2010](#)), it offers open thermocouple detection, the inputs of the AD8495 are PNP type transistors, which means that the bias current always flows out of the inputs. This way, the input bias current drives any unconnected output high, which saturates the output to the maximum possible reading, being in this case 1000°C or 5V (considering the fixed 5mv/°C gain). In Section [4.2](#), it was defined that the system must measure temperatures up to 600°C, with the fixed gain of 5mv° this means an output voltage of 3V. The so called *Thermocouple Sensor Detection* must be able to detect whenever the output exceeds 3V. In order to do that, the circuit displayed in Figure [29](#) was designed.

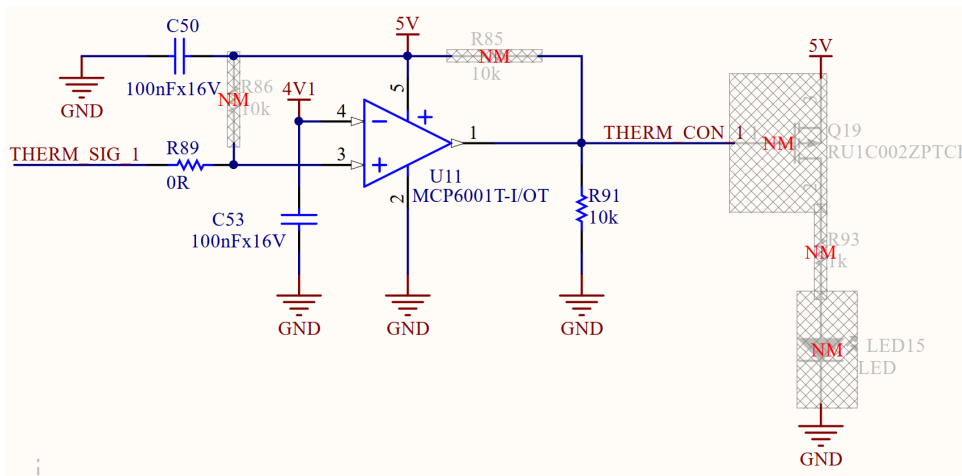


Figure 29 – Overvoltage Detection Circuit

U11 is a OPAMP working as a comparator, whenever the thermocouple signal is higher than the 4V1 the OPAMP output will saturate to the 5V (the supply voltage applied to the OPAMP). The net 4V1 will be further explained in Section [4.11.2.1](#), whereas it is a constant voltage produced on the Power Supplies circuit block. The resistor R_{91} is a pull-down resistor used to guarantee that signal will go to low-logic level in case the voltage in the inputs is not present. The capacitors C50 and C53 is just bypass capacitors used to stabile both the 4V1 and 5V supplies voltage.

4.6 Brake Pressure Acquisition Channel

4.6.1 Load Cell Signal

Load cells have very low output levels, usually from 2 to 3mV/V, and therefore an amplification is fundamental. It is not necessary to know the nature of the strain gauges when a load cell is being calibrated since generally the manufacturers provide a calibration curve based on the signals V_O and V_{EX} of the Figure 8, it is worth noting that these signals can not have the same reference, otherwise it will not be possible to excite the wheatstone bridge correctly.

The most common way to amplify the signal of a load cell is using a instrumentation amplifier. Although it is a widely used configuration, assembling this amplifier using three different operational amplifiers and seven resistors as in Figure 10 may make it inaccurate due to manufacturing imperfections of the components. Another factor that greatly influences the output signal of a load cell is the excitation voltage of its wheatstone bridge, if it varies too much the output will vary greatly as well, which will hamper its calibration.

4.6.2 Load Cell Signal Conditioning

In order to solve these two problems there is a solution widely used in the market which is the *INA125* from Texas Instruments ([INSTRUMENTS, 1997](#)), this IC is an integrated single supply instrumentation amplifier with precision voltage reference. Other good feature of this amplifier is that as it has a great CMRR (*Common-Mode Rejection Ratio* check Section 2.3.5.1) of 100dB, making it very much suitable for condionting differential pair signals (such as the one from the Load Cell as Subsection 2.3.3 mentions), more information of CMRR in Subsection 2.3.5.1. The only external component needed is a resistor R_G , as shown in Figure 30. This resistor will determine the gain (G) for the amplification according to the Equation 4.10.

$$R_G = \frac{60k\Omega}{G - 4} \quad (4.10)$$

Taking into account the sensitivity of 2mV/V, this means that if the cell is excited with 2V5, its output will vary from 0 to 5mV.

Since the analog input of the chosen microcontroller (*Atmega32U4*) is 0 to 5V, we may to amplify the cell output signal by a factor of 1000 in order to use the most number of bits from de MCU's ADC. Using Equation 4.10, to obtain a gain of amplification ratio of the ideal R_G would be 60Ω , a resistor of this value and minimal tolerance (1%) is not commercially available, the closest one is 60.4Ω . This resistor will generate a gain of

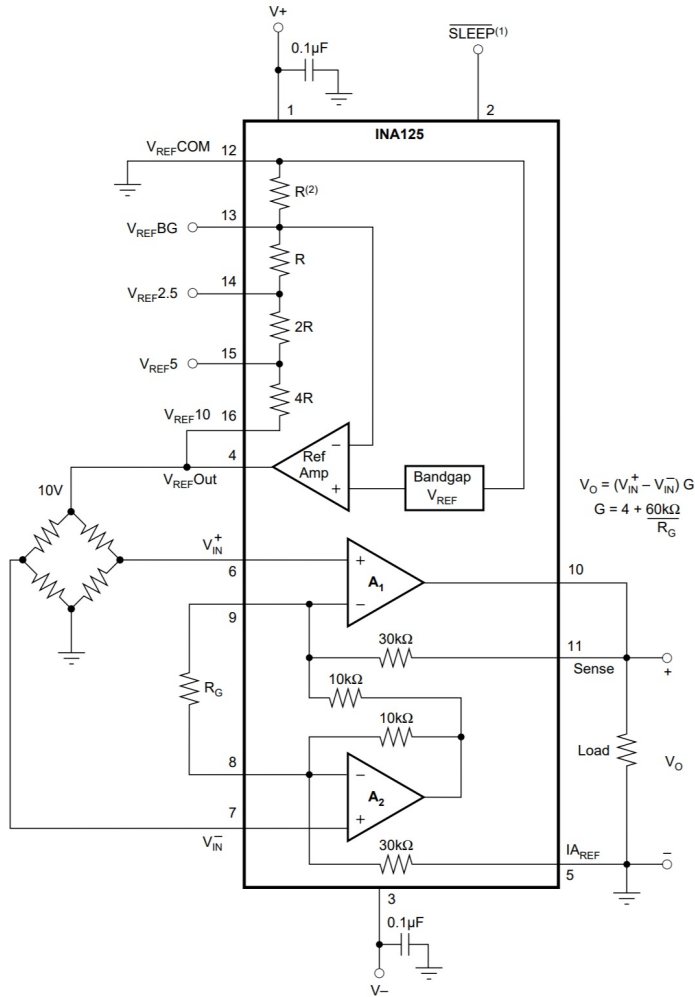


Figure 30 – INA125 Schematic (INSTRUMENTS, 1997)

approximately 997.378 and cause the IC output to range from about 0V to 4.986V, using 99.72% of the resolution of the microcontroller input.

Figure 31 shows the schematic of the load cell conditioning circuit with the INA125.

The main components of this circuit are

- *TVS Diodes:* INA125 only has overvoltage protection and not ESD protection, so the TVS Diodes were added to enhance the ESD protection.
- *Capacitors C18 and C19:* Bypass capacitors for the signal lines.
- *C15:* A capacitor to filter noise between both lines.
- *R39 and R43:* Jumpers that can be replaced by resistors in case a RFI filter is meant to be implemented using C24, C26 and C27.
- *R36:* The gain resistor.

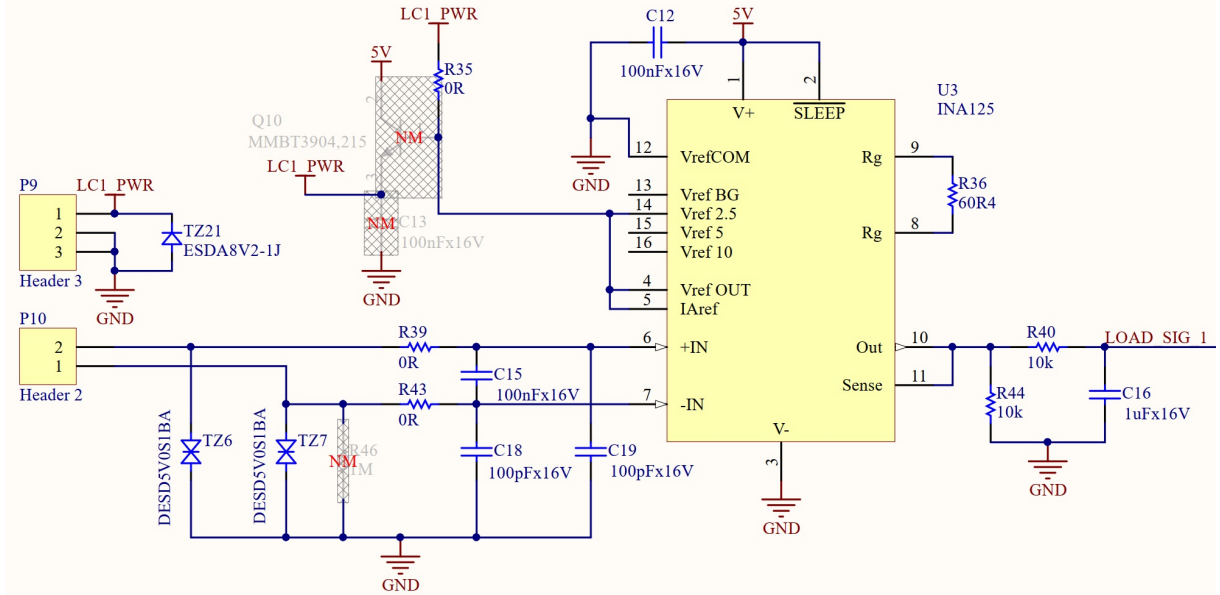


Figure 31 – Conditioning Circuit for the Load Cell

- R_{44} , R_{40} and C_{16} : R_{44} is used to set the impedance from the load cell signal. R_{40} and C_{16} are used to form a LPF with a cutoff frequency of 15.91Hz to filter any remaining noise from the load cell signal.

4.6.3 Load Cell Sensor Detection

As was explained in Subsection 4.6.2, the circuit will saturate the output to the supply voltage when the load cell sensor is disconnected. The circuit to detect this voltage saturation is exact the same from the one used previously on the thermocouple circuit, the circuit schematic and functional explanation can be found in Subsection 4.5.3.

4.7 Vibration Acquisition Channel

4.7.1 Accelerometer

The chosen accelerometer for this project was the *ADXL335* from *Analog Devices* (DEVICES, 2010). This accelerometer was chosen because it is the cheapest one available with the following characteristics:

- It has 3 axis sensing (easy to install).
- Low power operation ($350\mu\text{A}$).
- 10,000 g shock survival.
- 1V8-3V3 Single-supply operation.

- $\pm 3g$ measurements.

When powered up with 3V3 the sensor has a linear voltage output of 0V for -3g and 3V3 for 3g. This sensor is ideal for this project, the only issue is the installation. The sensor comes in a 16-LFCSP IC (Figure 32), and this IC needs to be installed where acceleration is intended to be measured, so a additional board is necessary to install it.

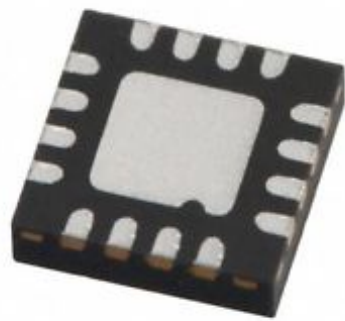


Figure 32 – 16-LFCSP ([DEVICES, 2016](#))

The are already embdded solutions that can solve this issue, such as the *Adafruit ADXL335 - 5V ready* ([ADAFRUIT, 2016](#)). This small (19mm x 19mm) board (Figure 33) has the ADXL335 with the capacitors recommended by the datasheet, with a 3V3 voltage regulator so the board can be powererd up with 5V and with the mounting holes to fix the board in any surface, making it ideal for this project.

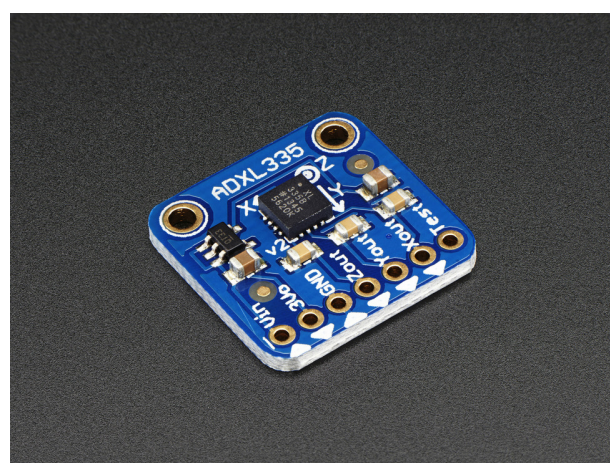


Figure 33 – Adafruit ADXL335 - 5V ready ([ADAFRUIT, 2018](#))

4.7.2 Signal Conditioning Circuit

The ADXL335 datasheet ([DEVICES, 2010](#)) says that for a -3g measured acceleration the device output is of 0V and for +3g measurement it is 3V3 voltage. The sensor conditioning circuit is displayed on Figure 34.

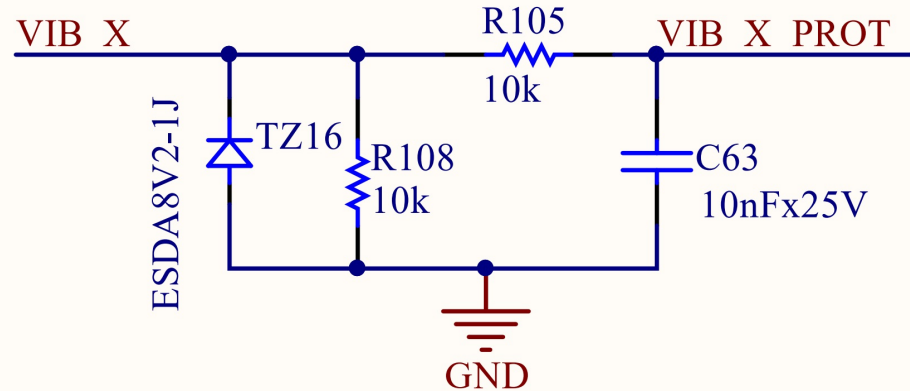


Figure 34 – Accelerometer Signal Conditioning Circuit

The circuit is composed only of a protection and filtering circuit. TZ16 is a TVS with a reverse standoff voltage of 5V, R105 and C63 form a LPF with cutoff frequency of approximately 1.6kHz, which should not interfere with the passband signal.

4.7.3 Sensor Detection Circuit

The chosen solution for the accelerometer (*Adafruit ADXL335 - 5V ready*), has a integrated 3V3 voltage regulator. In Figure 33 it is possible to see that the 3V3 voltage output from the voltage regulator has a connection point on the board. Hence, if a wire is connected to this point and to the main circuit board, whenever this point does not have 3V3 voltage the sensor is disconnected. Moreover, the detection circuit just need to detect when the net is in 0V or 3V3.

The detection circuit can be seen in Figure 35, D14 is a schottky diode used to protect the input from polarity change. TZ19 is a TVS used to protect the circuit from overvoltage, R111 and C66 forms a LPF with cutoff frequency close to 16Hz used to protect the NMOS gate from any fast transient.s

4.8 Speed Reference Output Channel

4.8.1 Speed Control

For the braketests, somethings as important as measuring the speed of the rotor is controlling it, as mentioned in Subsection 4.3.3. The rotor speed can be controlled in two ways:

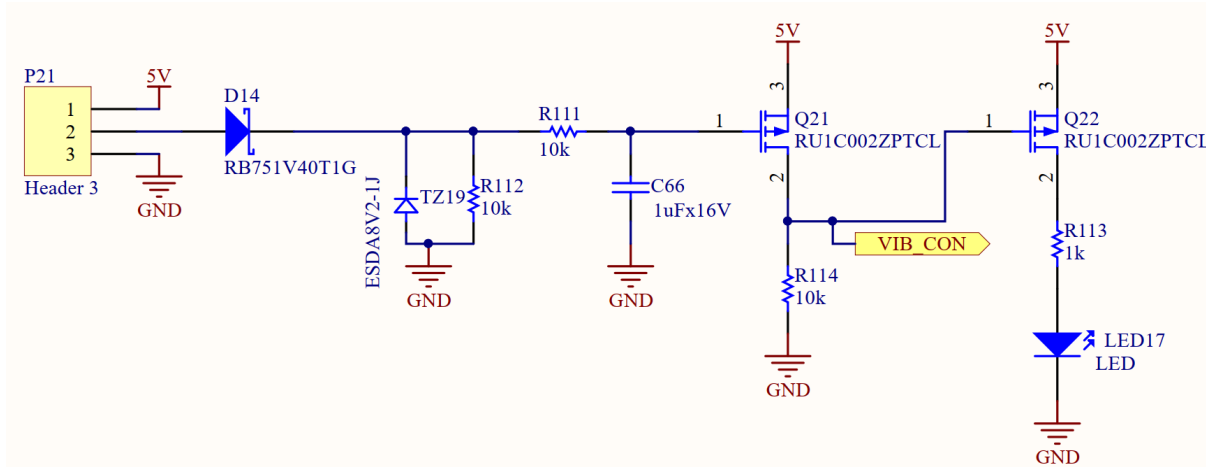


Figure 35 – Accelerometer Sensor Detection Circuit

- First way is the deceleration of the rotor with the aid of the brake system using the brake pads.
- Second way of controlling it by accelerating the rotor with the aid of the electric motor.

The electric motor used is a alternate current three-phase type, it in order to control it's speed a frequency inverter was used. The frequency inverter has many different controlling interfaces that lead to manipulating the three-phase electric system in order to control the engine's rotationary speed.

In this project the frequency inverter used was the *Weg CFW-08* (shown in Figure 36, according to ([WEG, 2009](#)) there are many port interfaces that can be used to control the desired speed remotely. One of this ways is using one of the device's 0-10V analog input with 8-bit resolution. According to the datasheet, this analog input can be used as a speed reference with programmable gain (0-20), the input parameters are the lower limit speed (when the input is on 0V) and the upper limit speed (when the input is at 10V).

The issue is that this project is microcontrolled, and MCU's do not have analog outputs, so a DAC circuit will need to be implemented. The MCU output will be a PWM signal, moreover as mentioned in Section 2.3.6.3, a PWM signal can encode information on a pulse train signal and this information can be decoded using a LPF, *i.e.* performing a digital to analog conversion.

4.8.2 Filter characteristics definition

Fortunately the microcontroller has pre-configured PWM (*Pulse Width Modulation*), a PWM signal can encode a analog voltage value proportional to it's duty cycle, and this is usually done with the aid of a low pass filter that will extract this analog



Figure 36 – Weg CFW-08 Frequency Inverter (WEG, 2017)

voltage from the PWM signal. As said in the previous paragraph the frequency inverter used in this project is the *Weg CFW-08*, and it's analog input has a zero to ten voltage input with eight bits of resolution. We can calculate the minimal voltage difference that will change the output frequency of the device using Equation 4.11, in which ΔV is the minimal voltage difference, V_{max} is the maximum voltage and "n" is the number of bits of the input resolution.

$$\Delta V = \frac{V_{max}}{2^n} \quad (4.11)$$

As mentioned in Section 4.10, the chosen MCU has a five volts high logic level, this voltage level will need amplification in order to best suit the zero to ten volts input from the frequency inverter. However, as already mentioned in Section 4.8.1 the analog input of the frequency inverter already has a 0-20 programmable gain that will be set to two.

The maximum ripple is the ΔV from Equation 4.11. Equation 4.12 (METIVIER, 2013) gives the necessary $\frac{dB}{decade}$ attenuation to guarantee a PWM converted signal desired ripple.

$$A_{dB} = 20 \cdot \log \left(\frac{V_{RIPPLE}}{V_{PWM}} \right) \quad (4.12)$$

As the V_{PWM} will already be amplified prior to filtering, $V_{PWM} = V_{max}$, this will produce the following Equation 4.13.

$$A_{dB} = -20 \cdot n \cdot \log (2) \quad (4.13)$$

And Equation 4.14 (METIVIER, 2013), is used to calculate the maximum needed cutoff frequency for the further to be designed LPF (*Low-Pass-Filter*) in order to convert the PWM signal to a analog voltage. The slope value is the filter slope and for first order filters and second order filters this slope value is equal respectively to 20dB/decade and 40dB/decade (METIVIER, 2013).

$$f_c = f_{PWM} \cdot 10^{-\frac{A_{dB}}{Slope}} \quad (4.14)$$

It is possible to combine all this equations into one single equation to calculate the needed cutoff frequency, is this done in Equation 4.15.

$$\begin{aligned} f_c &= f_{PWM} \cdot 10^{-\frac{A_{dB}}{Slope}} \\ f_c &= f_{PWM} \cdot 10^{-\frac{-20 \cdot n \cdot \log(2)}{Slope}} \\ f_c &= f_{PWM} \cdot 10^{\log\left(2^{\frac{20 \cdot n}{Slope}}\right)} \\ \text{Knowing :} \\ x \cdot \log(A) &= \log(A^x) \\ 10^{\log(A)} &= A \\ \text{So :} \\ f_c &= f_{PWM} \cdot 2^{\frac{20 \cdot n}{Slope}} \end{aligned} \quad (4.15)$$

As shown in Appendix B, the default PWM frequency for the defined pins are $f_{PWM} = 490Hz$, also $n = 8$ (number of bits of the ADC from the frequency inverter) and as according to (METIVIER, 2013), a second order LPF is better for converting a PWM signal to voltage and it has by default $Slope = -40dB/decade$, using Equation 4.15 it is possible to calculate a maximum cutoff frequency of 30.625Hz.

4.8.3 Sallen-Key Low Pass Active Filter

The Sallen-Key LPF setup is probably one of the best second order filters architectures available (DORF; SVOBODA, 2014), this setup is displayed on Figure 37.

According to (TEXAS INSTRUMENTS, 1999), this filter setup has a cutoff frequency defined by Equation 4.16.

$$f_c = \frac{1}{2 \cdot \pi \sqrt{R_1 \cdot R_2 \cdot C_1 \cdot C_2}} \quad (4.16)$$

Using values of $R1=100k\Omega$, $R2=100k\Omega$, $C1=100nF$ and $C2=100nF$ means having a cutoff frequency of 15.91Hz

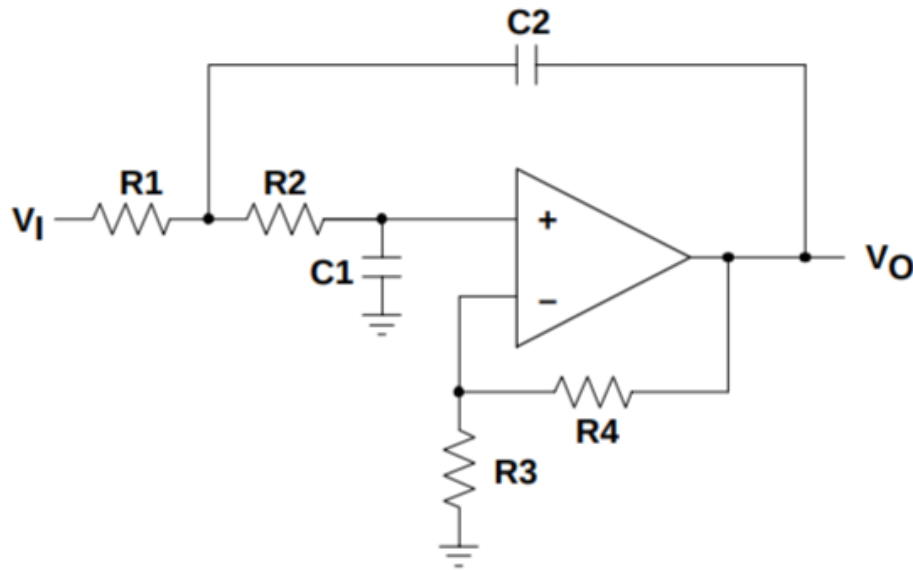


Figure 37 – Sallen-Key Active Low Pass Filter ([TEXAS INSTRUMENTS, 1999](#))

4.8.4 Complete Circuit

Based on all the previously calculations and on ([TEXAS INSTRUMENTS, 1999](#)), the final circuit will be the one in Figure 38. Besides the main components of the filter the added components were two bypass capacitors (C1 and C4), TZ1 is a TVS used to protect the circuit from any transient voltage coming from the cable. Moreover, R1 was added to limit the current that is drained from the analog output. The port *AOUT_1* is a feedback that goes to a analog input of the MCU so the output voltage can be adjusted by varying the duty cycle.

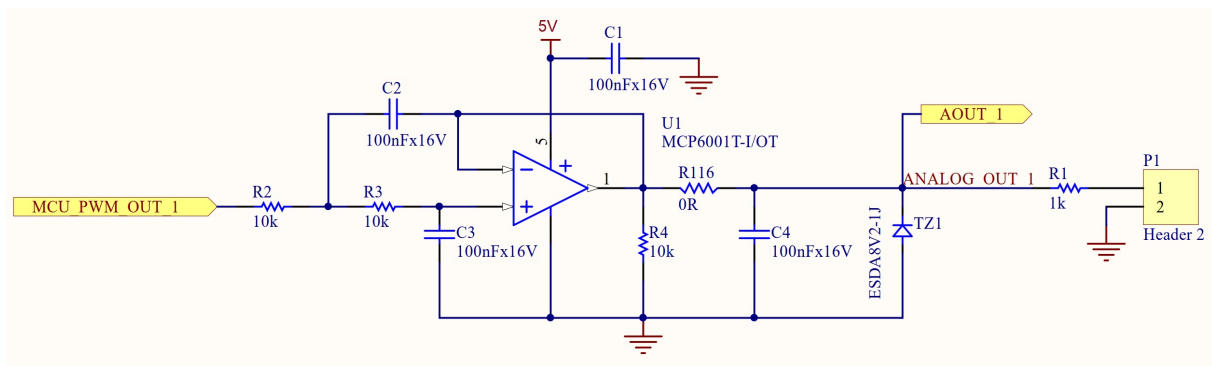


Figure 38 – PWM to Speed Reference Circuit

Although only one analog output is needed, another one will be placed on the PCB in order to allow the circuit to be used on other appliances on possible future projects.

4.9 Digital Interfaces

4.9.1 Digital Outputs

4.9.1.1 Low-side Driver

Item 9 from Section 4.2 states that the system must have a digital output channel to control a relay). According to ([SONGLE, 2018](#)), a standard 5V relay will have a nominal current of 89.3mA, the microcontroller's datasheet ([MICROCHIP, 2018](#)) says that the maximum DC current per I/O pin is 40mA though. Hence it is not possible to activate a relay connected directly to a MCU's I/O pin.

In order to solve this a relay driver circuit needs to be used, in this case a low side mosfet driver similar to the one from Figure ([ELECTRONICS TUTORIALS, 2018](#)) will be used.

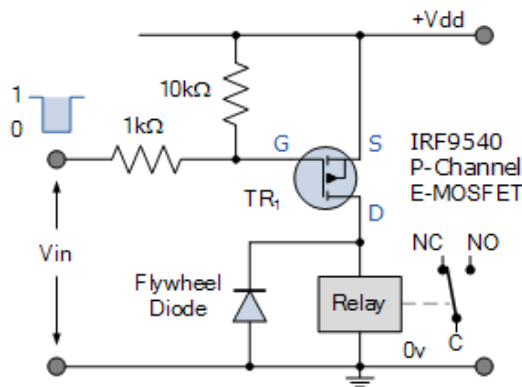


Figure 39 – PMOS low side driver ([ELECTRONICS TUTORIALS, 2018](#))

This is a low-side driver, when the PMOS is submitted to a high logic level (5V) in its gate it will enter on the cutoff region and will not conduct current, hence not activating the relay. On the other hand, when a low logic level (0V) is applied to the device's gate it will enter the saturation region and will conduct current, hence activating the relay.

4.9.1.2 Digital Output Circuit

The digital output circuit will be very similar to the one from Figure 39. The power supply connected to the mosfet will be the 5V source (check Section 4.11.1.1), on the PMOS drain there will be a TVS diode (SMBJ12A from *Littlefuse* ([LITTLEFUSE, 2015](#))) (check Section 2.3.7.2), this TVS will help protecting the PMOS from reverse current and from overvoltages. Figure 40 show the equivalent circuit for the digital output.

The selected PMOS is the NDS332P from *Fairchild* ([FAIRCHILD, 1997](#)), it has a maximum operating continuos current of 1A, maximum gate threshold voltage of 1V,

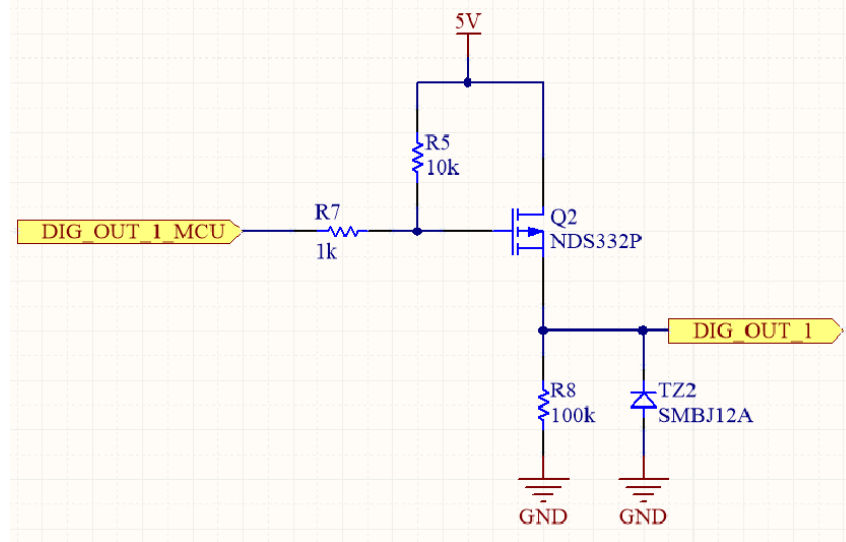


Figure 40 – Digital Output Circuit

maximum drain-source voltage of 20V and maximum gate source voltage of $\pm 8V$. It is adequate for this purpose. Resistor R7 is used to limit the magnitude of the current spike that can occur when a driver switches fast and has to charge or discharge a large gate capacitance. Resistor R5 is a pull-up for the gate, it will ensure that the PMOS will be in cutoff region if there is no input for the MCU. Resistor R8 is optional, for activating relays it is not needed, but other loads may require a pull-down, that is why it was placed on the PMOS drain. It was decided to keep any relay out of the board to save space. Moreover, keeping the relay out of the board gives room for using this digital output for other purposes. Although the project Requirements only specifies two digital outputs, as there were unused MCU digital ports, a third digital output will also be placed on the PCB layout.

4.9.2 Digital Inputs

This project does not have any requirement for digital inputs. However, in order to make the project more versatile for the future, making it able to capture switch states and possible external event, three digital inputs were added to the PCB. Figure 41 show the circuit to interface the digital inputs.

According to (ON SEMICONDUCTOR, 2014), the schottky diode on the input has a reverse voltage of 30V and a foward voltage of 280mV. When a voltage lower than 280mV is present on the input, the voltage on the PMOS gate will be lower than than its threshold (according to device's datasheet (ROHM SEMICONDUCTOR, 2016)) the PMOS will start to conduct current and the signal *MCU_DIN_1* will go to 5V. When the voltege on the input is higher than 280mV, the voltage on the PMOS gate will be higher than the treshold voltage and the PMOS will not conduct current, therefore, because of the pull down resistor R32, the signal *MCU_DIN_1* will go to 0V.

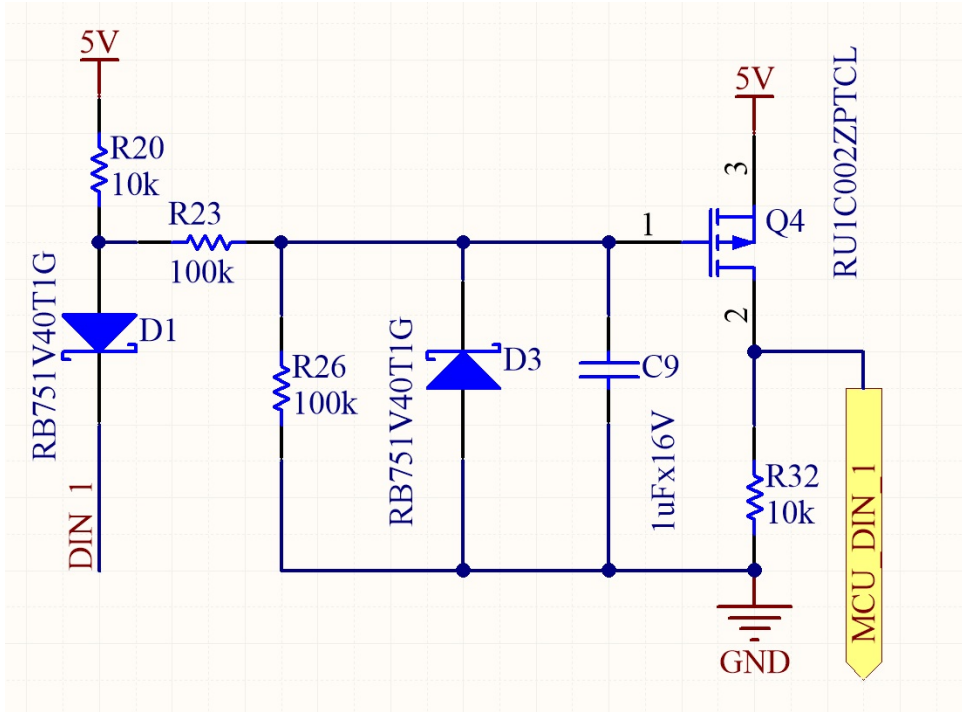


Figure 41 – Digital Input Circuit

4.10 MCU

The chosen MCU for the system is the *ATMEGA32U4* manufactured by *Microchip*. According to ([MICROCHIP, 2017a](#)) and ([MICROCHIP, 2018](#)) the main features of this MCU are:

- *Program Memory (Flash)*: 32KB.
- *Communication Peripherals*: 1-USB, 1-UART, 2-SPI, 1-I2C.
- *ADC*: 12-channels, 10-bit ADC.
- *Operating Voltage Range*: 2.7 to 5.5V.

This microcontroller family is widely used in academic environment (specially after the Arduino project started, when microcontroller programming became much more feasible and reachable), and is famous for being easy and reliable to use. The *ATmega32U4* is really versatile and more important it meets this project requirements, listed in Section 4.2. A very useful feature of this MCU is that it has a USB 2.0 controller built-in, this eliminates the need for an additional transceiver circuit, moreover this MCU can be easily reprogrammable through the USB port, this being a very useful feature when the hardware is fully assembled. Figure 42 shows the pinout of this device.

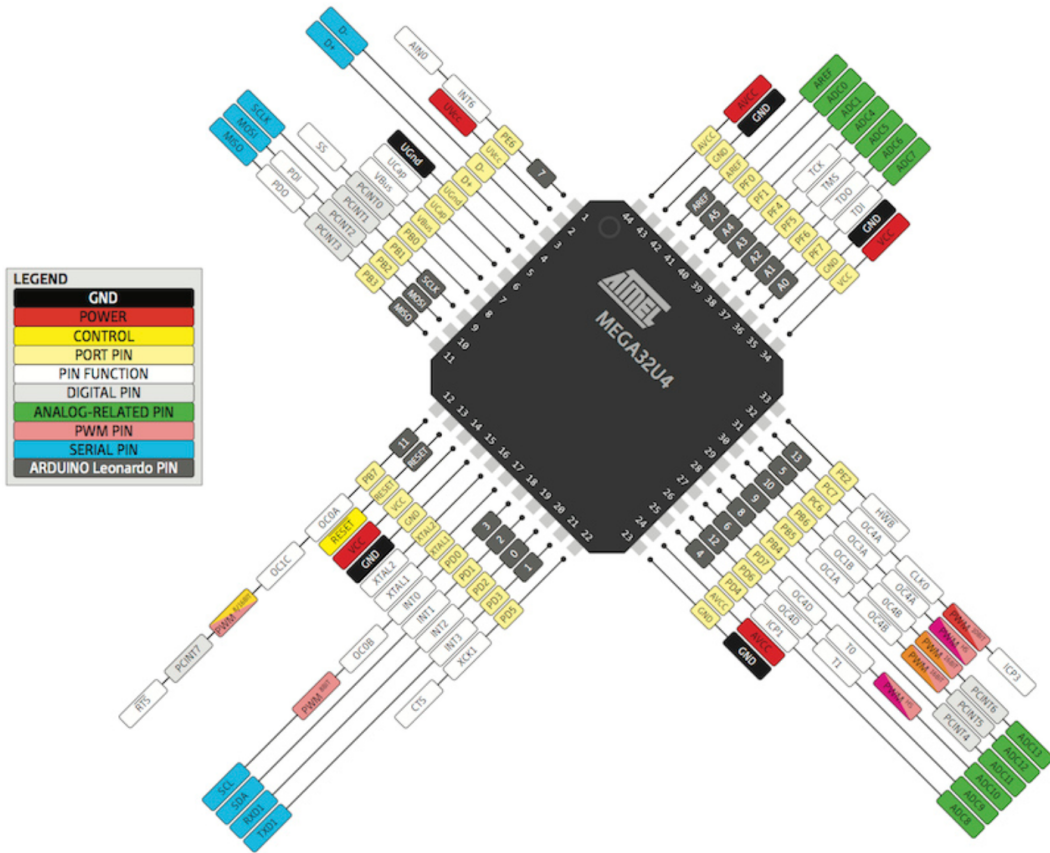


Figure 42 – ATmega32U4 pinout ([PIGHIXX, 2018](#))

4.10.1 MCU circuit

This MCU is the same used on the Arduino Leonardo Board ([ARDUINO..., 2016](#)), whereas, in order to avoid implementation problems the MCU peripheral components were chosen based on the Arduino board schematic ([ARDUINO, 2010](#)). The circuit with all the peripheral components to the ATmega32U4 can be divided in five parts.

4.10.1.1 Core Circuit

Figure 43 shows the core circuit for the MCU.

The components of his circuit and their respective functions are:

- *U7*: The ATmega32U4 chip itself.
- *C28* and *C29*: This are bypass capacitors recommended by the datasheet.
- *S1*, *D7* and *R60*: RST is the reset pin of the MCU, it resets the MCU when low logic voltage is detected. *S1* is a push-button used to short circuit the RST pin to ground and reset the MCU. *R60* is a pull-resistor used to guarantee that RST pin will remain in high logic voltage when the push-button is not being pressed.

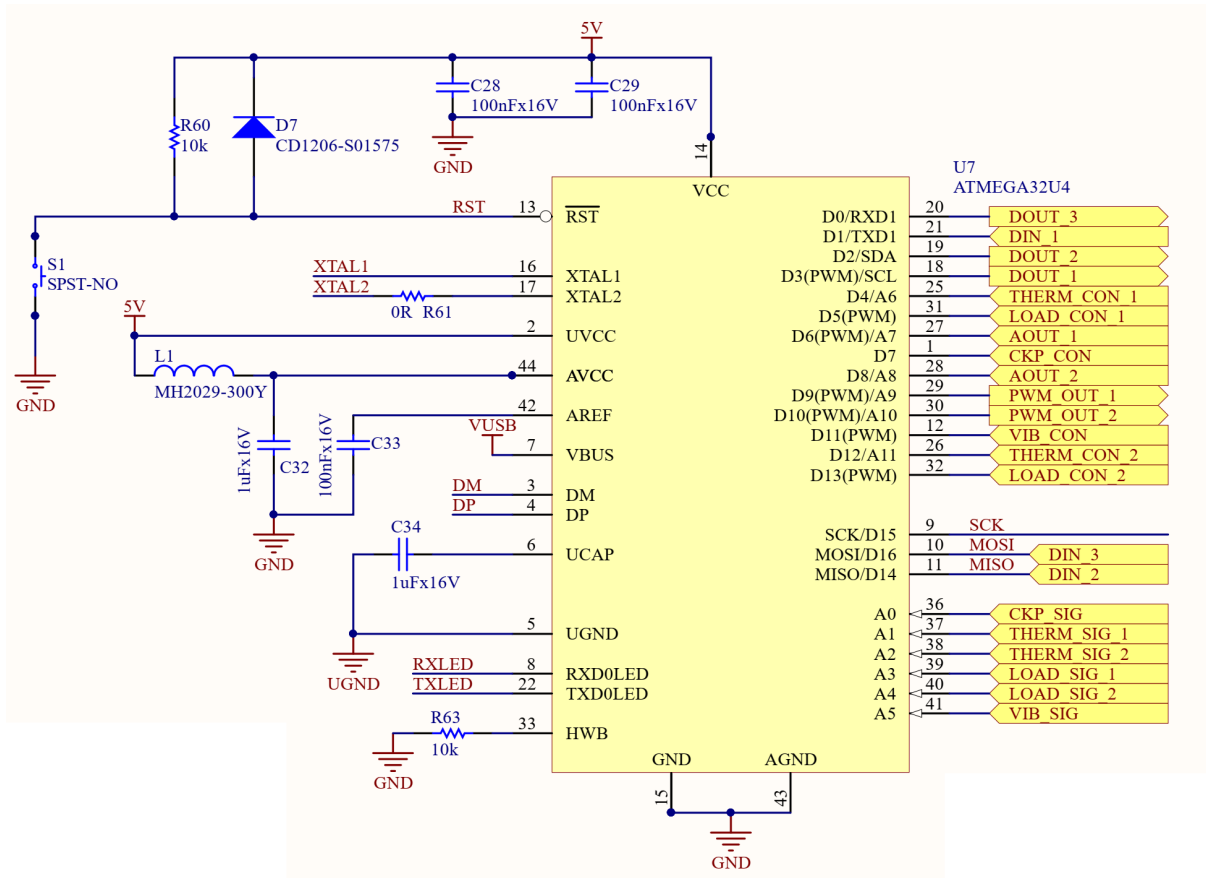


Figure 43 – MCU Core Circuit

- *R61*: This jumper will be explained in Section 4.10.1.2.
- *L1* and *C32*: These components form a LPF for the AVCC pin, which is the power supply for the MCUs ADC.
- *C33* and *C34*: Both are bypassing capacitors recommended by the datasheet, C33 for the ADC internal voltage supply and C34 for the USB 2.0 controller.
- *R63*: It is a pull-down resistor that enables hardware boot.

The MCU ports were defined as the following:

- *DOUT_1*, *DOUT_2* and *DOUT_3*: Digital Output ports
- *DIN_1*, *DIN_2* and *DIN_3*: Digital input ports.
- *CKP_SIG*, *THERM_SIG_1*, *THERM_SIG_2*, *LOAD_SIG_1*, *LOAD_SIG_2* and *VIB_SIG*: Those are respectively the analog input ports for the signal of: speed sensor, first temperature sensor, second temperature sensor, first force sensor, second force sensor, cibration sensor.

- *CKP_CON, THERM_CON_1, THERM_CON_2, LOAD_CON_1, LOAD_CON_2 and VIB_CON*: Those are digital inputs used to detect if one of the sensors from the previous item were disconnected.
- *PWM_OUT_1, AOUT_1, PWM_OUT_2 and AOUT_2*: Those are respectively: first PWM output, MCU analog input to monitor the first system analog output, second PWM output, MCU analog input to monitor the second system analog output.
- *SCK, MOSI and MISO*: Those are signal used to program the MCU through ISP(In System Programming).
- *XTAL1 and XTAL2*: Respectively the input and output for the crystal oscillator circuit.
- *VUSB*: This is the supply voltage pin for the USB controller, it is being powered by a external USB host connected to the board.
- *DM and DP*: USB data lines.
- *RXLED and TXLED*: Pins that goes to low logic level when data is being transmitted and high logic level when not.

4.10.1.2 Crystal Oscillator Circuit

According to ([MICROCHIP, 2018](#)), in order to work in full-speed mode, the MCU needs a external crystal oscillator with a frequency of 8 to 16MHz and bypassing capacitors from 12 to 22pF on the crystal pins. Based on ([ARDUINO, 2010](#)) besides this capacitor a $1\text{M}\Omega$ bias resistor has been placed between crystal pins. Also a 0R jumper (first mentioned in Item 4.10.1.1 from Section 4.10.1) was placed between one of the crystal pins and pin XTAL2 in case a low pass filter is needed (using this resistor and the internal capacitance of the MCU port). The desired circuit for the crystal oscillator is shown in Figure 44 (except for the 0R jumper which can be seen in Figure 43).

4.10.1.3 USB Port Protection Circuit

The USB Port Protection circuit was entirely based on the on the circuit from Arduino Leonardo, the only component specified by the MCU datasheet are the 22Ω series resistors as shown in Figure 45.

L2 and L3 are ferrite beads used to filter high frequency noise. Z1 and Z2 are ESD suppressors, alongside with the series resistors used to protect the MCU's USB data lines. Finally, C35 and C36 are bypass capacitors used to stabilize the voltage on the USB power line.

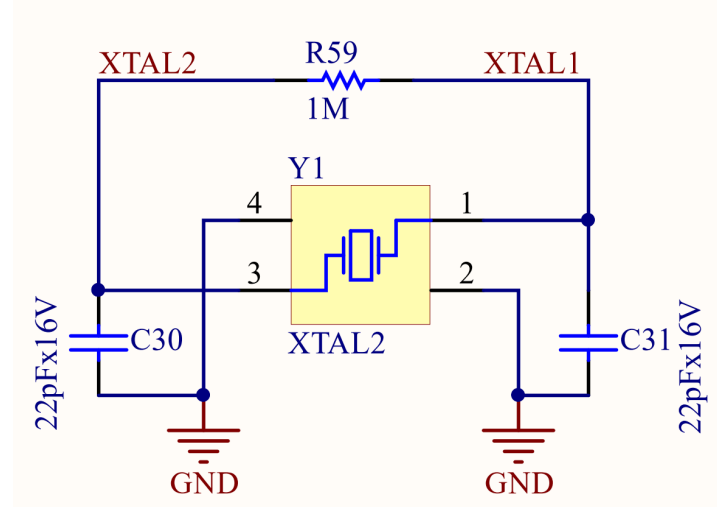


Figure 44 – Crystal Oscillator Circuit

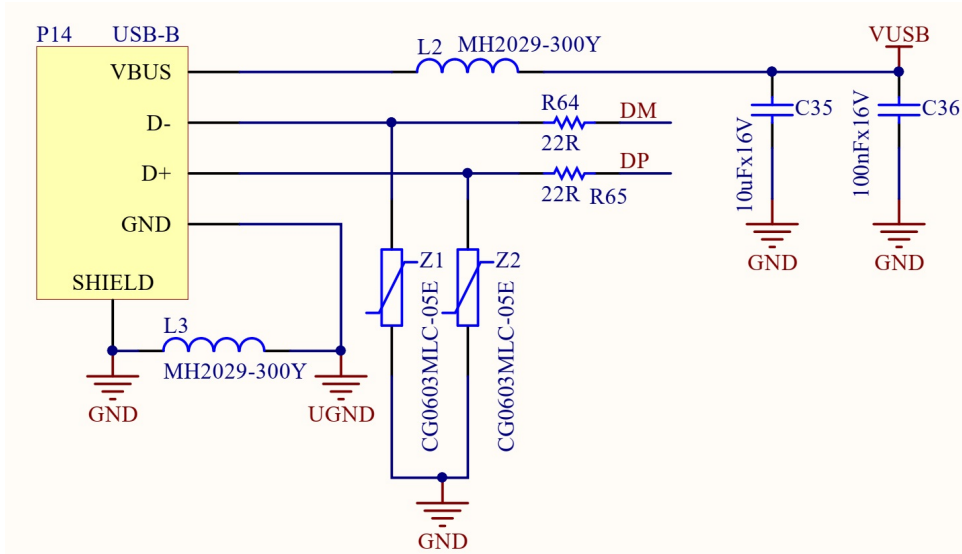


Figure 45 – USB Port Protection Circuit

4.11 Voltage Supplies

4.11.1 Power Supplies

In order to avoid any interference of the AC line, this project will work with a DC voltage input and any other necessary voltages will be acquired from this higher input voltage supply. There are many different types of voltage regulators, nowadays the most common DC/DC being switching regulators. They are more efficient than linear regulators and consequently they dissipate less heat, the downside is that they tend to have some ripple at the output (SCHWEBER, 2017). However, as the ripple can easily be filtered and that a switching power supply allows the input voltage to be of a much bigger range, this solution was considered the best for the project.

4.11.1.1 5V Supply

The voltage supply was chosen to be a 5V DC supply because all the components can work with this voltage. The chosen voltage regulator for the 5V supply was the TL2575-05 from *Texas Instruments* ([TEXAS INSTRUMENTS, 2014](#)), it has a output up to 1A, voltage drop of 2V, typical efficiency of 88% and can work with a 7 to 42V input. Figure 46 shows the circuit used for the 5V supply.

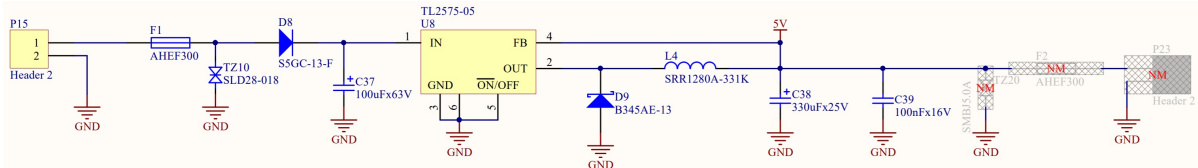


Figure 46 – 5V Power Supply Circuit

According to ([TEXAS INSTRUMENTS, 2014](#)), the main components to be chosen for the switching regulator are L4, C38 and D9. The inductor and the capacitor are used to form a LPF to transform the PWM output of the switching regulator to a DC voltage. D9 is a flyback diode used to shunt any negative current from the switching to ground and protect the device. The datasheet recommends using a 3A reverse current diode, a 330uH inductor and 330uF capacitor for the 5V regulator.

The other components of the circuit are:

- *TZ10*: TVS diode to clamp to protect the input from ESD.
- *F1*: resetable fuse, they will limit the current that flows into the circuit and protect the TVS.
- *D8*: A diode to protect the input from inverse polarity.
- *C37*: Input bypass capacitor recommended by the device's datasheet.
- *C39*: Another bypass capacitor on the output to filter any residual noise.

4.11.2 Voltage References

In this project any power supply that the precision and stability of the output voltage is more concerning than the maximum output current will be called a voltage reference.

4.11.2.1 4V1 Reference

As said in Section 4.5.3, the sensor detection circuit needs a 4V1 voltage reference for the comparator. This is achieved using the LM4040-4.1 from *Microchip* ([MICROCHIP](#),

2017b). This is a fixed 4V1 precise voltage reference and according to the datasheet it has a tolerance of $\pm 1.15\%$. Figure 47 shows the circuit for the 4V1 voltage reference.

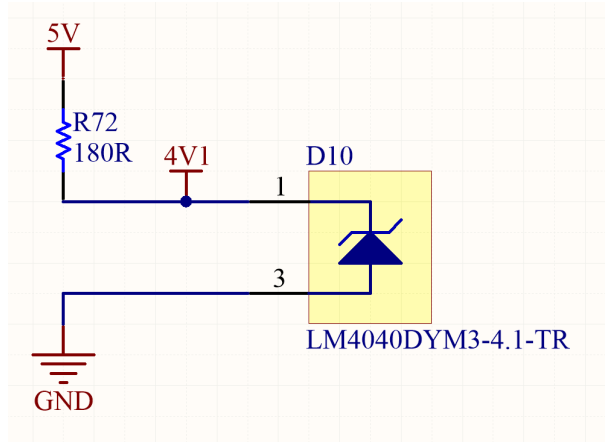


Figure 47 – 4V1 voltage reference circuit

According to the datasheet the current flowing through the LM4040-4.1 must be never be greater than 15mA, voltage reference pins do need very little current, so a third of this 15mA will be taken as goal. Considering the voltage drop of 0.9V (5V - 4.1V) and the current of 5mA we need a 180Ω resistor in series with the regulator.

4.12 Circuit Fabrication and Assembly

4.12.1 PCB Design

The PCB layout for this project was developed using the Altium Designer 17 Software (ALTIUM..., 2017). During the layout design some things were considered to ensure functionality:

- Instead of soldering the connectors directly to the board, empty pads for soldering wires were placed, this way connectors can be chosen later and fixed on the board housing instead of on the board.
- Protection devices such as TVS, Fuses and current limiting resistors were placed very close from the terminal pads in order to prevent cooper tracks to be damaged.
- SMT (Surface Mount Technology) was a priority during design in order to save space on the board.
- Cooper tracks width: The width of every track was chosen according to the electrical signal it is carrying.

Figures 48 and 49 shows respectively the top and the bottom side of the board during design, there are almost no cooperless areas, most of empty spaces were replaced by GND planes in order to make the board corrosion faster and to make a stronger gnd connection. Other interesting fact is the width of power supply tracks, it is easy to notice they are much more thick than normal signal tracks. The board dimmensions are 130mm x 80mm.

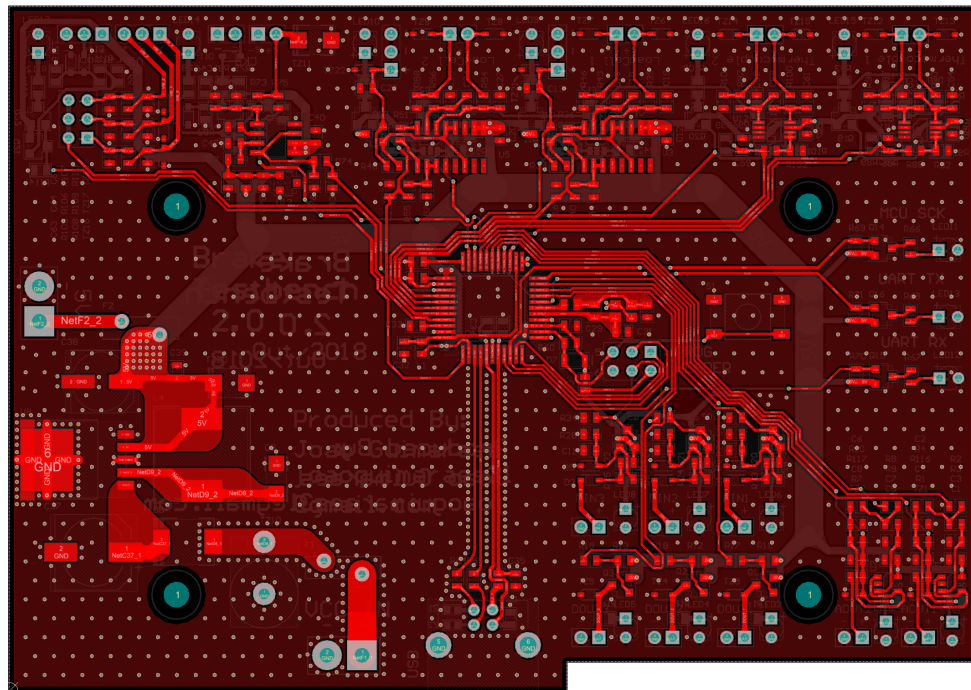


Figure 48 – PCB Top 2D View

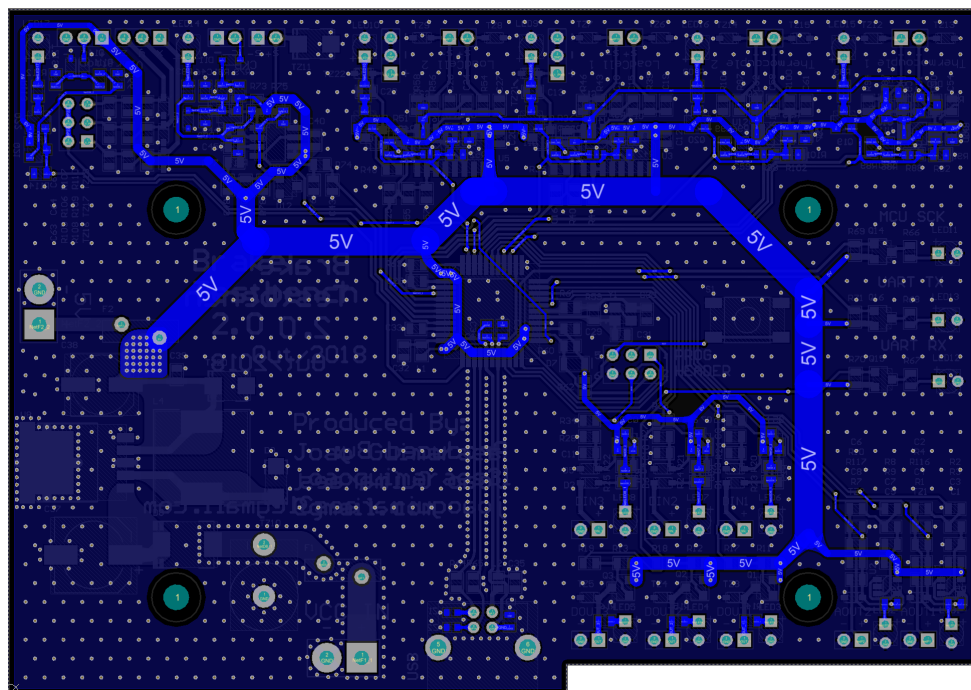


Figure 49 – PCB Bottom 2D View

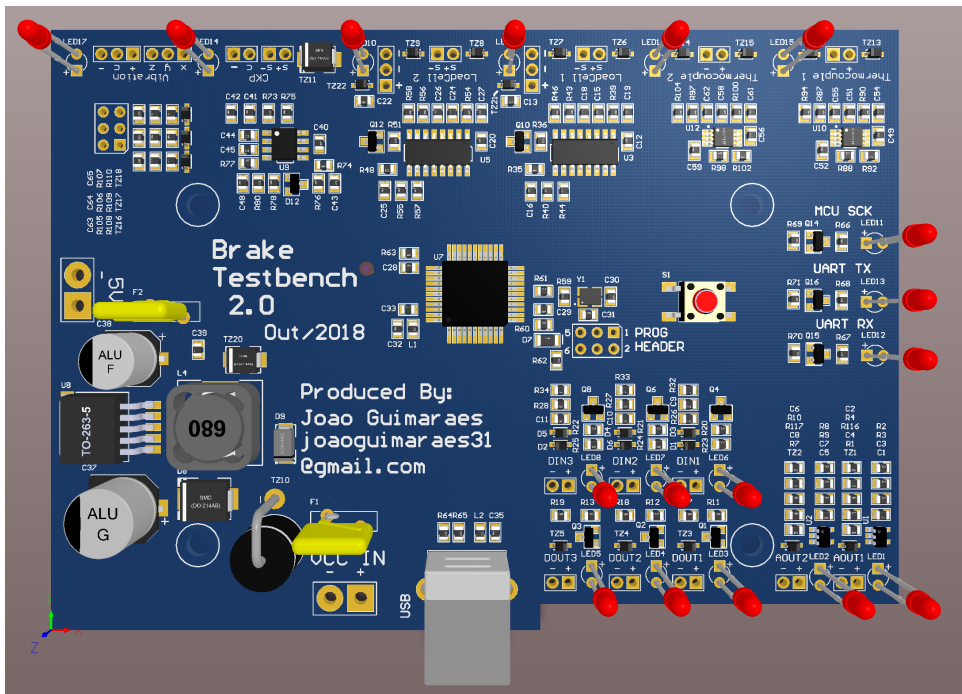


Figure 50 – PCB Top View

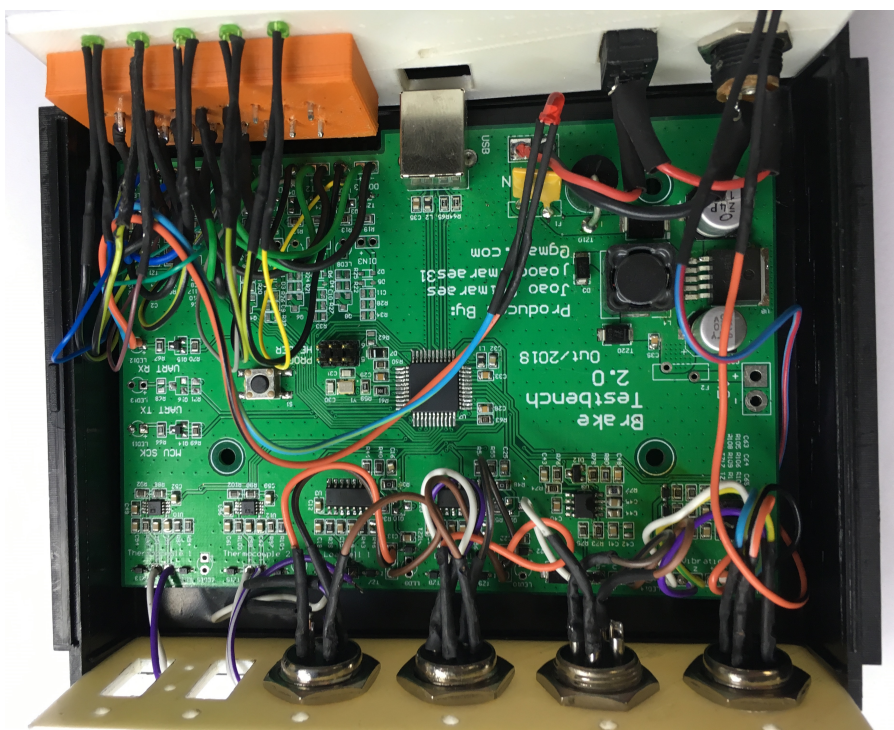


Figure 51 – Real PCB Assembled

5 Firmware Project

5.1 Microcontroller programming basics

A microcontroller code is composed basically of two parts:

- *Setup*: This part of the code is only executed once, as the name may indicate, it is used to set properties, configure timers, inputs and other features of the hardware.
- *Loop*: This part of the code is executed continuously or until some condition is reached.

Other important component of a microcontroller code are interruptions. It is possible to interrupt the standard execution of a program when an event happens, or as it is more common to say, when an event triggers an interruption. This event may be a timer overflow, a event triggered by an input change among other things. Interrupt routines are really useful when working with instrumentation and timers, because using interruptions it is feasible to meet real-time requirements in a project ([MUKARO; CARELSE, 1999](#)).

5.2 Code Map

The Figure [52](#) show a functional map of the microcontroller code that can be found entirely in Appendix [B](#).

As soon as the microcontroller is turned on it enters in the *Setup*, on this part the following things are setted:

- *Acquisition Timer*: Timer max count value is setted and a interruption service routine is appointed, this timer is used for the analog sampling/reading function.
- *LED Timer*: Same thing done for *Acquisition Timer* is done for *LED Timer*, this timer controls the blinking frequency of the MCU debug LED.
- *Serial Port*: The serial port baud rate is defined and the serial port is opened.
- *Port mapping*: The port mapping is done, *i.e.* digital I/O ports are defined as inputs (high impedance) or as outputs (low impedance) and the analog ports are setted.

After setting up, the code enters in a state in which it waits for a command that can be from three different groups. These commands are coded into ASCII characters ([ASCII, 2017](#)). Table [2](#) shows all proposed commands.

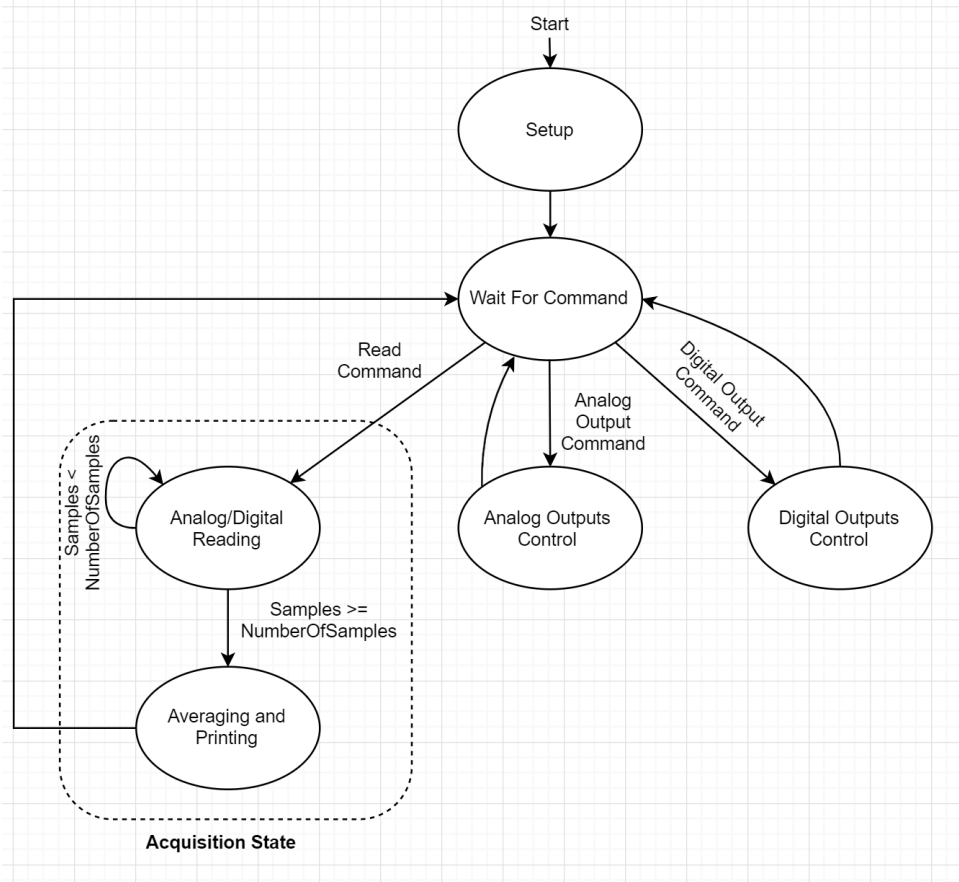


Figure 52 – Microcontroller Code Map

Each group of commands will lead to a specific block described in Figure 52.

- *Digital Output Control:* As mentioned in Section 4.3.3.1, there are three digital outputs on the circuit board. Hence, there will be two commands for each digital channel (on and off) plus a command to turn all the digital outputs off.
- *Analog Output Control:* Commands from this block will set the duty cycle for the MCU PWM outputs that will be converted to analog outputs, as explained in Section 4.8.
- *Acquisition State:* There is only one command that will lead the code to this loop (*Filter Read*). When in this loop, the code will read the analog outputs for a specific number of times (*Number Of Samples*), *i.e.* sampling the signals. Each samples is summed up and when the desired number of samples is reached, the code divides the sum of all samples by this number, giving a averaged read. Then, this read is printed together with the digital inputs read to the upstream data port.

Additional to these commands there are the commands *Print Version* and *One Read*, the first is a command that prints the firmware version, the latter performs one read of the analog inputs and is only used for debugging.

ASCII	Command	ASCII	Command	ASCII	Command
32	Print Version	65		98	PWM 1 - DT 92%
33	Filter Read	66		99	PWM 1 - DT 96%
34	One Read	67		100	PWM 1 - DT 100%
35	DOUT - Reset	68		101	PWM 2 - DT 0%
36	DOUT 1 - ON	69		102	PWM 2 - DT 4%
37	DOUT 1 - OFF	70		103	PWM 2 - DT 8%
38	DOUT 2 - ON	71		104	PWM 2 - DT 12%
39	DOUT 2 - OFF	72		105	PWM 2 - DT 16%
40	DOUT 3 - ON	73		106	PWM 2 - DT 20%
41	DOUT 3 - OFF	74		107	PWM 2 - DT 24%
42		75	PWM 1 - DT 0%	108	PWM 2 - DT 28%
43		76	PWM 1 - DT 4%	109	PWM 2 - DT 32%
44		77	PWM 1 - DT 8%	110	PWM 2 - DT 36%
45		78	PWM 1 - DT 12%	111	PWM 2 - DT 40%
46		79	PWM 1 - DT 16%	112	PWM 2 - DT 44%
47		80	PWM 1 - DT 20%	113	PWM 2 - DT 48%
48		81	PWM 1 - DT 24%	114	PWM 2 - DT 52%
49		82	PWM 1 - DT 28%	115	PWM 2 - DT 56%
50		83	PWM 1 - DT 32%	116	PWM 2 - DT 60%
51		84	PWM 1 - DT 36%	117	PWM 2 - DT 64%
52		85	PWM 1 - DT 40%	118	PWM 2 - DT 68%
53		86	PWM 1 - DT 44%	119	PWM 2 - DT 72%
54		87	PWM 1 - DT 48%	120	PWM 2 - DT 76%
55		88	PWM 1 - DT 52%	121	PWM 2 - DT 80%
56		89	PWM 1 - DT 56%	122	PWM 2 - DT 84%
57		90	PWM 1 - DT 60%	123	PWM 2 - DT 88%
58		91	PWM 1 - DT 64%	124	PWM 2 - DT 92%
59		92	PWM 1 - DT 68%	125	PWM 2 - DT 96%
60		93	PWM 1 - DT 72%	126	PWM 2 - DT 100%
61		94	PWM 1 - DT 76%	127	
62		95	PWM 1 - DT 80%		
63		96	PWM 1 - DT 84%		
64		97	PWM 1 - DT 88%		

Table 2 – ASCII Commands Reference

6 Experimental Tests

After the board assembly and fabrication phases were finished to ensure that this project attends its requirements. This chapter presents the experimental procedure, the results as well with the discussion and possible improvements.

The experimental procedure is based on the brake test procedures proposed by (SAE, 2003) described in Section 2.2.2. Basically the test will comprehend turning the electric motor on (with the aid of the frequency inverter) and by monitoring the Speed Acquisition Channel (check Section 4.4) wait until the rotor frequency reaches a pre-defined upper limit and then after a configured delay time, stop accelerating the motor and starts to brake until the system reaches a lower speed limit. During the entire procedure the brake pressure, and the temperature on the disc shall be measured. This procedure should be repeated for a set number of times called snubs.

6.1 Materials

The few materials needed to perform the braketest, most of the materials needed for the validation tests were borrowed from the *Wear of Materials Laboratory* from *University of Brasília*, the way the materials are disposed can be seen in Figure 53.

The frequency inverter used on the tests is the WEG-CFW08, it is an important part of the tests as it is responsible for controlling the speed and acceleration of the motor by varying the current on the three-phase lines that feeds the motor. It has four digital inputs, two analog inputs, two digital outputs alongside with two analog outputs (WEG, 2009). For the tests only the digital inputs will be used to turn the motor on and off, Figure 54 shows the device installed and fixed on the Laboratory's panel.

The electric motor used is manufactured by WEG, this is a three-phase motor that has 12.5 cv of power, 1755 max RPM and has an efficiency of 87.7% and it is connected to the brake disc machine through a pulley system. Figure 55 the motor itself.

Brake Disc Machine is a machine welded on *Wear of Materials Laboratory* in order to simulate a car's axle submitted to inertial masses. One end of the axle is connected to the electric motor through a pulley system and the other end is connected to the disc brake components as Figures 56, 57 and 58.

The Load Cell used to measure the brake force has a sensibility of 2mV/V and a maximum load of 500kgf, meaning when it is powered with 2V5 (check Section 4.6.2) and submitted to its maximum load the voltage output will be of 5mV. Figure 59 shows how

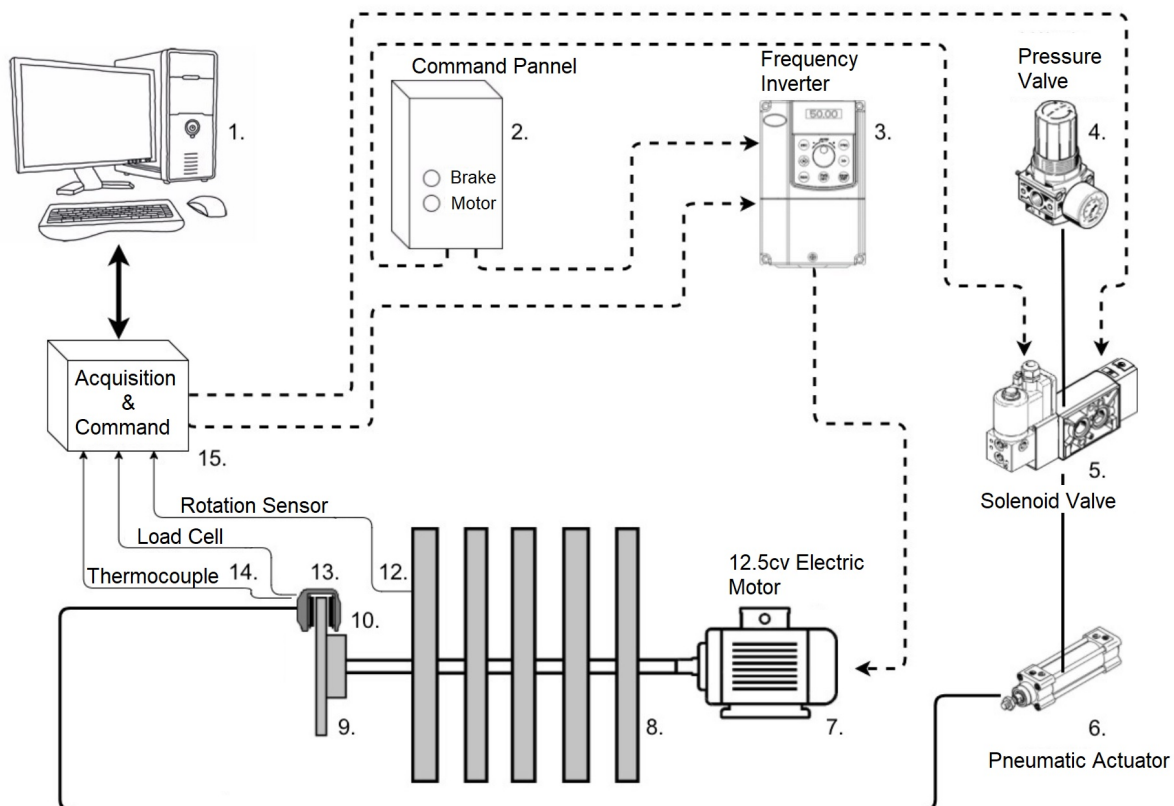


Figure 53 – Materials Disposition



Figure 54 – Frequency Inverter WEG-CFW08



Figure 55 – Electric Motor WEG



Figure 56 – Brake Disc Machine



Figure 57 – Brake Disc Machine Pulley System

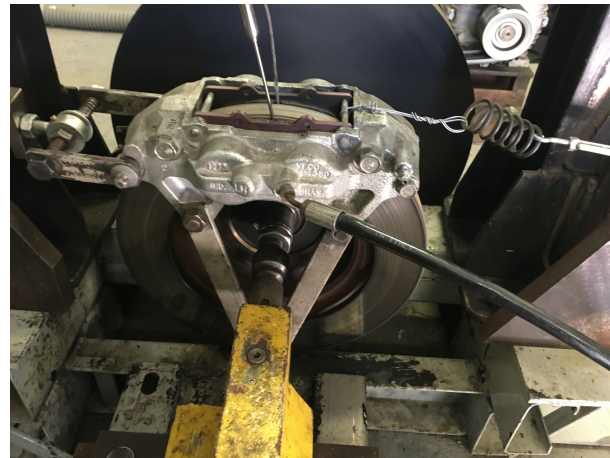


Figure 58 – Brake Disc Arrangement

the load cell can be used to measured the braking force and Figure 60 shows the actual load cell installed on the Brake Disc Machine.

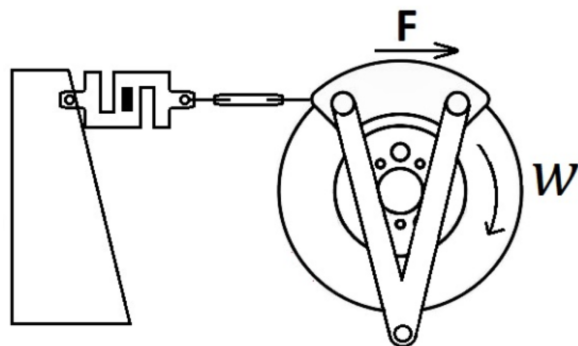


Figure 59 – Load Cell Installation Scheme ([CAIXETA, 2017](#))



Figure 60 – Load Cell Installed

This project uses two generic type K thermocouples at each end of the braking disc, as Figure 61 shows.



Figure 61 – Thermocouples Installed

This project also includes a generic Crankshaft Position Sensor, to enhance the CKP signal amplitude six small magnets were placed around the inertial disc that the CKP is perpendicular mounted to, the only important consideration when doing this is that the CKP will actually measure a frequency six times higher than the actual rotation frequency of the axel. Figure 62 shows how the CKP sensor was placed.

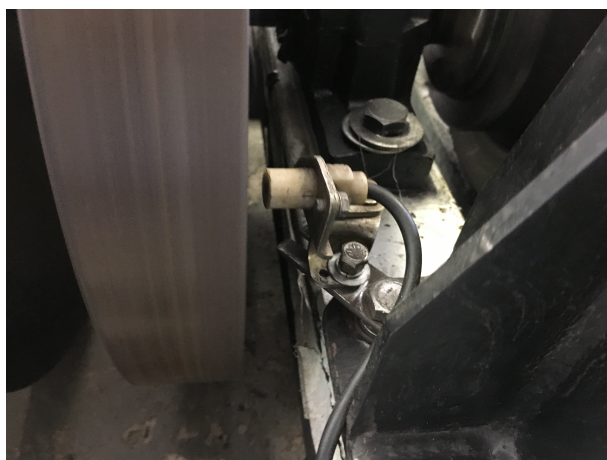


Figure 62 – CKP installed

Additional materials used for the test are the developed hardware and the laptop used to run the test.

6.2 Test Application

In order to perform the test a *LabView* application was developed to control the lower level hardware and perform data processing, the application main screen can be

seen in Figure 63.

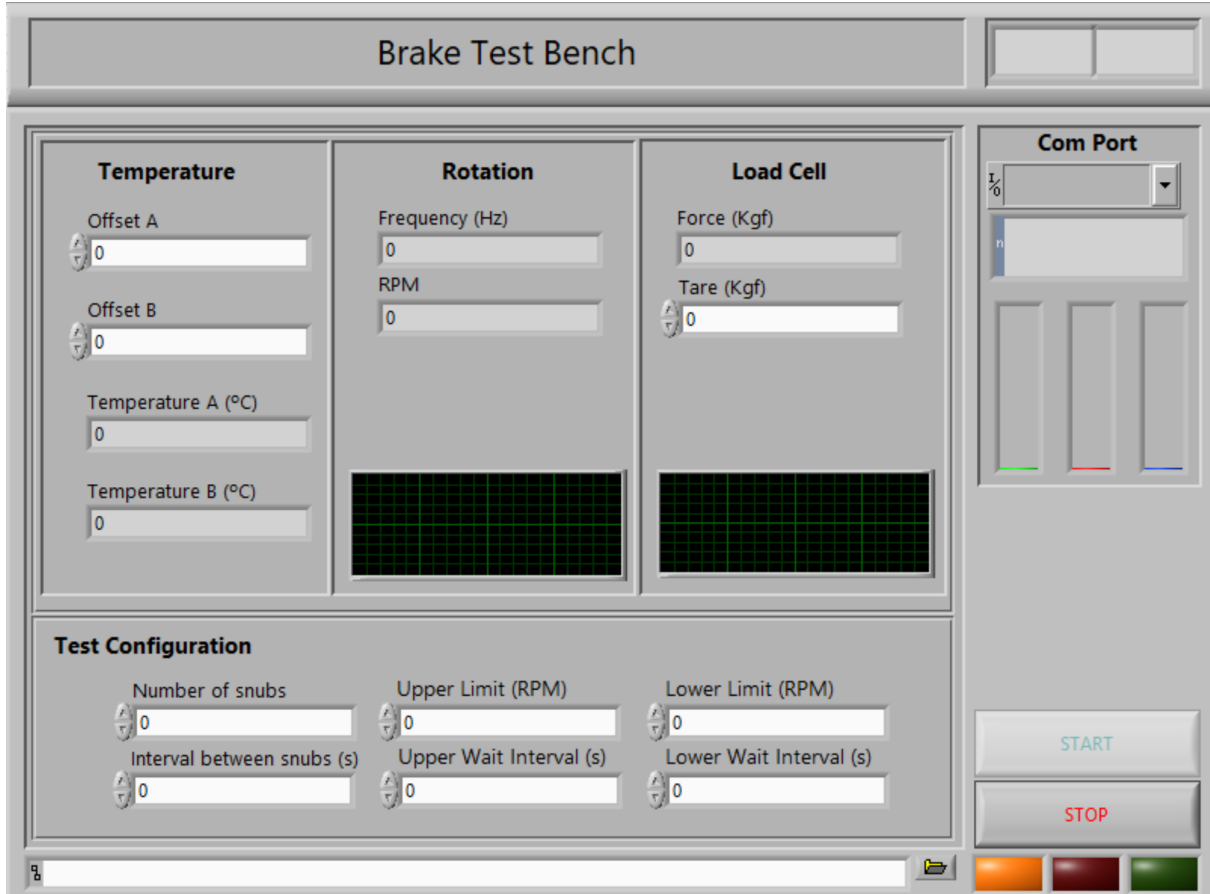


Figure 63 – Test Application Main Screen

The main screen is divided in three parts, first part displays the sensors readings, thermocouples measured temperature, rotation frequency and RPMs and load cell braking force. On the bottom of the screen the test configurations, them being:

- *Number of Snubs*: The number of times each brake interaction will be done.
- *Interval between snubs (s)*: The amount of seconds that a interface will wait at the end of a brake interaction before accelerating the motor again.
- *Upper Limit (RPM)*: At each snub the system will accelerate the electric engine until the rotor reaches this pre-defined rotation rhythm.
- *Upper Wait Interval (s)*: After reaching the upper rotation limit the system will wait for this interval before braking.
- *Lower Limit (RPM)*: The system will perform braking until the rotor reaches this lower RPM limit.
- *Lower Wait Interval (s)*: After reaching the Lower Limit the system will for this interval.

The software itself will take full control of the test, it will turn the electric motor on when needed, turn the brakes one

6.3 Brake Test

6.3.1 Full Stop Test

The desired test will be the full stop test, described by ([CAIXETA, 2017](#)) as a test where the speed is set to a upper limit and then to nought rotation at the end. In order to evaluate the reliability from developed hardware.the test shall be carried a hundred times.

In order to start the brake test the following parameters were configured on the *Labview* Test Application as Table 3 shows.

Parameter	Value	Description
Number of Snubs	100	To achieve reliable data.
Interval Between Snubs	5s	Allows the brakes to cool down after each Snub.
Upper Limit	500 rpm	Almost the maximum rotation of the rotor (580rpm)
Upper Wait Interval	3s	Just enough so that the speed can stabilize
Lower Limit	0 rpm	The ideia is to fully stop the system.
Lower Wait Interval	1s	Just enough to guarantee no momentum is present.

Table 3 – Test Parameters Setup

The goal of this tests is not to evaluate braking performance of components of a brake system but rather to achieves that the developed hardware can be used for that, i.e. showing that the measured quantities are directly related to the tests are being carried out. Hence, it is expected that temperature should increase after each snub. Moreover, as the measured braking pressure increases and the CKP signal frequency should decrease rapidly. Moreover, it shall be possible to see a variation in brake efficiency when the brakes starts to get hotter.

6.3.2 Results and Discussion

Figure 64 shows a graph with the measured quantities on the first ten of the hundred snubs.

Based on experiment results, it is possible to see the correlation between the measured quantities. Clearly the measured rotation falls rapidly as the brake force saturates to a maximum brake force value. Moreover, at each brake event, detected when the brake force increases, the temperature measured on each of thoose thermocouples increases.

Taking a more detailed look at the temperature variation at each snub, Figure 65 show the measured brake force regard the measured temperature at the first ten snubs.

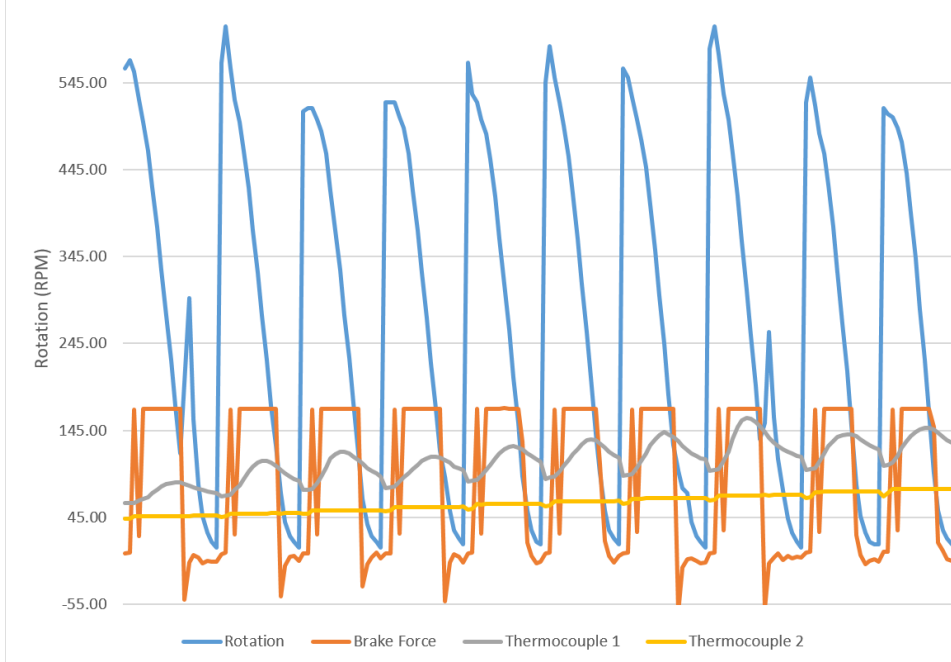


Figure 64 – Measurements of the first ten snubs of the test

This graph states the coorelation between the temperature of the brake pads and the braking action, and the fact that the temperature increases during the braking act is perfectly in agreement with the fact that a braking system can be analysed as a kinetic to thermal energy converter, at is was explained in Section 2.1.

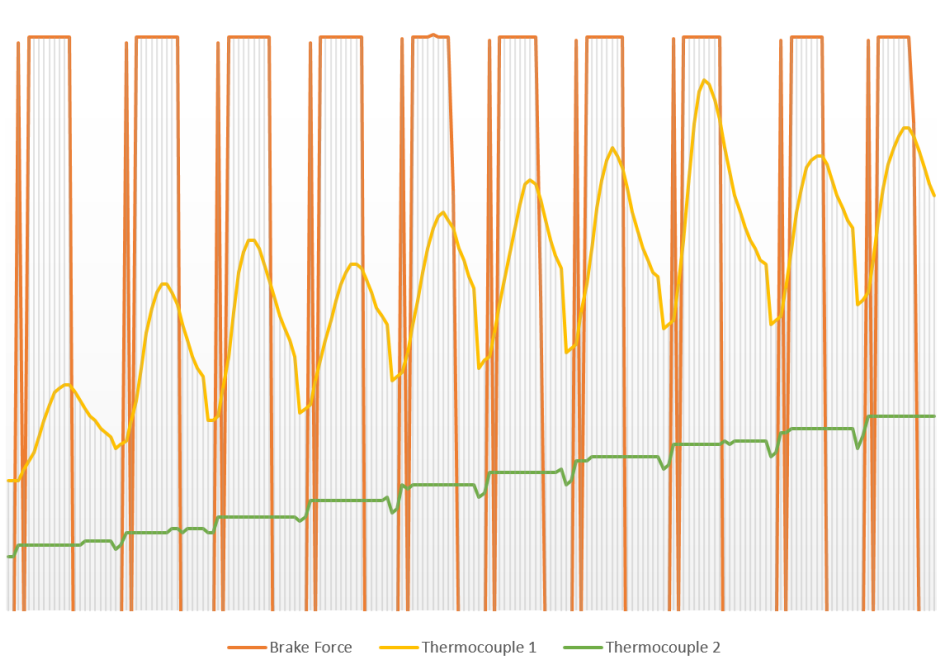


Figure 65 – Temperature and Brake Force Measurements of The First Ten Snubs

Whereas the temperature increases at each snub, there may be a point where the temperature reaches a equilibrium, Figure 66 shows the variation of temperature during

the 100 snubs, it is possible to see that even that the temperature bounces at each snub, there may be a point were the temperature stabilizes close to a certain temperature.

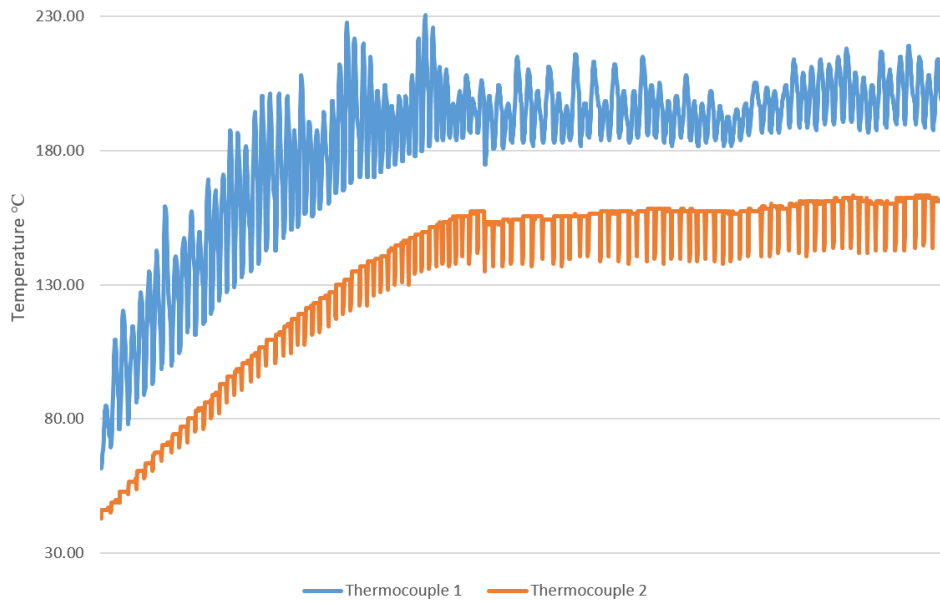


Figure 66 – Temperature Variation During The Whole Test

Another interesting point to analyse is the effect of the temperature of the pads and the rate of desacceleration of the rotor. Figure 67 shows the desacceleration curves at each snub and shows that during the test the brake efficiency was slightly reduced as the temperature would increase.

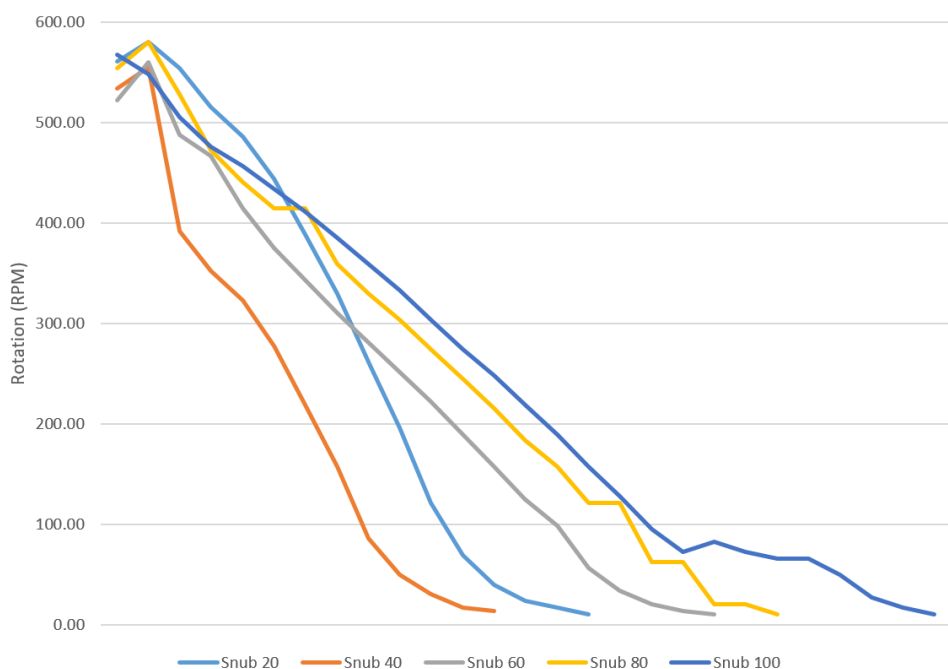


Figure 67 – Deceleration During the Whole Test

6.4 Analog Output Tests

6.4.1 Analog Output Duty Cycle Tests

In order to test the analog output of the system a additional test using just a serial terminal was performed to validate the analog output and its usage. Before starting this test the frequency inverter was configured to take the 0-10V analog input as its speed reference with a gain of two and maximum rotation of 500rpm. Whereas, when 5V is present at this analog input the rotor should spin at a rotation close to 500rpm and when 2.5V is present at the input the rotor should spin at a rotation close to 250rpm.

The test was carried out varying the analog output from 50 to 100% duty cycle (2.5 to 5V), taking 50 samples at every 10% interval, *i.e.* taking 50 samples at 50%, 50 samples at 60%, 50 samples at 70%, 50 samples at 80%, 50 samples at 90% and finally 50 samples at 100%. At each sample the CKP acquisition channel and the analog output feedback channel were monitored.

6.4.2 Results and Discussion

Figure 68 shows the analog output voltage in respect with the duty cycle.

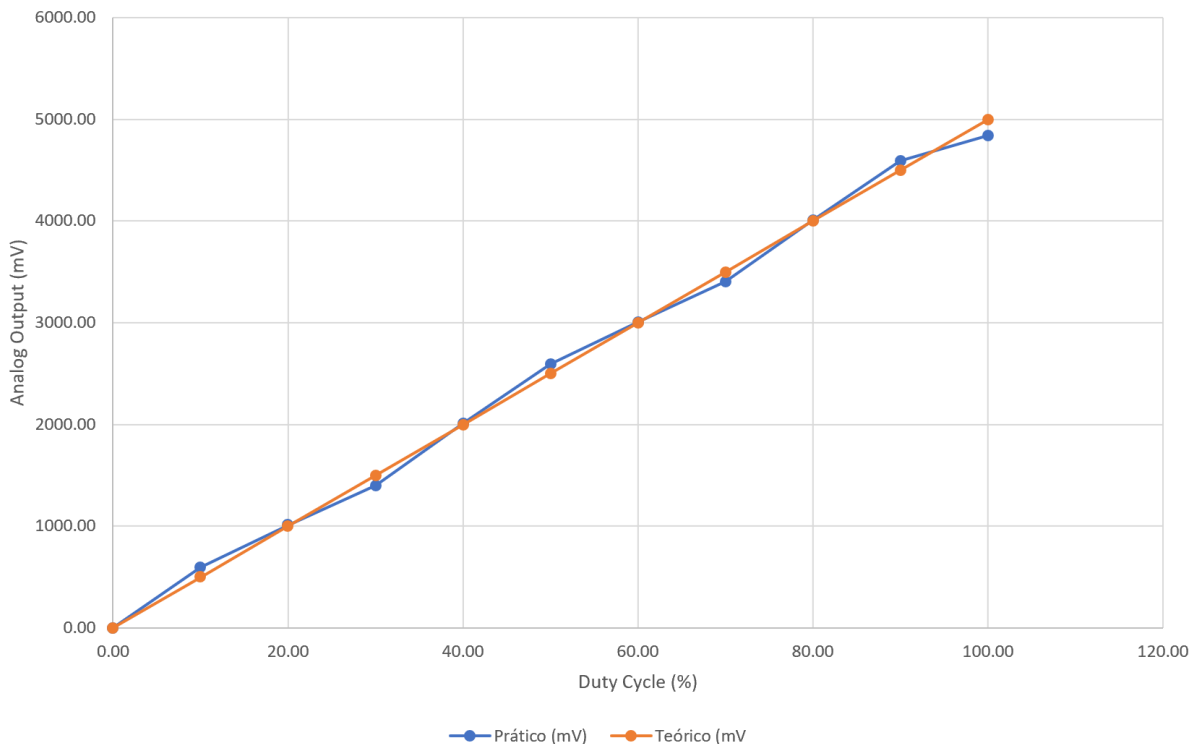


Figure 68 – Analog Output in Respect with Duty Cycle

It is possible to see that the measured output was really faithful to the theoretically calculated output, the average error was just 3.35% which is pretty low. If we disconsider

the measured values from 0% and 100% this error falls to 1.58%, probably this is related to the fact that 0% and 100% produces a theoretically output of 0V and 5V, which is respectively the negative and positive supply of the operational amplifier from the analog output circuit (check Section 4.8.4). Although the error for 0% and 100% is more than two times the error from the rest of the possible duty cycles, it still is quite small, and this happens because the chosen amplifier for the analog output circuit has rail-to-rail input/output.

Different from the brake tests from Sections 6.3.1 and 6.3.2, the frequency inverter was always on, the consequence of this is that the noise from the electric motor and the frequency inverter was always interfering with the CKP sensor signal. Figure 69 shows the measured rotation in respect with the duty cycle.

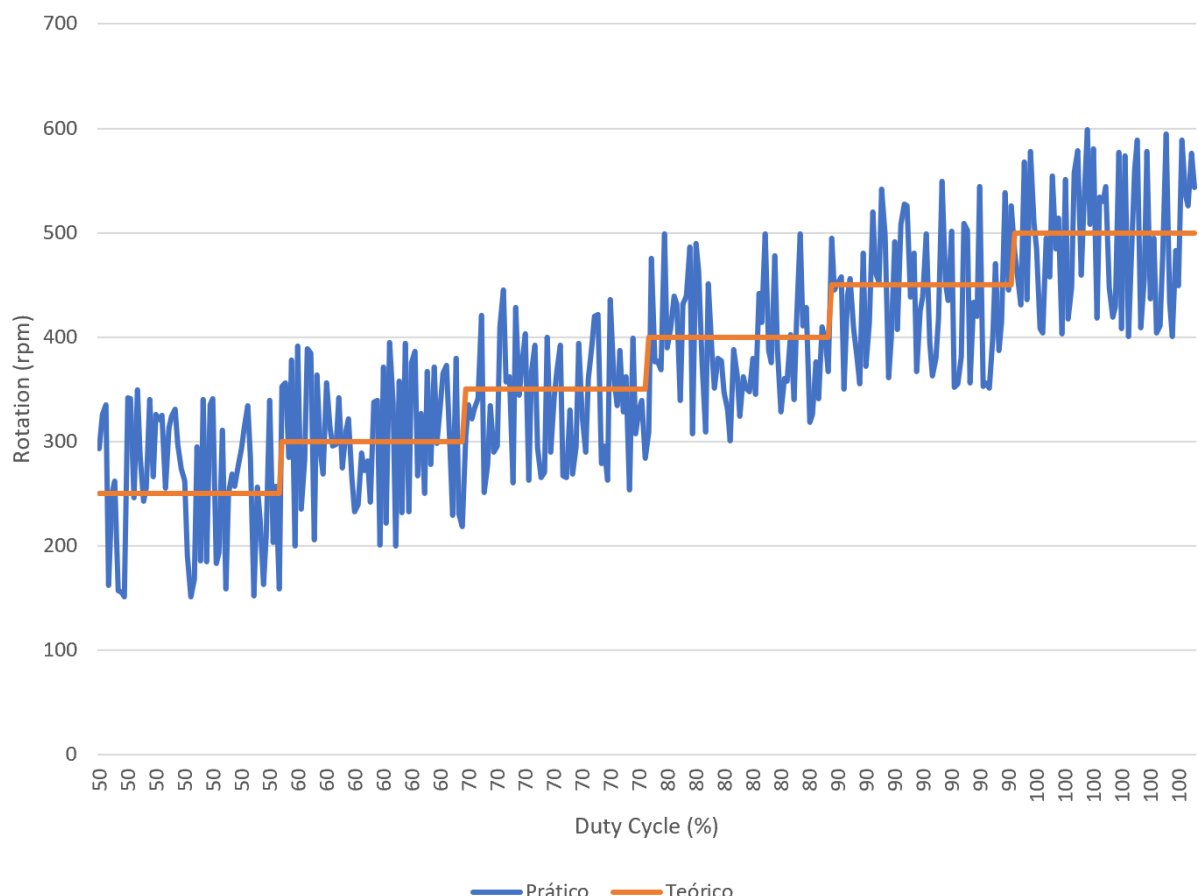


Figure 69 – Rotation in Respect with Duty Cycle

The signal is extremely noisy, compared to the theoretical rotation. However, even with all that noise it is possible to see that the signal is varying within a range close to the desired rotation. Maybe with a more sophisticated software it would be possible to treat this signal better to achieve better results.

7 Conclusions and Future Endavours

7.1 Conclusions

The initial goals of this paper can be summarized as being the project of a electronic test bench to perform brake tests in automotive components, and this goal was achieved.

As the tests proved the testbench can perform the required data acquisition of the specified physiscal quantities listed on Section 4.1 and also meet the mandatory requirements from Section 4.2 as well as the system can control the actuators needed for the brake tests.

During the project phase of this system, versatility was always in mind, the system does not only have the basical functionalities specified on *SAEJ2522*, it also achieved all the optional requirements from Section 4.2. At the end, a multifunctional hardware with transient protection in all ports was delivered. A interesting point of the developed hardware is that as it operates with pre-defined commands comming from its generic USB emulated serial port, any higher level software can theoretically be used to control it, as long as it respects the defined communication protocol.

The results of the brake tests performed shows a crucial point of this system, repeatability, the braketests were carried out for a hundred snubs without any interruption or bug, making the system extremely reliable. The transient protections circuits worked really well, even in the noisy and transient-dangerous environment created by the three-phase motor and frequency-inverter, not a single circuit was damaged during the tests.

As mentioned before, this system is extremely versatile, making it able to perform many different functions. Although this system was initially was developed with the final goal of performing braketests, at another point of view it can be seen as a control and acquisition system. For example, considering it has thermocouple reading inputs and digital inputs, it could be used to control a SMT (Surface Mount Technology) reflow oven temperature. Moreover the force acquistion channels can be used to control a industrial precision scale. Considering a vibration channel was implemented, even a vibration test-bench could be controlled and monitored. Possibilities are infinite, the only restriction is the amount of inputs and outputs of the designed hardware.

7.2 Future Endavours

A possible interesting improvement for this project would be developing a personalized software instead of using a default *LabView* application. A open source plataform could make the system more capable of being readily changed and maybe developing a system using Java could even make it easier to migrate the system to a web plataform.

A future version of this project could maybe consider switching from a integrated architecture to a distribuited one, instead of putting all acquisition channels in one board, a single board for each acquisition channel could be created and all this boards could communicate through a I2C bus for example. That way the system versatility would be only limit to the number of allowed devices on the bus. Moreover, as the sensors cables could be smaller (peripheral boards would be placed closer to the sensors), there would probably be less noise captured by those cables.

References

- ABENDROTH, H. A new approach to brake testing. *SAE transactions*, JSTOR, p. 438–450, 1985. Cited in page 23.
- ADAFRUIT. *Adafruit ADXL335 - 5V ready*. 2016. Cited in page 64.
- ADAFRUIT. *ADXL335 - 5V ready triple-axis accelerometer*. 2018. Disponível em: <<https://cdn-shop.adafruit.com/1200x900/163-02.jpg>>. Cited 2 times in page 11 and 64.
- ALTER, D. M. *Using PWM Output as a Digital-to-Analog Converter on a TMS320F280x Digital Signal Controller*. [S.l.], 2008. Cited in page 41.
- ALTIUM Designer 17. 2017. Disponível em: <<https://www.altium.com/s>>. Cited in page 78.
- AMETHERM. *Types of Temperature Sensors*. 2018. Disponível em: <<https://www.ametherm.com/blog/thermistors/temperature-sensor-types>>. Cited in page 32.
- ANALOG DEVICES. *AD8495: Precision Thermocouple Amplifiers with Cold Junction Compensation*. [S.l.], 2010. Cited 4 times in page 57, 58, 59, and 60.
- ARDUINO. *Arduino Leonardo Schematic*. 2010. Cited 2 times in page 73 and 75.
- ARDUINO Leonardo. 2016. Disponível em: <https://www.arduino.cc/en/Main/Arduino_BoardLeonardo>. Cited in page 73.
- ASCII. *ASCCII Table and Description*. 2017. Disponível em: <<http://www.asciitable.com/>>. Cited in page 81.
- ATMEL. *ATmega16/32U4 Block Diagram*. 2018. Disponível em: <<https://www.pjrc.com/teensy/atmega32u4.pdf>>. Cited 2 times in page 11 and 39.
- BARTZ, M.; ZHAKSILIKOV, M.; OGAMI, K. Y. *Data driven method and system for monitoring hardware resource usage for programming an electronic device*. [S.l.]: Google Patents, 2004. US Patent 6,785,881. Cited in page 38.
- BOJORGE, N. *Curva de Variação da F.E.M dos Termopares*. 2014. Disponível em: <http://www.termopares.com.br/teoria_sensores_temperatura_termopares_curvas_variacao_fem/curvas.gif>. Cited 2 times in page 11 and 32.
- BRYANT, J. et al. Protecting instrumentation amplifiers. *Sensors*, p. 6, 2000. Cited 2 times in page 57 and 58.
- CAIXETA, L. G. d. R. Projeto de dinamômetro inercial automatizado para analisar o comportamento em desgaste de sistemas de freio de veículos leves. 2017. Cited 3 times in page 12, 88, and 91.
- CARPARTS. *A Short Course on Brakes*. 2018. Disponível em: <<https://www.carparts.com/brakes.htm>>. Cited in page 27.

- CNW. *Volkswagen Gol 1.0 Ficha Técnica*. 2017. Disponível em: <<http://www.carrosnaweb.com.br/fichadetalhe.asp?codigo=1528>>. Cited in page 23.
- CNW. *Volkswagen Gol Plus 1.0 Ficha Técnica*. 2017. Disponível em: <<http://www.carrosnaweb.com.br/fichadetalhe.asp?codigo=431>>. Cited in page 23.
- CONTRAN. *Resolução N° 519*. 2015. Cited in page 24.
- COUNTS, L.; KITCHEN, C. A designer's guide to instrumentation amplifiers. In: _____. 3. ed. [S.l.]: Analog Devices, 2006. cap. 2, p. 3. Adapted. Cited 2 times in page 36 and 58.
- DESCONHECIDO. *Typical instrumentation amplifier schematic*. 2016. Disponível em: <https://upload.wikimedia.org/wikipedia/commons/thumb/e/ed/Op-Amp_Instrumentation_Amplifier.svg/400px-Op-Amp_Instrumentation_Amplifier.svg.png>. Cited 2 times in page 11 and 36.
- DEVICES, A. Adxl335: Small, low power, 3-axis \pm 3 g accelerometer. *ADXL335 Data Sheet Rev B, Jan*, p. 52, 2010. Cited 2 times in page 63 and 65.
- DEVICES, A. *AD8495 Functional Block Diagram*. 2011. Cited 2 times in page 11 and 57.
- DEVICES, A. *16-LFCSP Footprint*. 2016. Cited 2 times in page 11 and 64.
- DILLON, B. N.; GRIFFEN, N. C.; WEIHS, M. E. *Load cell*. [S.l.]: Google Patents, 1989. US Patent 4,815,547. Cited in page 34.
- DORF, R. C.; SVOBODA, J. A. *Introduction to Electrical Circuits*. 2014. Cited in page 68.
- DUFF, M.; TOWEY, J. *Two Ways to Measure Temperature Using Thermocouples Feature Simplicity, Accuracy, and Flexibility*. [S.l.], 2010. Cited 3 times in page 57, 58, and 59.
- ECIL. *Medição com Termopares*. 2016. Disponível em: <<http://www.ecil.com.br/imagens/seedback2.jpg>>. Cited 2 times in page 11 and 33.
- ELECTRONICS TUTORIALS. *P-channel MOSFET Relay Switch Circuit*. 2018. Disponível em: <<https://www.electronics-tutorials.ws/articles/switch8.gif>>. Cited 2 times in page 12 and 70.
- FAIRCHILD. *NDS332P: P-Channel Logic Level Enhancement Mode Field Effect Transistor*. [S.l.], 1997. Cited in page 70.
- FERNANDES, J. C. *Segurança nas Vibrações sobre o Corpo Humano*. [S.l.], 2000. 11 p. Cited in page 35.
- GARDINALLI, G. J. Comparação do desempenho de frenagem simulada x experimental de um veículo de passeio com freios hidráulicos e abs. *Trabalho de Conclusão de Curso apresentado à Escola Politécnica da Universidade de São Paulo para obtenção do título de Mestre em Engenharia Automotiva*, 2005. Cited in page 23.

- GOODYEAR. *Brake Calipers: The Top 3 Things You Need to Know*. 2018. Disponível em: <<https://www.goodyearautoservice.com/en-US/brakes/calipers>>. Cited 2 times in page 27 and 29.
- GUMS, J. *Types of Temperature Sensors*. 2018. Disponível em: <<https://www.digikey.com/en/blog/types-of-temperature-sensors>>. Cited in page 32.
- HALDERMAN, J. D.; MITCHELL, C. D. *Automotive brake systems*. [S.l.]: Prentice Hall, 2016. Cited in page 23.
- HERNANDES, D. *Relembre todos os carros que já lideraram as vendas no Brasil em 60 anos de história*. 2017. Disponível em: <<https://www.flatout.com.br/relembre-todos-os-carros-que-ja-lideraram-as-vendas-no-brasil-em-60-anos-de-historia/>>. Cited in page 23.
- HOLMES, D. G.; LIPO, T. A. *Pulse width modulation for power converters: principles and practice*. [S.l.]: John Wiley & Sons, 2003. v. 18. Cited in page 41.
- INC.(NORWOOD, M. A. D. *Operational Amplifiers Selection Guide 2011-2012: Detachable Charts Inside for Quick Product Selection & Design Equations*. [S.l.]: Analog Devices, 2011. Cited in page 37.
- INSTRUMENTS, N. *Definition of Strain*. 2016. Disponível em: <<http://www.ni.com/cms/images/devzone/tut/a/83a1fe69763.gif>>. Cited 2 times in page 11 and 34.
- INSTRUMENTS, N. *Wheatstone Bridge Circuit*. 2016. Disponível em: <<http://www.ni.com/cms/images/devzone/tut/a/a28b553b1069.gif>>. Cited 2 times in page 11 and 34.
- INSTRUMENTS, T. Instrumentation amplifier. 1997. Cited 3 times in page 11, 61, and 62.
- INSTRUMENTS, T. *INA 118*. 2000. Cited 2 times in page 11 and 37.
- INSTRUMENTS, T. *INA118 Precision, Low Power Instrumentation Amplifier*. [S.l.], 2000. 29 p. Cited in page 37.
- JAMES, C. Fundamentals of linear electronics: Integrated and discrete. *Fundamentals of linear electronics: integrated and discrete*. Cengage Learning, 2001. Cited in page 40.
- JR, K. N. Equivalence principle for massive bodies. ii. theory. *Physical Review*, APS, v. 169, n. 5, p. 1017, 1968. Cited in page 35.
- KAWAGUCHI, H. Comparação da análise de conforto de frenagem subjetiva x objetiva de um veículo de passeio. São Paulo, Brazil, p. 101, 2005. Cited in page 24.
- KINZIE, P. A.; RUBIN, L. G. Thermocouple temperature measurement. *Physics Today*, v. 26, p. 52, 1973. Cited in page 33.
- LIMPERT, R. *Brake design and safety*. [S.l.: s.n.], 1999. Cited in page 27.
- LITTLEFUSE. *Transient Voltage Suppression Diodes, SMBJ Series*. [S.l.], 2015. Cited in page 70.
- LITTLELFUSE. *ESD Test Wave*. 2015. Cited 2 times in page 11 and 42.

LITTLELFUSE. *Transient Voltage Suppressors (TVS Diode) Applications Overview.* [S.l.], 2015. Cited in page 41.

MATHIVANAN, N. *PC-based instrumentation: concepts and practice.* [S.l.]: PHI Learning Pvt. Ltd., 2007. Cited in page 41.

METIVIER, R. *Method for Converting a PWM Output to an Analog Output When Using Hall-Effect Sensor ICs.* [S.l.], 2013. Cited 2 times in page 67 and 68.

METTINGVANRIJN, A.; PEPER, A.; GRIMBERGEN, C. Amplifiers for bioelectric events: a design with a minimal number of parts. *Medical and Biological Engineering and Computing*, Springer, v. 32, n. 3, p. 305–310, 1994. Cited in page 36.

MICROCHIP. *Atmega32U4 Features.* 2017. Disponível em: <<https://www.microchip.com/wwwproducts/en/ATmega32u4#additional-features>>. Cited in page 72.

MICROCHIP. Lm4040/lm4041 precision micropower shunt voltage reference. *Technical Document, Literature*, 2017. Cited 2 times in page 55 and 78.

MICROCHIP. *Microchp ATmega16U4/32U4 datasheet.* [S.l.]: ed, 2018. Cited 3 times in page 70, 72, and 75.

MUKARO, R.; CARELSE, X. F. A microcontroller-based data acquisition system for solar radiation and environmental monitoring. *IEEE transactions on instrumentation and measurement*, IEEE, v. 48, n. 6, p. 1232–1238, 1999. Cited in page 81.

NATIONAL INSTRUMENTS. *O Que é Aquisição de Dados?* 2018. Disponível em: <<https://www.ni.com/data-acquisition/what-is/pt/>>. Cited in page 38.

NEWTON, R. *Brake Temperatures.* 2016. Disponível em: <<http://cartechstuff.blogspot.com.br/2016/04/brake-temperatures.html>>. Cited in page 32.

NICE, K. *How Disc Brakes Work.* 2017. Disponível em: <<https://s.hswstatic.com/gif/disc-brake3.jpg>>. Cited 2 times in page 11 and 27.

O'MAHONY, J. J.; GELFAND, M.; MERRICK, E. B. *Pressure sensor disconnect detection for a blood treatment device.* [S.l.]: Google Patents, 2011. US Patent 7,886,611. Cited in page 60.

ON SEMICONDUCTOR. Rb751v40t1 schottky barrier diode. 2014. Cited in page 71.

PALLÃ, R.; WEBSTER, J. G. et al. *Sensors and signal conditioning.* [S.l.]: John Wiley & Sons, 2012. Cited in page 33.

PATRICK, W. L. The history of the accelerometer: 1920s-1996 - prologue and epilogue. Ft. Worth - Texas, Estados Unidos da América, p. 9, 2007. Cited in page 35.

PETROLHEAD GARAGE. *CKP sensor signal example.* 2014. Disponível em: <<https://petrolheadgarage.com/wp-content/uploads/2014/10/EDISDiagram.jpg>>. Cited 2 times in page 11 and 31.

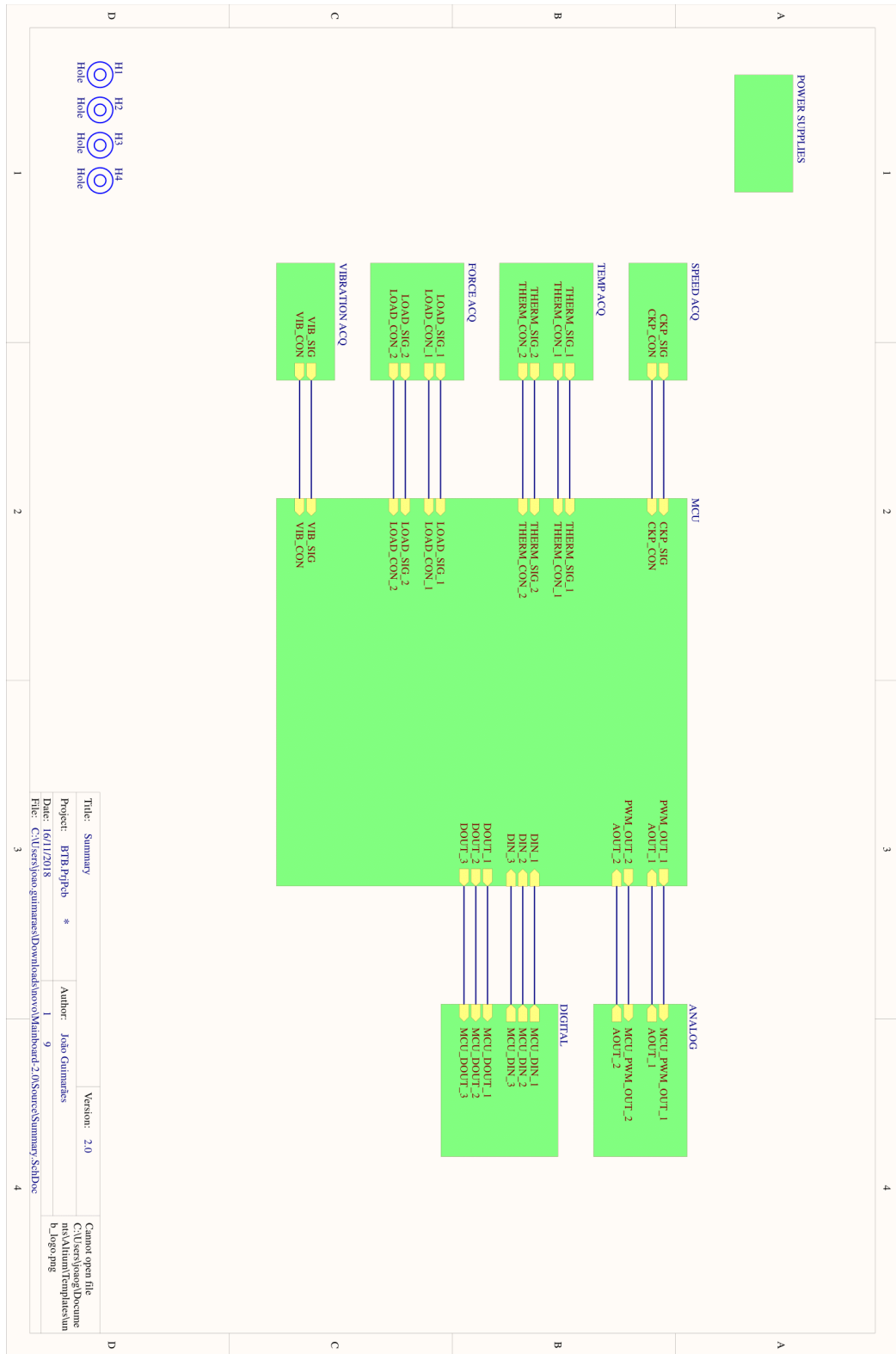
PIGHIXX. *ATmega32U4 Pinout.* 2018. Disponível em: <<https://www.flickr.com/photos/28521811@N04/8467610175>>. Cited 2 times in page 12 and 73.

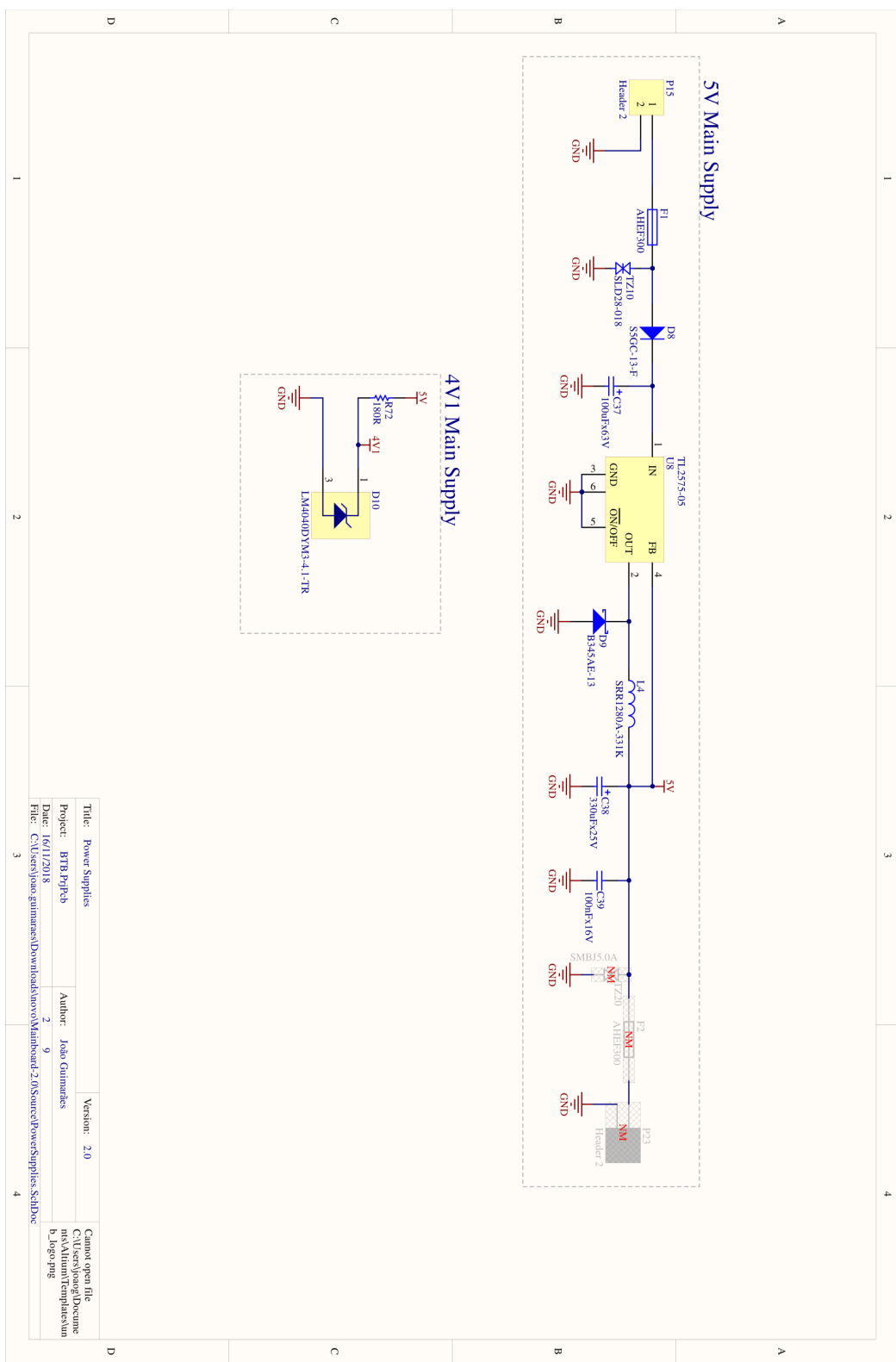
- POLLOCK, D. D. *Thermocouples: theory and properties*. [S.l.]: CRC press, 1991. Cited in page 32.
- REMAN, M. C. *GM Replacement 10456042 Crankshaft Position Sensor*. 2016. Disponível em: <<http://ep.yimg.com/ay/motorcityreman/general-motors-oe-10456042-crankshaft-position-sensor-1.gif>>. Cited 2 times in page 11 and 30.
- RENESAS. *Application Note 1977: Transient Voltage Suppressors: Operation and Features*. [S.l.], 2016. Cited in page 42.
- RENESAS. *Camping action of a bi-directional TVS*. 2016. Cited 2 times in page 11 and 43.
- RENESAS. *Camping action of a uni-directional TVS*. 2016. Cited 2 times in page 11 and 43.
- RENESAS. *V X I characteristic of a bi-directional TVS*. 2016. Cited 2 times in page 11 and 43.
- RENESAS. *V X I characteristic of a uni-directional TVS*. 2016. Cited 2 times in page 11 and 43.
- ROHM SEMICONDUCTOR. *RU1C002ZP Small Signal Mosfet*. [S.l.], 2016. Cited in page 71.
- ROMERO, N. A. Johnson noise. *power*, v. 2, p. 4, 1998. Cited in page 57.
- ROUSE, M. *microcontroller*. 2012. Disponível em: <<http://internetofthingsagenda.techtarget.com/definition/microcontroller>>. Cited in page 38.
- RZTRONICS. *Duty Cycle*. 2016. Disponível em: <<https://i1.wp.com/rztronics.com/wp-content/uploads/2016/10/pwm.gif?zoom=1.89999976158142&resize=390%2C427>>. Cited 2 times in page 11 and 40.
- SAE. *Dynamometer Global Brake Effectiveness*. Rio de Janeiro, Brasil, 2003. 18 p. Cited 4 times in page 28, 31, 32, and 85.
- SAE. *SAE*. 2016. Disponível em: <<http://www.sae.org/>>. Cited 2 times in page 23 and 25.
- SCHROEDER, T. *Crankshaft position sensor*. [S.l.]: Google Patents, 2002. US Patent 6,346,808. Cited in page 30.
- SCHWEBER, B. *Understanding the Advantages and Disadvantages of Linear Regulators*. 2017. Disponível em: <<https://www.digikey.com/en/articles/techzone/2017/september/understanding-the-advantages-and-disadvantages-of-linear-regulators>>. Cited in page 76.
- SONGLE. *Songle Relay*. 2018. Cited in page 70.
- SOUZA, S. Xavier-de et al. The benefits of low operating voltage devices to the energy efficiency of parallel systems. *arXiv preprint arXiv:1709.08689*, 2017. Cited in page 41.

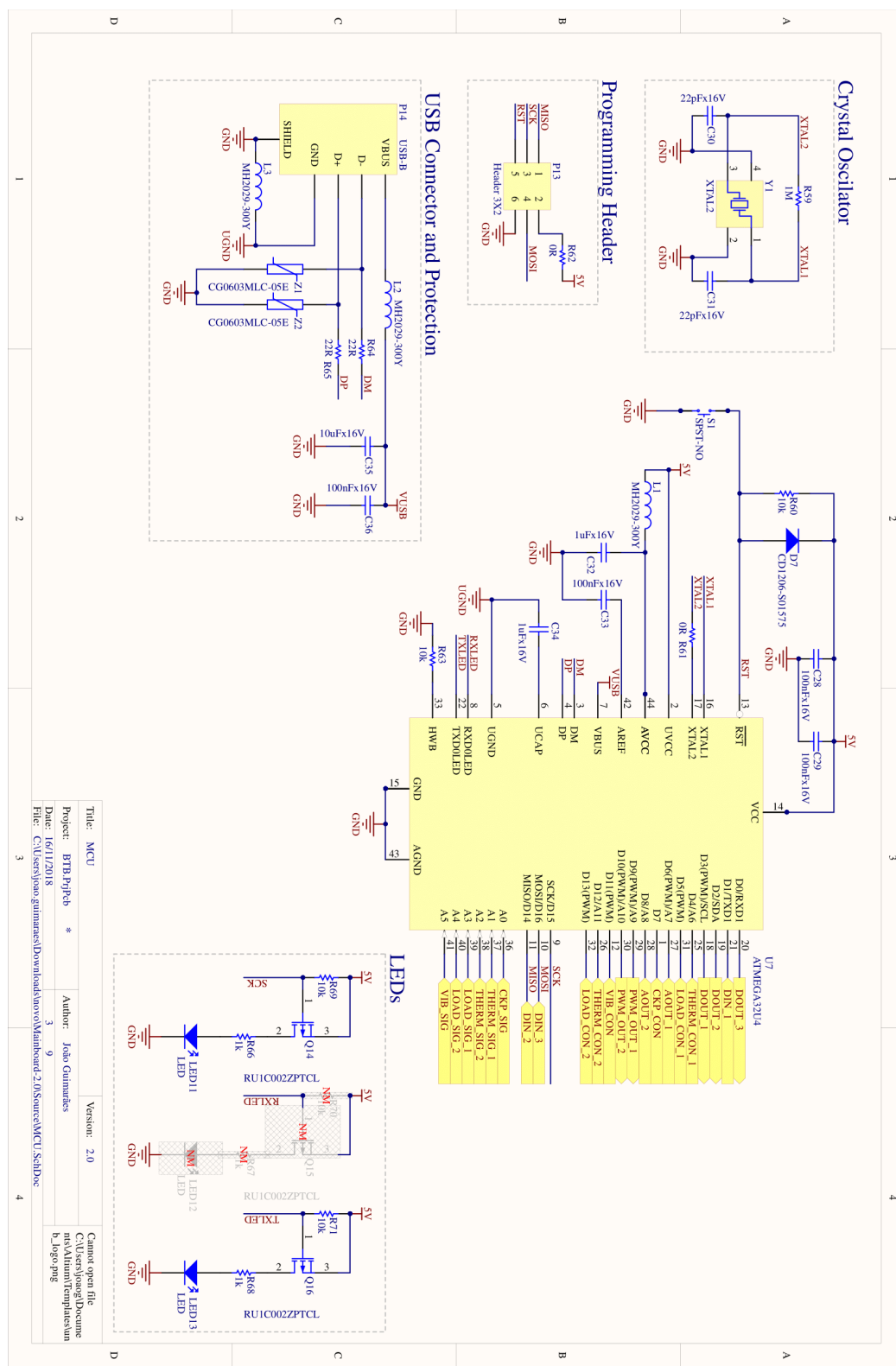
- STANDARD, F. 1037c. telecommunications: Glossary of telecommunication terms. *Institute for Telecommunications Sciences*, v. 7, 1996. Cited in page 40.
- STANDLER, R. *Use of low-pass filters to protect equipment from transient overvoltages on the mains*. 1988. 66–73 p. Cited in page 42.
- TEXAS INSTRUMENTS. *Analysis of the Sallen-Key Architecture*. Dallas, Texas 75265, 1999. Cited 3 times in page 12, 68, and 69.
- TEXAS INSTRUMENTS. *LM2907 and LM2917 Frequency to Voltage Converter*. [S.I.], 2000. Cited 5 times in page 11, 51, 52, 54, and 55.
- TEXAS INSTRUMETS. *LM2907 Tachometer with Adjustable Zero Speed Voltage Output*. 2018. Cited 2 times in page 11 and 53.
- TEXAS INSTURMENTS. *TL2575, TL2575HV 1-A Simple Step-Down Switching Voltage Regulators*. [S.I.], 2014. Cited in page 77.
- THOMSEN, A. et al. *Application of a conditionally stable instrumentation amplifier to industrial measurement*. [S.I.]: Google Patents, 2003. US Patent 6,525,589. Cited in page 36.
- TODAS as Medidas de Pneu. 2018. Disponível em: <<https://www.pneusfacil.com.br/comprepneus>>. Cited in page 54.
- UK, M. O. *Compression Accelerometer*. 2016. Disponível em: <[http://www.maintenanceonline.co.uk/maintenanceonline/content_images/figure-2\(1\).jpg](http://www.maintenanceonline.co.uk/maintenanceonline/content_images/figure-2(1).jpg)>. Cited 2 times in page 11 and 35.
- WAIT, J. V.; HUELSMAN, L. P.; KORN, G. A. *Introduction to operational amplifier theory and applications*. [S.I.]: McGraw-Hill Companies, 1975. Cited in page 36.
- WALTERS, K. *How To Select Transient Voltage Suppressors*. [S.I.], 2016. Cited in page 42.
- WEG. *CFW-08 Frequency Inverter*. [S.I.], 2009. Cited 2 times in page 66 and 85.
- WEG. *WEG CFW08 Frequency Inverter*. 2017. Disponível em: <http://ecatalog.weg.net/files/produtos/CFW-08_G.jpg>. Cited 2 times in page 12 and 67.
- WINDOW, A. L.; HOLISTER, G. S. et al. *Strain gauge technology*. [S.I.]: Applied science publishers, 1982. Cited in page 33.

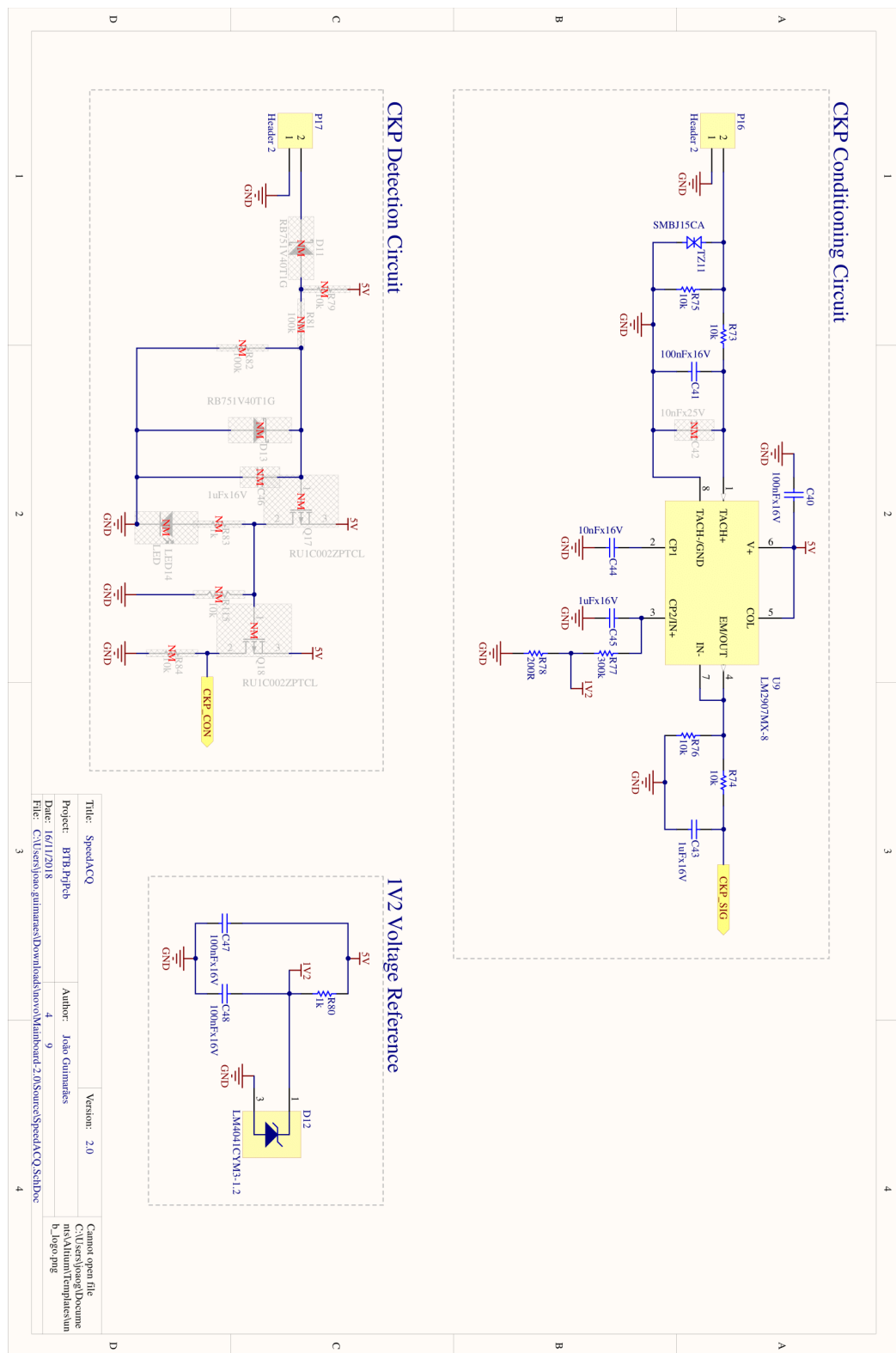
Appendix

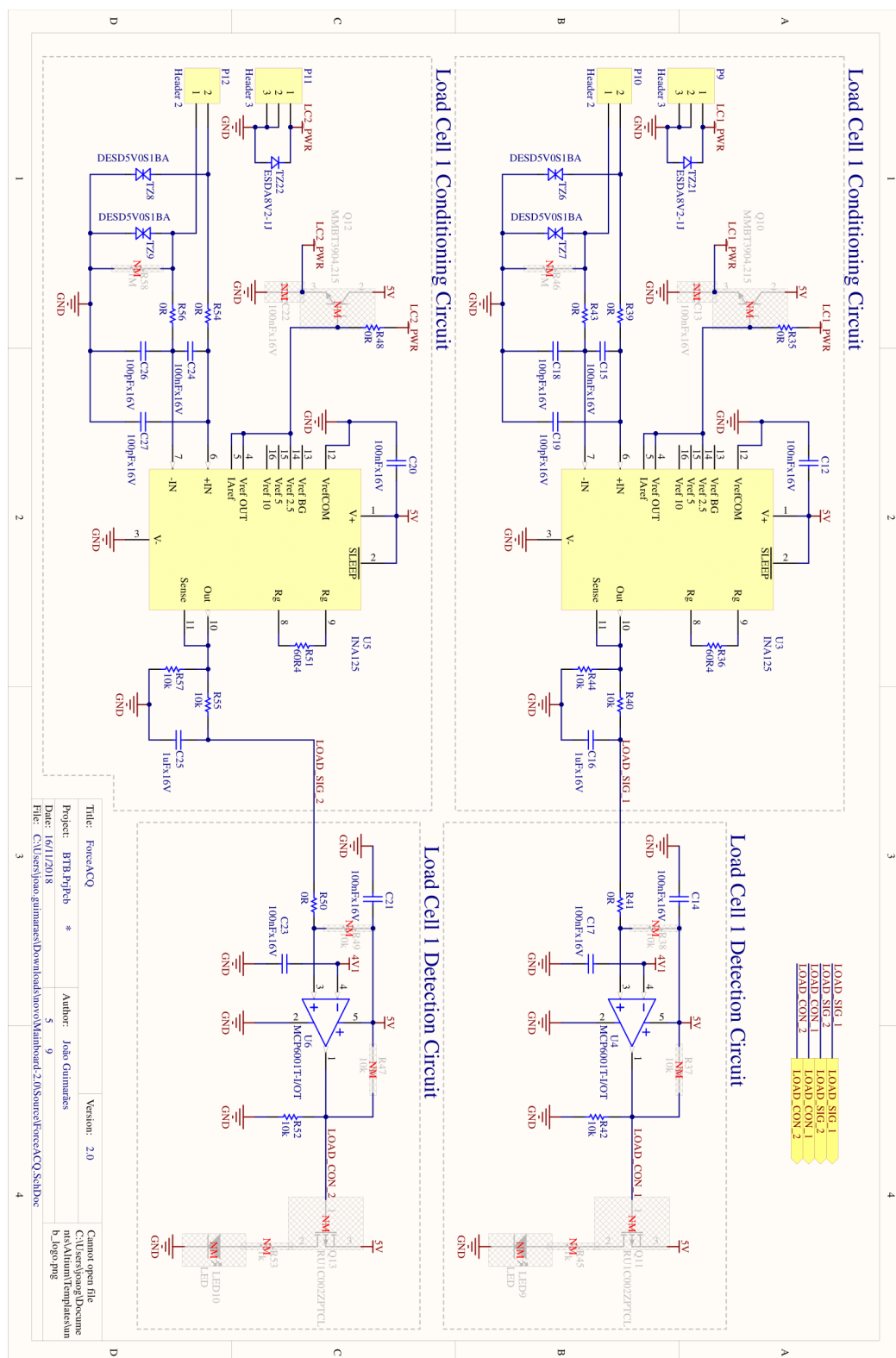
APPENDIX A – Schematic Prints

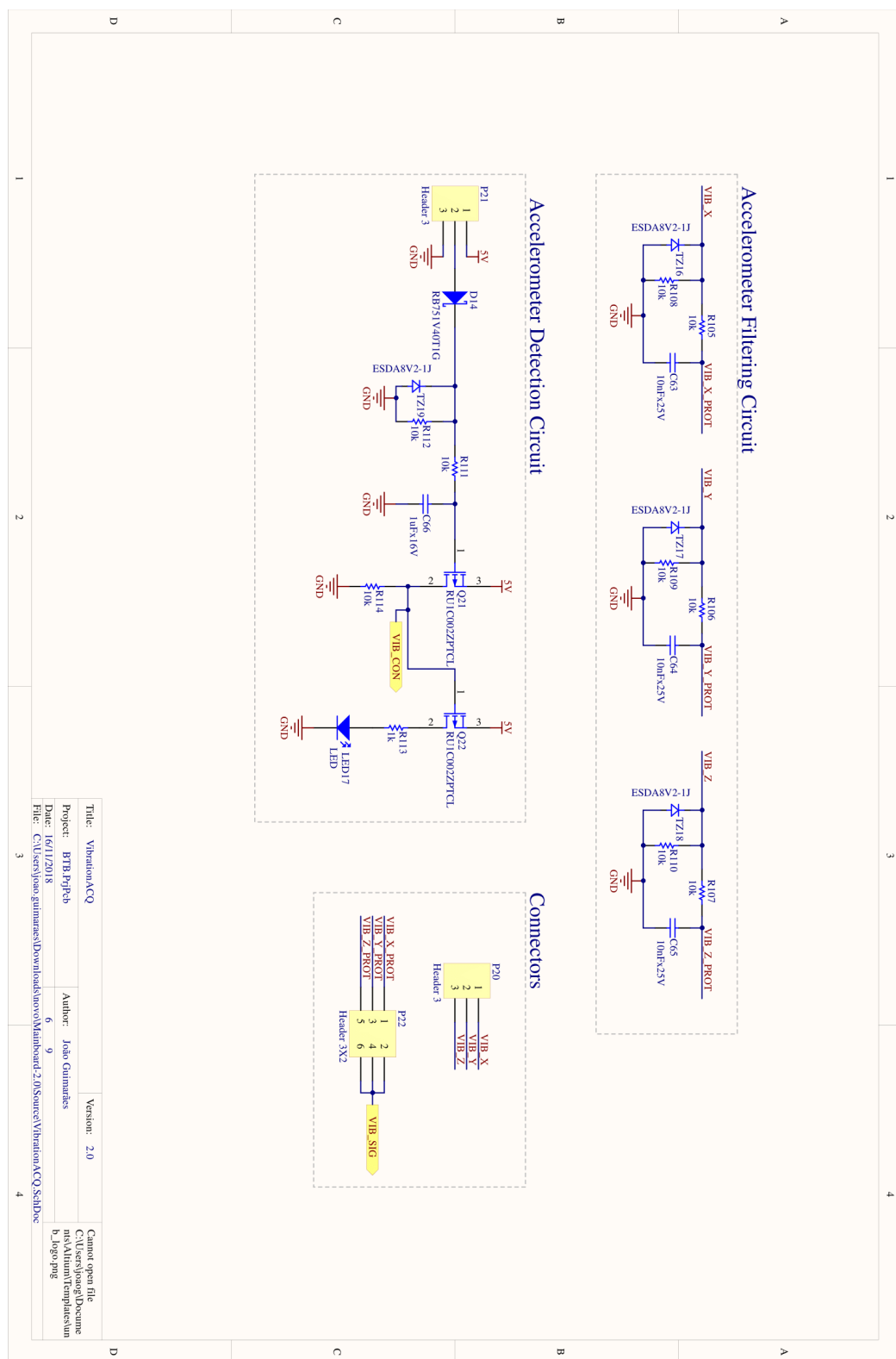


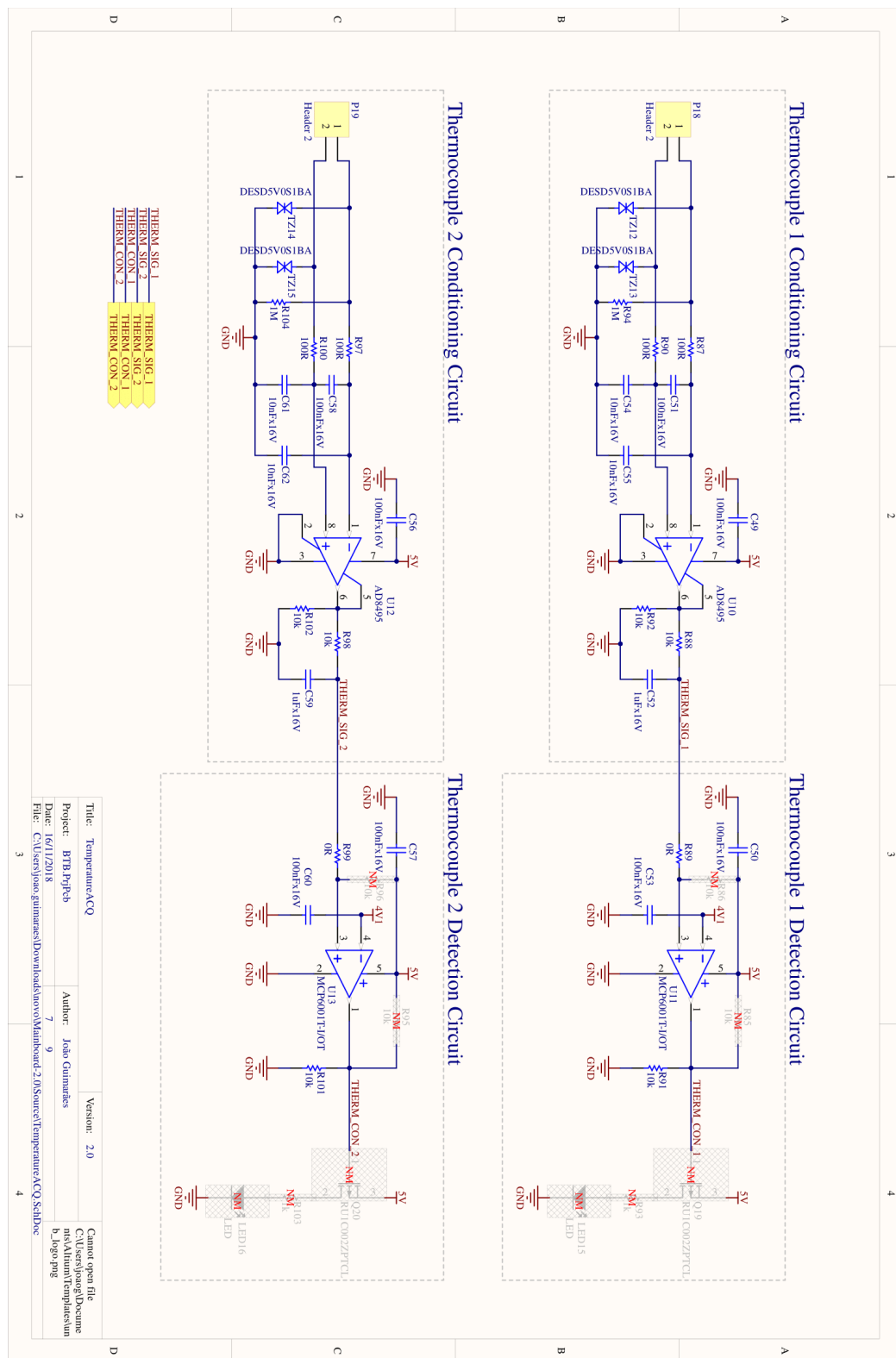


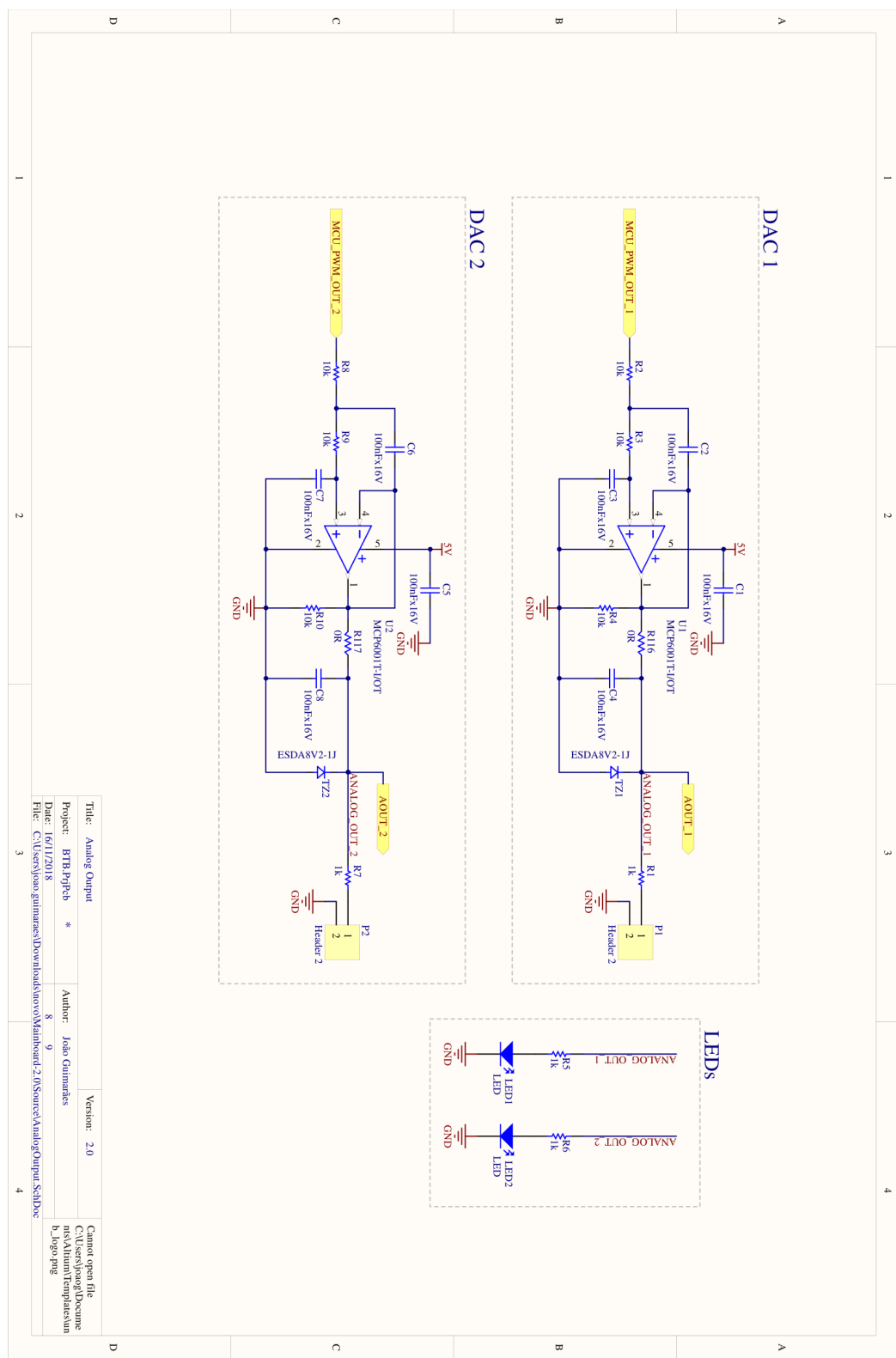


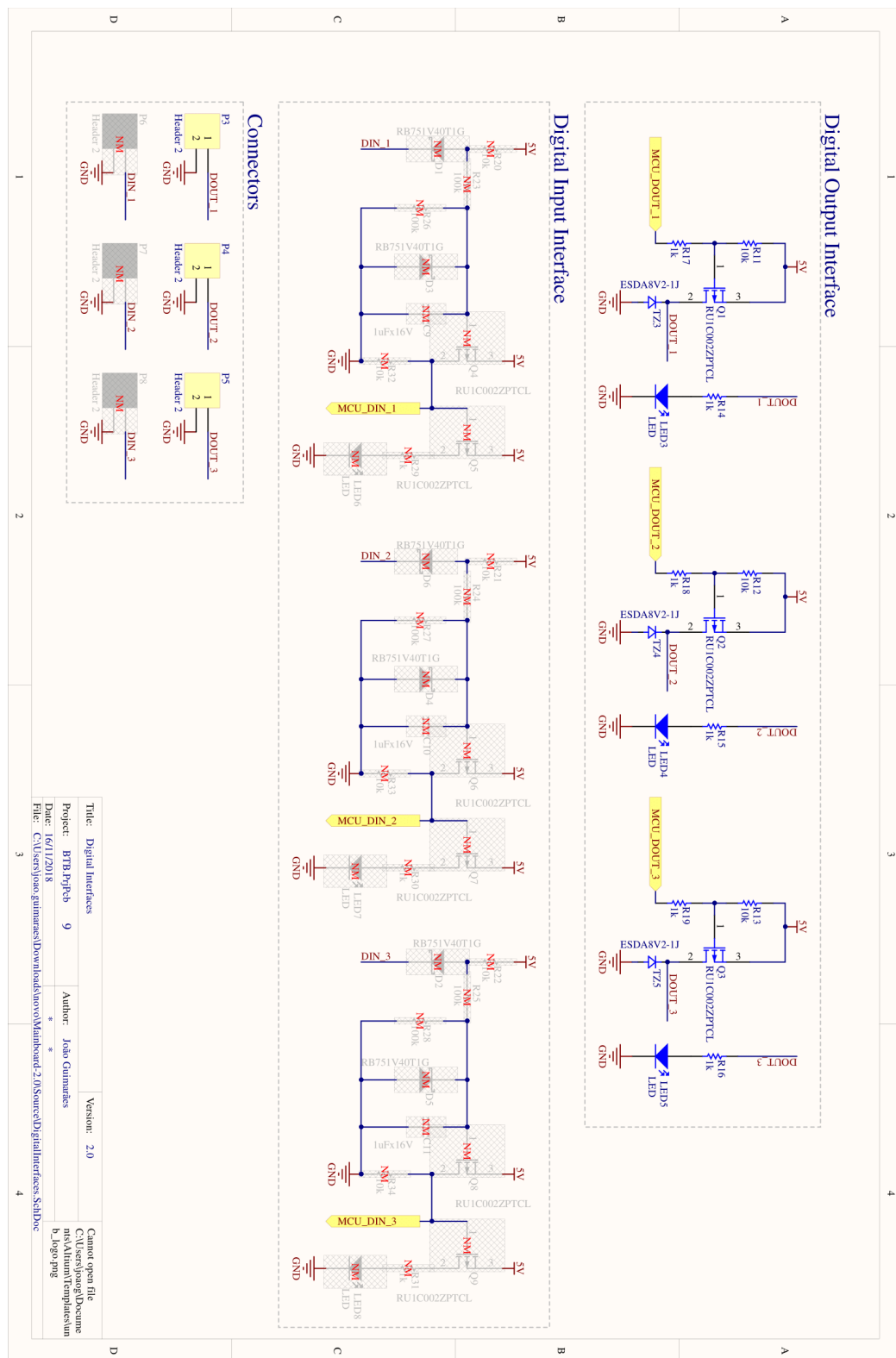












APPENDIX B – Firmware Code

```

//HARDWARE DEFINITIONS

//Digital Inputs
#define CKP_CON_1          7
#define THERM_CON_1         4
#define THERM_CON_2         12
#define LOAD_CON_1          5
#define LOAD_CON_2          13
#define VIB_CON_1           11
#define DIG_IN_1             1
#define DIG_IN_2             14
#define DIG_IN_3             16

//Digital Outputs
#define DIG_OUT_1            3
#define DIG_OUT_2            2
#define DIG_OUT_3            0
#define MCU_LED_1            15

//Analog Inputs
#define CKP_SIG_1            A0
#define THERM_SIG_1           A1
#define THERM_SIG_2           A2
#define LOAD_SIG_1            A3
#define LOAD_SIG_2            A4
#define VIB_SIG_1              A5
#define AOUT_SIG_1            A7
#define AOUT_SIG_2            A8

//Analog Outputs
#define PWM_OUT_1             9
#define PWM_OUT_2             10

//COMMUNICATIONS DEFINITIONS
#define BAUD_RATE           115200
#define PRINT_VERSION_BYTE    32
#define FILTER_READ_BYTE      33
#define ONE_READ_BYTE         34
#define ACQ_CMD_OFF_BYTE      35

```

```
#define NULL_DIGITAL_BYTE      36
#define MAX_DIGITAL_BYTE        43
#define CH1_NULL_SPEED_BYTE     75
#define CH1_MAX_SPEED_BYTE      100
#define CH2_NULL_SPEED_BYTE     101
#define CH2_MAX_SPEED_BYTE      126

//GENERAL DEFINITIONS
#define SET                      1
#define RESET                   0

//Running Setup
#define ACQ_LED_BLINK_MS        150
#define NUMBER_OF_SAMPLES        100
#define SAMPLE_RATE               250

//TIMER DEFINITIONS
#define MCU_LED_BLINK_FREQ       2
#define SAMPLE_RATE_HZ            10000

//GLOBAL VARS
boolean enableAcquisition = false;
boolean enableMcuLed = false;
float adcReads[] = {RESET, RESET, RESET, RESET, RESET, RESET, RESET,
                    RESET};
int samples = RESET;
boolean state = RESET;
int inputPins[] = {CKP_CON_1, THERM_CON_1, THERM_CON_2, LOAD_CON_1,
                  LOAD_CON_2, VIB_CON_1, DIG_IN_1, DIG_IN_2, DIG_IN_3};
int outputPins[] = {DIG_OUT_1, DIG_OUT_2, DIG_OUT_3, MCU_LED_1};

//////TIMER CONFIGURING FUNCTIONS
//Function that sets Timer 1 - PWM frequency
void configurePwmTimer() {
    TCCR1B = (TCCR1B & 0xF8) | 0x02; //sets the frequency to 3900Hz (0x01 -
                                         32kHz, 0x02 - 3900Hz, 0x03 - 490Hz default, 0x04 - 120Hz, 0x05 - 30Hz)
}

//Function that sets Timer 3 - Acquisition Timer
void configureAcquisitionTimer() {
    TCCR3A = 0; TCCR3B = 0; TCCR3C = 0; TCNT3 = 0; //clearing timer registers
```

```

TCCR3B |= (1 << WGM32) | (1 << CS31) | (1 << CS30); //setting up the
    clock divider (clk/1);
OCR3A = 16000000 / 64 / SAMPLE_RATE_HZ; //16MHz/64/1000kHz //Configuring
    the compare value, sample rate)
TIMSK3 |= (1 << OCIE3A); //Enable Interrupt on compare input 3A
}

//Function that sets Timer 4 - MCU LED timer
void configureMcuLedTimer() {
    TCCR4A = 0; TCCR4B = 0; TCCR4C = 0; TCCR4D = 0; TCNT4 = 0; //clearing
        timer registers
    TCCR4B |= (1 << CS43) | (1 << CS42) | (1 << CS41) | (1 << CS40);
        //setting up the clock divider (clk/16384);
    OCR4A = 488; //16000 / 16384 / MCU_LED_BLINK_FREQ; //16MHz/16384/2Hz=488
        ~ 1.95Hz
    TIMSK4 |= (1 << OCIE4A); //Enable Interrupt on compare input 4A
}

//Timer 3 Interrupt Service Routine - Acquisition
ISR(TIMER3_COMPA_vect) {
    if (enableAcquisition) {
        if (samples <= NUMBER_OF_SAMPLES) {
            //Reading Analog Inputs
            adcReads[0] += analogRead(CKP_SIG_1);
            adcReads[1] += analogRead(THERM_SIG_1);
            adcReads[2] += analogRead(THERM_SIG_2);
            adcReads[3] += analogRead(LOAD_SIG_1);
            adcReads[4] += analogRead(LOAD_SIG_2);
            adcReads[5] += analogRead(VIB_SIG_1);
            adcReads[6] += analogRead(AOUT_SIG_1);
            adcReads[7] += analogRead(AOUT_SIG_2);
            samples++;
        }
    }
}

//Timer 4 Interrupt Service Routine - Acquisition
ISR(TIMER4_COMPA_vect) {
    if (enableMcuLed) {
        digitalWrite(MCU_LED_1, digitalRead(MCU_LED_1) ^ 1); // toggle MCU Led
        Pin
    } else {
}

```

```
    digitalWrite(MCU_LED_1, LOW); //Turn MCU LED on
}
}

//Function that turns all the outputs off
void resetCommandOutput() {
    //resetting digital outputs
    digitalWrite(DIG_OUT_1, HIGH);
    digitalWrite(DIG_OUT_2, HIGH);
    digitalWrite(DIG_OUT_3, HIGH);
    //resetting analog outputs
    analogWrite(PWM_OUT_1, RESET);
    analogWrite(PWM_OUT_2, RESET);
}

//Function that prints acquisition results in serial port
void printResults(int * result) {
    for (int i = RESET; i < 8; i++) {
        Serial.print(result[i]);
        Serial.print(",");
    }

    for (int i = RESET; i < 3; i++) {
        if (digitalRead(inputPins[i])) {
            Serial.print("1");
        } else {
            Serial.print("0");
        }
        if (i<2){
            Serial.print(",");
        }else{
            Serial.println(";");
        }
    }
}

//Function that does one analogRead of each channel and prints the results
// to the serial port
void oneReadPrint() {
    int oneRead[] = {RESET, RESET, RESET, RESET, RESET, RESET, RESET, RESET};
    oneRead[0] = analogRead(CKP_SIG_1);
    oneRead[1] = analogRead(THERM_SIG_1);
```

```
    oneRead[2] = analogRead(THERM_SIG_2);
    oneRead[3] = analogRead(LOAD_SIG_1);
    oneRead[4] = analogRead(LOAD_SIG_2);
    oneRead[5] = analogRead(VIB_SIG_1);
    oneRead[6] = analogRead(AOUT_SIG_1);
    oneRead[7] = analogRead(AOUT_SIG_2);

    printResults(oneRead);
}

void printFwVersion(){
    Serial.println("");
    Serial.println("Braketestbench - FW Version 2.0 (28-Oct/2018)");
    Serial.println("Made by Joao Guimaraes - joaoguimaraes31@gmail.com");
    Serial.println("https://github.com/braketestbench/firmware");
    Serial.println("");
}

void setup() {
    //Initializing Serial port
    Serial.begin(BAUD_RATE);

    //Port Map
    for (int i = RESET; i < sizeof(inputPins); i++) {
        pinMode(inputPins[i], INPUT);
    }
    for (int i = RESET; i < sizeof(outputPins); i++) {
        pinMode(outputPins[i], OUTPUT);
    }
    resetCommandOutput();

    //Configuring Timers
    configurePwmTimer();
    configureAcquisitionTimer();
    configureMcuLedTimer();

    //statusLED
    enableMcuLed = true;

    //printFwVersion
    printFwVersion();
}
```

```
//Funcao loop - executada continuamente
void loop() {
    //parar o timer quando o numero de amostras for o desejado
    if (samples >= NUMBER_OF_SAMPLES) {
        enableAcquisition = false;
        enableMcuLed = true;
        TCNT3 = 0; //clearing timer count register
        static int resultAcq[sizeof(adcReads)];
        for (int counter = RESET; counter < 8; counter++) {
            resultAcq[counter] = (int)roundf((adcReads[counter] / samples));
            adcReads[counter] = RESET;
        }
        samples = RESET;
        printResults(resultAcq);
    }

    //Verificado dado da porta serial
    if (Serial.available()) {

        //Lendo o byte mais recente
        unsigned char byteRead = Serial.read();

        switch (byteRead) {

            //Recebeu comando iniciar aquisicao
            case FILTER_READ_BYTE:
                {
                    if (!enableAcquisition) {
                        TCNT3 = 0; //clearing timer count register
                        enableAcquisition = true;
                        enableMcuLed = false;
                    }
                }
                break;
            case ONE_READ_BYTE:
                {
                    if (!enableAcquisition) {
                        oneReadPrint();
                    }
                }
                break;
        }
    }
}
```

```
case ACQ_CMD_OFF_BYTE:
{
    resetCommandOutput();
    enableAcquisition = false;
}
break;

case PRINT_VERSION_BYTE:
{
    printFwVersion();
}
break;

default:
{
    if ((byteRead >= NULL_DIGITAL_BYTE) && (byteRead <=
        MAX_DIGITAL_BYTE)) { //Controla los comandos
        unsigned char command = byteRead - NULL_DIGITAL_BYTE;
        switch (command) {
            case 1:
                digitalWrite(DIG_OUT_1, LOW);
                digitalWrite(DIG_OUT_2, HIGH);
                digitalWrite(DIG_OUT_3, HIGH);
                break;

            case 2:
                digitalWrite(DIG_OUT_1, HIGH);
                digitalWrite(DIG_OUT_2, LOW);
                digitalWrite(DIG_OUT_3, HIGH);
                break;

            case 3:
                digitalWrite(DIG_OUT_1, LOW);
                digitalWrite(DIG_OUT_2, LOW);
                digitalWrite(DIG_OUT_3, HIGH);
                break;

            case 4:
                digitalWrite(DIG_OUT_1, HIGH);
                digitalWrite(DIG_OUT_2, HIGH);
                digitalWrite(DIG_OUT_3, LOW);
        }
    }
}
```

```
        break;

    case 5:
        digitalWrite(DIG_OUT_1, LOW);
        digitalWrite(DIG_OUT_2, HIGH);
        digitalWrite(DIG_OUT_3, LOW);
        break;

    case 6:
        digitalWrite(DIG_OUT_1, HIGH);
        digitalWrite(DIG_OUT_2, LOW);
        digitalWrite(DIG_OUT_3, LOW);
        break;

    case 7:
        digitalWrite(DIG_OUT_1, LOW);
        digitalWrite(DIG_OUT_2, LOW);
        digitalWrite(DIG_OUT_3, LOW);
        break;

    default: //NULL_DIGITAL_BYTE COMMAND RECEIVED
        digitalWrite(DIG_OUT_1, HIGH);
        digitalWrite(DIG_OUT_2, HIGH);
        digitalWrite(DIG_OUT_3, HIGH);
        break;
    }

}

if ((byteRead >= CH1_NULL_SPEED_BYTE) && (byteRead <=
CH1_MAX_SPEED_BYTE)) {
analogWrite(PWM_OUT_1, (255 * (byteRead - CH1_NULL_SPEED_BYTE)
/ (CH1_MAX_SPEED_BYTE - CH1_NULL_SPEED_BYTE)));
}

if ((byteRead >= CH2_NULL_SPEED_BYTE) && (byteRead <=
CH2_MAX_SPEED_BYTE)) {
analogWrite(PWM_OUT_2, (255 * (byteRead - CH2_NULL_SPEED_BYTE)
/ (CH2_MAX_SPEED_BYTE - CH2_NULL_SPEED_BYTE)));
}

break;
```

```
    }  
}  
}  
}
```
